SKB

TECHNICAL REPORT 91-15

Uraninite alteration in an oxidizing environment and its relevance to the disposal of spent nuclear fuel

Robert Finch, Rodney Ewing

Department of Geology, University of New Mexico

December 1990

SVENSK KÄRNBRÄNSLEHANTERING AB
SWEDISH NUCLEAR FUEL AND WASTE MANAGEMENT CO

BOX 5864 S-102 48 STOCKHOLM

TEL 08-665 28 00 TELEX 13108 SKB S
TELEFAX 08-661 57 19

URANINITE ALTERATION IN AN OXIDIZING ENVIRONMENT AND ITS RELEVANCE TO THE DISPOSAL OF SPENT NUCLEAR FUEL

Robert Finch, Rodney Ewing

Department of Geology, University of New Mexico

December 1990

URANINITE ALTERATION IN AN OXIDIZING ENVIRONMENT AND ITS RELEVANCE TO THE DISPOSAL OF SPENT NUCLEAR FUEL

Robert Finch
Rodney Ewing

Department of Geology
University of New Mexico

Submitted to
Svensk Kärnbränslehantering AB (SKB)

December 21, 1990

ABSTRACT

Uraninite is a natural analogue for spent nuclear fuel because of similarities in structure (both are fluorite structure types) and chemistry (both are nominally UO_2). Effective assessment of the long-term behavior of spent fuel in a geologic repository requires a knowledge of the corrosion products produced in that environment. UO_2 retains the fluorite structure when oxidized to $UO_{2.25}(U_4O_9)$. Further oxidation in laboratory experiments indicates formation of $UO_{2.33}(U_3O_7)$,$UO_{2.67}(U_3O_8)$ and amorphous UO_3; analogous anhydrous oxides have not been confirmed in nature. Hydrous uranyl oxides schoepite ($UO_3 \cdot 2H_2O$), dehydrated schoepite ($UO_3 \cdot 0.8\text{-}1.0H_2O$), becquerelite ($CaU_6O_{19} \cdot 10H_2O$); and hydrous uranyl silicates, including uranophane $Ca(UO_2)_2(SiO_3OH) \cdot 5H_2O$), boltwoodite $(K(H_3O)(UO_2)SiO_4 \cdot nH_2O$, sklodowskite $(Mg(UO_2)_2(SiO_3OH) \cdot 5H_2O)$, and perhaps haiweeite $(3CaO \cdot 4UO_3 \cdot 10SiO_2 \cdot 24H_2O)$, have also been identified in corrosion studies on UO_2 or spent fuel; these phases are all known in nature. The uranyl oxide hydrates possess layer-type structures similar to orthorhombic U_3O_8 with large, low-valence cations (e.g. Ca^{2+}, Ba^{2+}, Pb^{2+}) and water molecules occupying exchangeable interlayer sites. This is important to the alteration and paragenesis of these phases and for the potential role of the uranyl oxide hydrates as "scavengers" for radionuclides and fission products. No uranyl phosphates or other complex uranyl phases have been identified in laboratory experiments, although such phases are common in the nature. More than 160 naturally-occurring uranyl phases are known, but fewer than 20 uranyl phases have been identified to date in laboratory corrosion studies.

Several important natural analogue sites are reviewed, illustrating a wide variety of environments from oxidizing to reducing, including, among others: Cigar Lake, Canada, a uraninite-bearing ore body at depth within a strictly reducing environment; the ore body has "seen" extensive groundwater interaction with virtually no significant oxidation or mobilization of U apparent. Koongara, Australia is a highly altered uraninite-bearing ore body partially exposed to meteoric water; alteration at depth has resulted from interaction with groundwater having a somewhat reduced Eh compared to the surface. Uraninite, Pb-uranyl oxide hydrates and uranyl silicates control U solubility at depth; uranyl phosphates and U adsorption onto clays and FeMn-oxides control U solubility near the surface. Poços de Caldas, Brazil displays a redox front moving through uraninite-bearing rocks near the surface and shows local remobilization of U. Oklo, Gabon, a uraninite- and coffinite-bearing ore body, locally affected by intense hydrothermal alteration during fission reactions, demonstrates restricted radionuclide and fission product transport within a reducing environment. A current study being conducted by the authors at Shinkolobwe, Zaire, a uraninite-bearing ore body exposed to highly oxidizing conditions at the surface, provides over 50 species of uranyl phases for detailed study, and illustrates a complex uranyl phase paragenesis over several million years, from earliest-formed uranyl oxide hydrates and uranyl silicates to later-formed uranyl phosphates.

URANINITE ALTERATION IN AN OXIDIZING ENVIRONMENT AND ITS RELEVENCE TO THE DISPOSAL OF SPENT NUCLEAR FUEL

TABLE OF CONTENTS

INTRODUCTION 1

URANINITE AND RELATED U(IV) PHASES 3

U(VI) MINERALS 13

Synthetic Uranyl Oxide Hydrates 13

Natural Uranyl Oxide Hydrates 14

RADIATION EFFECTS 26

Alpha-recoil Damage 26

Alpha Radiolysis of Water 27

NATURAL UO_{2+x} AS AN ANALOGUE FOR SPENT FUEL CORROSION 28

Laboratory Studies 29

Natural Analogue Studies 39

Cigar Lake, Saskatchewan, Canada 39

Koongarra, Northern Territories, Australia 42

Poços de Caldas, Minas Gerais, Brazil 47

Oklo, Gabon 52

Palmottu, Finland 54

Krunkelbach mine, Menzenschwand, Germany 56

Needle's Eye, Scotland 57

Shinkolobwe mine, Shaba, Zaire 58

SUMMARY 62

TABLE OF CONTENTS *(cont'd)*

REFERENCES 66

APPENDIX A 85
MINERALS CONTAINING THE URANYL ION

APPENDIX B 93
URANYL MINERALOGY OF SELECTED URANIUM DEPOSITS

APPENDIX C 97
UNM URANIUM MINERAL COLLECTION

APPENDIX D 115
SCANNING ELECTRON MICROGRAPHS OF SELECTED URANYL MINERALS

Acknowledgements

AEM, SEM, and EMPA were performed at the Electron Microbeam Analysis Facility of the Geology Department and Institute of Meteoritics at the University of New Mexico. XRD was performed in the X-ray Diffraction Laboratory at the University of New Mexico. This work is supported by Svensk Kärnbränslehantering AB (SKB).

INTRODUCTION

Assessing the long-term behavior of spent fuel exposed to the geochemical conditions of a geologic repository is difficult because of the long time required for the effective isolation of hazardous radionuclides (on the order of 10,000 years). Laboratory studies of spent fuel are critical for understanding the initial, or short-term corrosion behavior of spent fuel (during temporary storage and permanent disposal), but predicting the behavior of spent fuel after thousands of years requires the extrapolation of experimental data for periods up to 10,000 . Fortunately, uraninite (UO_{2+x}) and its alteration products are natural analogues for the corrosion of spent fuel. These natural analogues may provide a key to understanding spent fuel behavior over the long term; however, a complete understanding of these natural phases, and of the environmental conditions under which they form, is required in order to confidently and competently employ natural analogue studies in the performance assessment of a spent fuel repository.

This paper is a partial summary of literature on laboratory studies on the corrosion and dissolution behavior of UO_2 and spent fuel as well as several natural analogue studies. The two approaches are substantially different in their scope. Laboratory studies are primarily concerned with near-field phenomena over relatively short periods (months to years), while natural analogue studies tend to focus on far-field phenomena over geologically significant periods (millions of years). By integrating these two diverse approaches using the appropriate geochemical models, the confident assessment of spent fuel behavior may be possible.

Spent fuel from nuclear reactors is greater than 95 percent UO_2. The most common uranium mineral in nature is uraninite (UO_{2+x}). They are similar both chemically and structurally. Therefore, the study of uraninite and its alteration products provides valuable insight into the long-term behavior of spent fuel in the natural environment. When exposed to oxidizing solutions, spent fuel will oxidize and corrode, and uranyl oxide hydrates will form as corrosion products. The uranyl phases in equilibrium with groundwater will ultimately control the concentration of uranium in solution.

Uranium exists in two valence states in nature; the uranous ion, (U^{4+} or U(IV)) and the uranyl ion (U^{6+} or U(VI)). The chemistries of the two ions are dramatically different, owing to charge and size differences. The uranous ion has a solubility in most aqueous solutions on the order of 10^{-9} mol·kg^{-1}, making uraninite extremely stable in reducing environments. However, Giblin and Appleyard (1987) have shown that significant dissolution of uraninite will occur in saline reducing aqueous environments. The uranyl ion

solubility is potentially much higher, depending on the solution chemistry.

Since World War II, a great deal of study has focused on the uranium-oxygen system. The literature regarding the behavior of spent fuel, especially with respect to nuclear waste disposal is generally restricted to the last two decades. Hoekstra and Siegel (1973) reviewed the UO_3-water system. The uranium-oxygen-water system is further discussed by Smith and others (1982), who also provide an extensive bibliography. An excellent review of spent fuel corrosion studies is provided by Johnson and Shoesmith (1988).

Several reviews are published on the uranium phases found in nature. Frondel (1958) described in detail the uranium minerals known at that time. Since Frondel's work, many new uranyl minerals have been described. The most complete lists of known uranyl minerals currently compiled are Fleischer (1987, 1989) and Smith (1984). Smith (1984) provides descriptions of many uranium minerals not listed in Frondel's (1958) work, as well as providing substantial bibliographic background. Detailed mineralogical descriptions of several uranyl oxide hydrates are provided by Christ and Clark (1960), Deliens (1977), Pagoaga (1983), and Pagoaga and Others (1987). A mineralogical description of the uranyl silicates is given by Stohl and Smith (1981).

URANINITE AND RELATED U(IV) PHASES

Uraninite (UO_{2+x}, $0.01 < x < 0.25$) precipitates as stoichiometric UO_2 in most sedimentary environments (pegmatitic uraninite usually contains thorium and lanthinides, Berman, 1957); however, due to post-depositional oxidation, x is always greater than zero in the formula UO_{2+x} (Langmuir, 1978). Uraninite crystallizes in the cubic system (fluorite structure type, Fm3m; Fig. 1), but as the oxidation state increases, the excess oxygen atoms distort the structure. The limit of oxidation for cubic symmetry has been reported as either

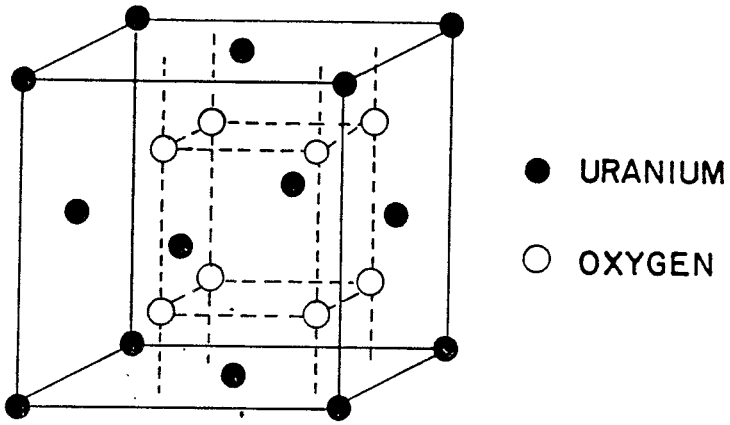

Figure 1 Unit Cell for Uraninite (from Cordfunke, 1969)

$UO_{2.25}$ (U_4O_9; Smith, 1984) or as $UO_{2.33}$ (U_3O_7; Johnson and Shoesmith, 1988). Uraninite probably retains the fluorite structure type until $UO_{2.33}$ (U_3O_7), and the tetragonal phase, α–U_3O_7, represents a distorted fluorite-type structure (Johnson and Shoesmith, 1988). In nature, α–U_3O_7 may only exist as a short-lived phase prior to uraninite dissolution. Although the mechanisms of corrosion of spent UO_2 fuel may differ somewhat from that of unirradiated UO_2 (Thomas *et al.*, 1989; Taylor *et al.*, 1989; Johnson and Shoesmith, 1989; Taylor *et al.*, 1980), the long-term corrosion products of spent fuel should be the same as

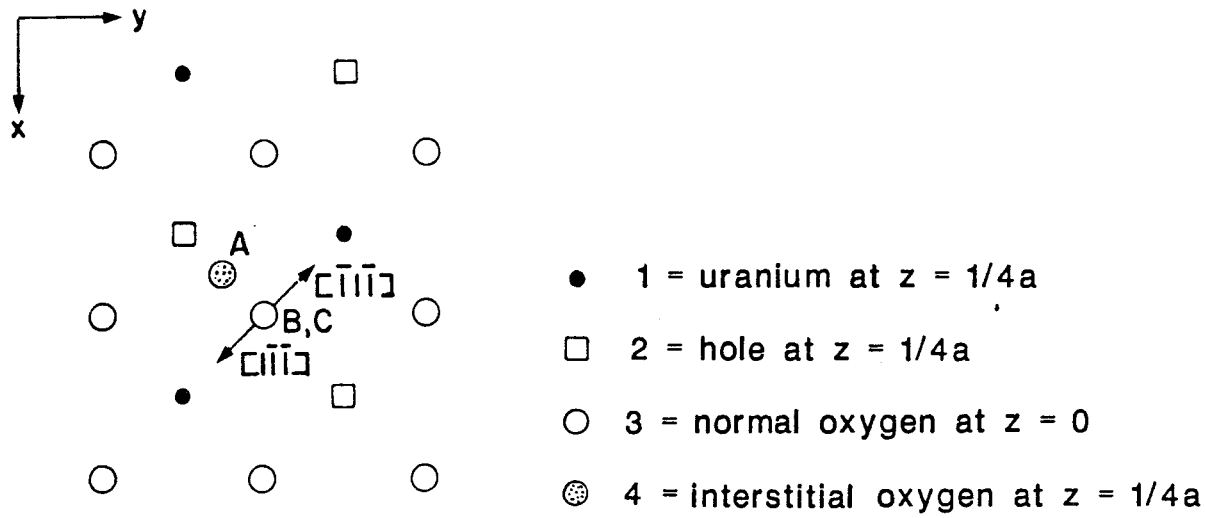

Figure 2 Formation of UO_{2+x}. The interstitial oxygen at A ejects the two nearest oxygen atoms at B and C which are displaced along the <111> direction towards the adjacent holes, which are converted to interstitial oxygens (Cordfunke, 1969; after Willis, 1963).

those reported for weathered uraninite under similar geochemical conditions.

The oxidation of uraninite is due to oxygen diffusion into the cubic unit cell. The excess oxygen enters the unoccupied uranium-equivalent interstices. In so doing, two adjacent close-packed oxygens are displaced to opposite interstices (Willis, 1978; Fig. 2). At the oxidation state $UO_{2.25}$, there is one excess oxygen atom per uraninite unit cell. $UO_{2.25}$ is also non-stoichiometric and is written $UO_{2.25-y}$ (y = 0.0 - 0.02). Oxygen enters a different interstitial site in each of the four adjacent cells in the three crystallographic directions giving rise to a 4a x 4a x 4a superstructure in $UO_{2.25}$ (a = 0.5441 nm; Smith *et al.*, 1982). Based on synthetic studies (Naito, 1974; Belbeoch *et al.*, 1967; Bell, 1961), uraninite consists of two coexisting phases: UO_{2+x} and $UO_{2.25-y}$. The oxidation of uraninite proceeds in a "step-wise" fashion as domains in the structure oxidize from UO_{2+x} to $UO_{2.25-y}$ (Smith *et al.*, 1982). This has significant bearing on the electronic properties of uraninite (and spent fuel) thereby affecting the dissolution mechanisms in oxidizing solutions (Johnson and Shoesmith, 1988). A TEM study of oxidized spent fuel has shown that reaction fronts ($UO_{2+x} \rightarrow UO_{2.25-y}$) for these domains move through the UO_2 grains from grain boundaries inward without the introduction of significant strain-induced defects (Thomas *et al.*, 1989),

except for some shrinkage cracks due to the reduced size of the unit cell for $UO_{2.25-y}$ compared to UO_{2+x}.

Uraninite, as $UO_{2.25}$, is the stable solid phase in contact with moderately oxidizing waters (Fig. 3; Langmuir, 1978) and is the uraninite oxidation state coexisting stably with the uranyl oxide hydrates. Dissolution of uraninite does not proceed until oxidation exceeds $UO_{2.25}$. A virtual barrier to the oxidation of uraninite beyond $UO_{2.25}$ in most moderately oxidizing groundwaters may be due to a kinetic barrier inhibiting the formation of higher oxides. The existence of naturally occurring α-U_3O_7, initially reported from Key Lake in Saskatchewan, Canada (Voultsidis and Clasen, 1978), and subsequently at Cigar Lake, Saskatchewan (Sunder *et al.* 1988) and in the Brousse-Broquiès Basin, Aveyron, France (Pagel *et al.*, 1986) has been questioned recently (J. Janeczek, pers. comm.) and verification

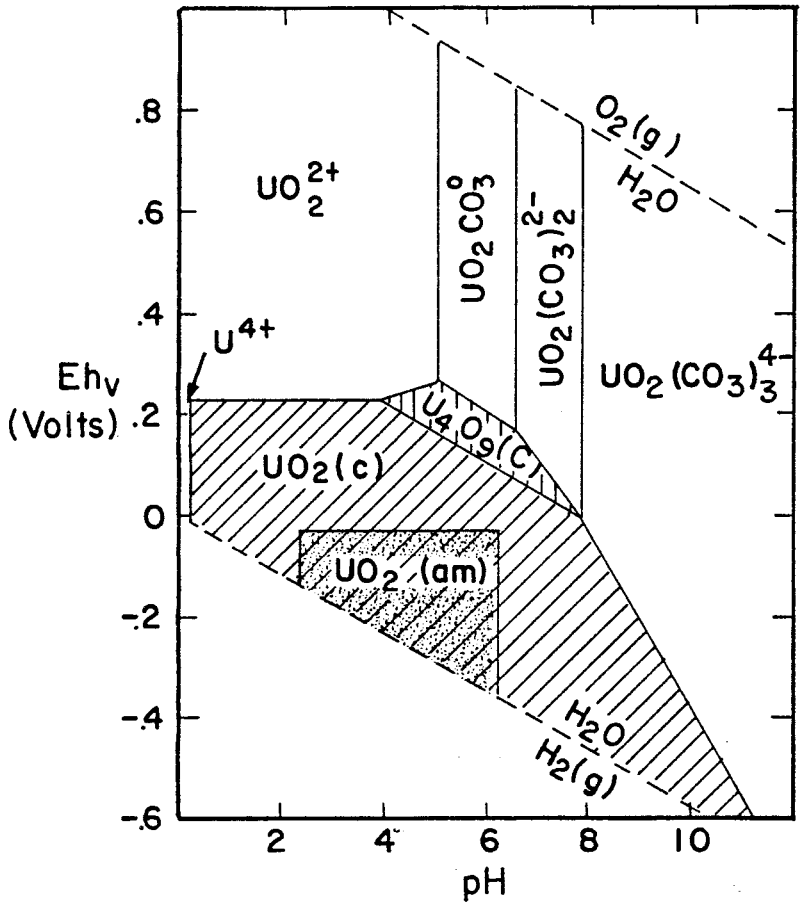

Figure 3 Eh-Ph diagram of the system: U-O_2-CO_2-H_2O at 25°C, P_{CO_2} = 10^{-2}atm. Solid/solution boundaries are drawn at [U] = 10^{-6} mol·kg^{-1}. UO_2(c) = ideal uraninite, UO_2(am) = amorphous UO_2 (Langmuir, 1978)

of this phase in nature requires further study. α-U_3O_7 would exist only in relatively reducing environments (cf. Garisto and Garisto, 1986). The oxidation of unused UO_2 fuel in the presence of water produces β-$UO_{2.33}$ and $UO_{2.67}$ only at elevated temperatures. These are short-lived intermediate phases formed on the surface of the fuel prior to the precipitation of UO_3-hydrates (Taylor *et al.*, 1980). $UO_{2.33}$ is the dissolving phase on the surface of oxidized spent fuel and occurs as a thin layer between the fuel matrix and UO_3-hydrates in contact with the oxidizing solutions (Grambow *et al.*, 1990). The rare mineral ianthinite ($U(UO_2)_5(OH)_{14}\cdot 3H_2O = UO_{2.87}\cdot 10H_2O$, found at such localities as Shinkolobwe, Zaire and Wölsendorf, Germany) is a verified natural example of a partially reduced uranium oxide

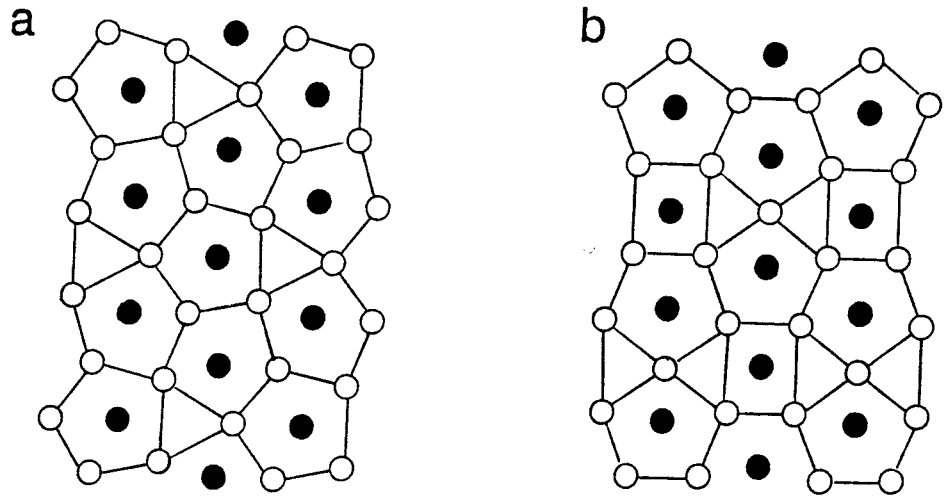

Figure 4 Sheet structures of **a)** α-U_3O_8 and **b)** β-U_3O_8 with coordination polyhedra outlined. Structural oxygens and hydroxyls are represented by open circles. Uranyl groups, $(UO_2)^{2+}$, are represented by filled circles (after Loopstra, 1970).

above $UO_{2.25}$. Ianthinite is a violet mineral; its dark color is due to the presence of U^{4+} in the structure. Occurring with weathered uraninite, ianthinite is found only in isolated vugs in which conditions are locally reducing. However, rather than being produced by the incomplete oxidation of uraninite, ianthinite may be the result of retrograde reduction of schoepite ($UO_3\cdot 2H_2O$) or meta·schoepite ($UO_3\cdot H_2O$) (P. Taylor, pers. comm.). Ianthinite is unstable in air and alters readily to schoepite. No anhydrous oxides above $UO_{2.33}$ have ever been reported in nature.

The phase $UO_{2.67}$ (α-U_3O_8) is orthorhombic (Cmm2). The phase change at $UO_{2.67}$ is reconstructive, and the coordination geometry of uranium changes from 8-coordinated cubic

to a 7-coordinated pentagonal dipyramid. This may be accomplished by the formation of $(UO_2)^{2+}$ at the surface followed by recrystallization of $UO_{2.67}$ (Johnson and Shoesmith, 1988). The structure of $UO_{2.67}$ is based on "sheets" of UO_6 or UO_7 polyhedra. Uranium ions (U^{6+}) are coordinated to six or seven oxygen atoms, two apical oxygens and either four or five equatorial oxygens. The polyhedra share equatorial oxygens to form the sheets. The sheets are, in turn, connected to each other by sharing the apical oxygens of the polyhedra (Fig. 4; Loopstra, 1964, 1970). Many uranyl oxide hydrates are based on this type of sheet structure.

The lack of anhydrous $UO_{2.67}$ in nature is probably due to a kinetic barrier to recrystallization following formation of the $(UO_2)^{2+}$ complex at the uraninite surface in the presence of water. The structural similarity between $UO_{2.67}$ and many uranyl oxide hydrates may provide an easier crystallization path for the uranyl oxide hydrates when $(UO_2)^{2+}$ is present. The $(UO_2)^{2+}$ ion may be adsorbed at the surface, or it may enter into solution, depending on pH and solution composition. If $(UO_2)^{2+}$ is present on the surface, the recrystallization of the higher oxides may occur; but, the presence of complexing ligands such as $(PO_4)^{3-}$, $(CO_3)^{2-}$, $(SO_4)^{2-}$, or $(SiO_4)^{2-}$ will tend to solubilize $(UO_2)^{2+}$ in solution. Even $(OH)^-$ will complex with the uranyl ion when pH is sufficiently high (Langmuir, 1978). Under such circumstances, the solid-state restructuring of uraninite to form anhydrous $UO_{2.67}$ is kinetically unfavorable in the presence of water.

$UO_{2.67}$ is apparently unstable in the presence of water, but liandratite $(U(Nb,Ta)_2O_8)$, an alteration product of petscheckite $(UFe(Nb,Ta)_2O_8)$, reported from a pegmatite in Madagascar (Mucke and Strunz, 1978), is a derivative of the U_3O_8 structure. Apparently, Nb or Ta substitute for the reduced uranium, and the structure is stabilized as an anhydrous phase. Liandratite, while found in uraninite-bearing pegmatites, is not associated with the direct alteration of uraninite. Liandratite has also been reported as an alteration product of Ti-pyrochlore (betafite) from Antanifotsy, Madagascar. Betafite, a pyroclore structure type, is a constituent of crystalline nuclear waste form assemblages (Lumpkin and Ewing, 1987).

Uraninite is commonly deposited as fine-grained aggregates, "pitchblende". Fine-grained material often shows x-ray diffraction line broadening, and this line broadening is characteristic of most natural samples. The fine-grained nature of pitchblende enhances the oxidation of uraninite as well as augmenting the diffusion of cations. Scanning electron microscopy (SEM) and X-ray diffractometry (XRD) indicate that uraninite exposed to oxidizing waters develops micropores (Hofmann, 1989). These micropores increase the effective surface area of the sample enhancing oxidation. Thomas and others (1989) have

shown that oxidation of spent UO_2 fuel occurs by the formation of γ-$UO_{2.25}$ along UO_2 grain boundaries. The reduced unit cell parameter of γ-$UO_{2.25}$ as compared to that for UO_2 leads to the opening of grain boundary cracks as oxidation proceeds. This leads to the embrittlement of the spent fuel as well as increasing potential diffusion pathways for species in solution.

X-ray diffraction patterns obtained from oxidized UO_2 surfaces show significantly increased peak splitting as oxidation proceeds (Taylor *et al.*, 1980; cf. Thomas *et al.*, 1989), and the x-ray diffraction line broadening characteristic of natural samples may be due to peak splitting caused by decreased symmetry as oxidation proceeds, or it may be caused by the separation of diffraction maxima corresponding to the two cubic phases UO_{2+x} and $UO_{2.25-y}$ (J. Janeczek, pers. comm.). Additionally, uraninite compositions listed as more oxidized than $UO_{2.25}$ may be mixtures of uraninite and domains of uranyl oxide hydrates within the structure (Frondel, 1958).

The oxidation potential at the solid-solution interface is of critical importance to the

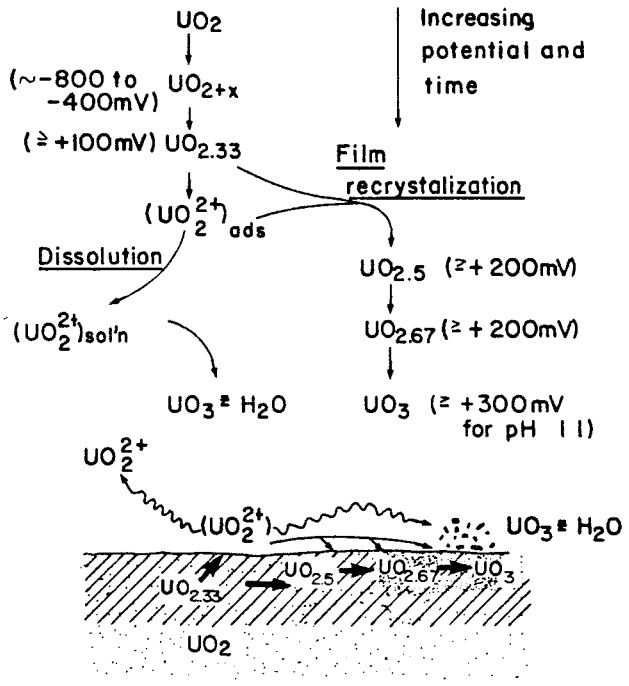

Figure 5 Reaction scheme for the anodic dissolution of UO_2 in neutral pH solutions (Johnson and Shoesmith, 1989).

stability of the anhydrous uranium oxides. The reaction scheme proposed by Johnson and Shoesmith (1989) for the anodic dissolution of UO_2 is presented along with the oxidation potentials for the various oxidation steps in figure 5. The potential required for the oxidation of UO_2 to UO_{2+x} is approximately -0.80 to -0.40 volts. The oxidation of UO_{2+x} to $UO_{2.33}$ requires at least +0.10V. Oxidation of $UO_{2.33}$ to $UO_{2.5}$ requires +0.20V. The potential for oxidation from $UO_{2.5}$ to $UO_{2.67}$ is also approximately +0.20V (the stability range for $UO_{2.5}$ is extremely narrow; it is not observed in nature). The production of UO_3 from $UO_{2.67}$ requires +0.30V (UO_3 is stable only at a pH above 11; Johnson and Shoesmith, 1989). Note that the reaction $UO_{2+x} \rightarrow UO_{2.25}$ would require an oxidation potential between -0.40V and +0.10V. Garisto and Garisto (1986) estimated the oxidation potential for $UO_{2.25}$ production from UO_2 to be approximately -0.15 V (Fig. 6). This is a redox potential found in many natural environments (Fig. 7).

Garisto and Garisto (1986) used thermodynamic data and reaction path calculations to

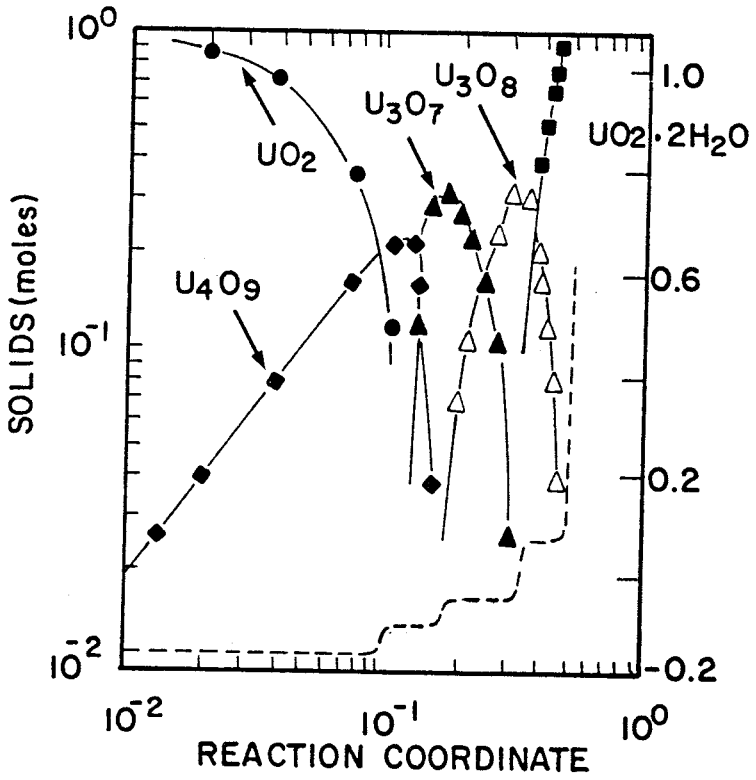

Figure 6 The abundance of solids produced by the oxidation of UO_2 in water as a function of the reaction coordinate (the number of moles of $O_{2(aq)}$ consumed in the reaction). The dashed line represents Eh along the reaction path (T = 298.15°C, pH = 10.5; SHE = standard hydrogen electrode; Garisto and Garisto, 1986).

predict the oxidation of UO_2 under hydrous conditions. While sufficient oxygen is available, UO_2 will oxidize completely to $UO_3 \cdot 2H_2O$. The nominal sequence of phases produced as oxidation proceeds is: $UO_2 \rightarrow UO_{2.25} \rightarrow UO_{2.33} \rightarrow UO_{2.67} \rightarrow UO_3 \cdot 2H_2O$. The higher oxides of uranium coexist with water only if the Eh of the environment remains within a narrow range (Fig. 6). UO_2 and U_4O_9 coexist when the oxidation potential (Eh) is approximately -1.5 volts (with respect to the standard hydrogen electrode; SHE). U_4O_9 and U_3O_7 coexist when Eh = -1.0V. U_3O_7 and U_3O_8 coexist when Eh = -0.5V. U_3O_8 and $UO_3 \cdot 2H_2O$ coexist when Eh = +0.75V. These thermodynamic calculations do not address the kinetics inhibiting uranium oxide formation discussed above.

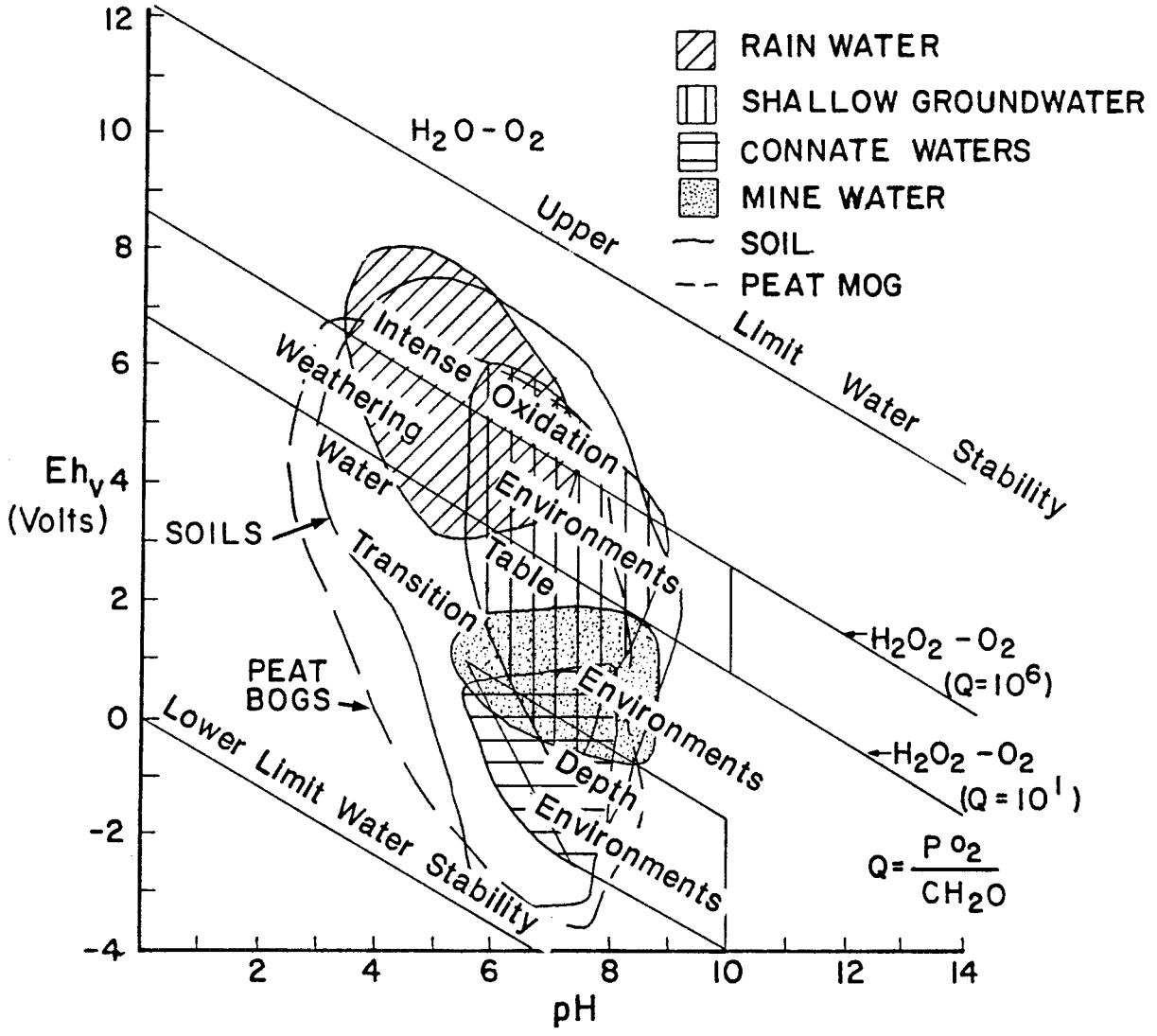

Figure 7 Geochemical environments in terms of Eh and pH (Hansuld, 1967).

Table 1(a) **Solid Formation Sequences at 298.15K in Carbonate Solutions**

pH	Total Carbonate ($mol \cdot kg^{-1}$)	Solid Formation Sequence
10.5	0	$UO_2 \rightarrow U_4O_9 \rightarrow U_3O_7 \rightarrow U_3O_8 \rightarrow UO_3 \cdot 2H_2O$
"	1.61×10^{-2}	$UO_2 \rightarrow U_4O_9 \rightarrow U_3O_7 \rightarrow U_3O_8$
"	8.04×10^{-2}	$UO_2 \rightarrow U_4O_9 \rightarrow U_3O_7$
"	1.74×10^{-1}	$UO_2 \rightarrow U_4O_9$
9.5	0	$UO_2 \rightarrow U_4O_9 \rightarrow U_3O_7 \rightarrow U_3O_8 \rightarrow UO_3 \cdot 2H_2O$
"	1.61×10^{-2}	$UO_2 \rightarrow U_4O_9 \rightarrow U_3O_7 \rightarrow U_3O_8$
"	8.04×10^{-2}	$UO_2 \rightarrow U_4O_9 \rightarrow U_3O_7$
"	1.74×10^{-1}	$UO_2 \rightarrow U_4O_9$
7.0	0	$UO_2 \rightarrow U_4O_9 \rightarrow U_3O_7 \rightarrow U_3O_8 \rightarrow UO_3 \cdot 2H_2O$
"	1.61×10^{-2}	$UO_2 \rightarrow U_4O_9 \rightarrow U_3O_7 \rightarrow U_3O_8 \rightarrow UO_2CO_3$
"	8.04×10^{-2}	$UO_2 \rightarrow U_4O_9 \rightarrow U_3O_7 \rightarrow U_3O_8 \rightarrow UO_2CO_3$
"	1.74×10^{-1}	$UO_2 \rightarrow U_4O_9 \rightarrow U_3O_7 \rightarrow UO_2CO_3$

Table 1(b) **Solid Formation Sequences at 298.15K in Phosphate Solutions**

pH	Total Phosphate ($mol \cdot kg^{-1}$)	Solid Formation Sequence
10.5	0	$UO_2 \rightarrow U_4O_9 \rightarrow U_3O_7 \rightarrow U_3O_8 \rightarrow UO_3 \cdot 2H_2O$
"	1.61×10^{-2}	$UO_2 \rightarrow U_4O_9 \rightarrow U_3O_7 \rightarrow U_3O_8$
"	8.04×10^{-2}	$UO_2 \rightarrow U_4O_9 \rightarrow U_3O_7$
"	2.06×10^{-1}	$UO_2 \rightarrow U_4O_9$
9.5	0	$UO_2 \rightarrow U_4O_9 \rightarrow U_3O_7 \rightarrow U_3O_8 \rightarrow UO_3 \cdot 2H_2O$
"	1.61×10^{-2}	$UO_2 \rightarrow U_4O_9 \rightarrow U_3O_7 \rightarrow U_3O_8$
"	8.04×10^{-2}	$UO_2 \rightarrow U_4O_9 \rightarrow U_3O_7$
"	2.06×10^{-1}	$UO_2 \rightarrow U_4O_9$
7.0	0	$UO_2 \rightarrow U_4O_9 \rightarrow U_3O_7 \rightarrow U_3O_8 \rightarrow UO_3 \cdot 2H_2O$
"	1.61×10^{-2}	UO_2
"	8.04×10^{-2}	UO_2

(Table 1 after Garisto and Garisto, 1986)

Garisto and Garisto (1986) also describe the effects of pH and ligand concentrations (CO_3^{2-} and PO_4^{3-}; table 1). At moderately high ligand concentrations in alkaline waters ($PO_4 = 8.04 \times 10^{-2}$ $mol \cdot kg^{-1}$ at a pH of 10.5, and $PO_4 = 1.61 \times 10^{-2}$ $mol \cdot kg^{-1}$ at a pH of

9.5), the higher oxides did not form. At neutral pH values, even moderate phosphate concentrations (PO_4: 1.61 x 10^{-2} mol·kg^{-1}, pH = 7.0) destabilized the higher oxides relative to dissolved species, and UO_2 goes into solution without the formation of any solids (table 1). The presence of $(CO_3)^{2-}$ in most alkaline waters, also acts to inhibit solid formation at pH values above 8.5, although relatively high carbonate concentrations are required (CO_3 = 8.04 x10^{-2} mol·kg^{-1}, pH = 9.5 and 10.5). This is due to the fact that these ligands solubilize the U(VI) by forming highly stable complexes in solution (Langmuir, 1978). Carbonate solutions at neutral ph (7.0) values did not destabilize the higher oxides, but instead lead to the formation of a uranyl carbonate, UO_2CO_3 (rutherfordine), from U_3O_8.

U(VI) MINERALS

The alteration of uraninite in an aqueous oxidizing environment always produces a variety of uranyl minerals. These are generally microcrystalline and intimately intergrown, making positive identification difficult and often impossible. Hence, these minerals are often ill-defined. During weathering, uraninite crystals undergo progressive oxidation and hydration to produce a suite of uranyl oxide hydrates, alkali and alkaline-earth uranyl oxide hydrates, uranyl silicates, uranyl phosphates, and other less common uranyl minerals. The earliest of these minerals to form are usually the uranyl oxide hydrates in which only uranium is the essential cation in the structure.

Synthetic Uranyl Oxide-Hydrates

Hoekstra and Siegel (1973) reviewed stability relationships in the UO_3-water system for synthetic phases. These offer likely analogues for natural uranyl oxide hydrates. There are five hydroxide/hydrates with uranium as the only essential cation ($UO_3 \cdot 2H_2O$, α–$UO_2(OH)_2$, β-$UO_2(OH)_2$, γ-$UO_2(OH)_2$, and $U_3O_8(OH)_2$). The structural unit of the uranyl hydrates is the 7-coordinated pentagonal dipyramid of the uranyl ion (Evans, 1963), also written as 2-5 coordination (Smith, 1984). These units form sheets of $UO_2(OH)_2$. Hence, the formula for schoepite is more correctly written $UO_2(OH)_2 \cdot H_2O$, and is seen to be a true hydrate with the water occupying sites between the $UO_2(OH)_2$ sheets. Hoekstra and Siegel (1973) did not distinguish between the three polymorphs of $UO_3 \cdot nH_2O$ found in nature (schoepite, meta·schoepite, and para·schoepite; Smith, 1984; Frondel, 1958).

Dehydration of natural schoepite produces a substoichiometric phase designated α-$UO_3 \cdot 0.8H_2O$ which is orthorhombic. The composition is variable up to $UO_3 \cdot H_2O$ ($UO_2(OH)_2$) and is structurally equivalent to the stoichiometric monohydrate (α–$UO_2(OH)_2$) of Taylor and Hurst (1971), with which α-$UO_3 \cdot 0.8H_2O$ likely forms a series (Smith *et al.*, 1982).

An orthorhombic monohydrate, synthesized in sealed capsules at 200°-290°C, is β-$UO_2(OH)_2$. This was prepared by Bannister and Taylor (1970). A monoclinic hydrate, for which no suitable synthesis has been reported, is detected as a second phase in several synthetic studies (Bergstrom and Lundgren, 1956; Cordfunke and Debets, 1964; Wheeler *et al.*, 1964). This phase has been designated γ-$UO_2(OH)_2$, but was not studied by Hoekstra and Siegel (1973).

A triclinic "hemihydrate" ($U_3O_8(OH)_2$ or $3UO_3 \cdot H_2O$) reported by Siegel and co-workers (1972) does not posses a layered structure. Instead, the structure has two distinct uranium atoms. U(1) is in 2-4 (octahedral) coordination and U(2) is in 2-5 (pentagonal dipyramidal) coordination. $U_3O_8(OH)_2$ is synthesized hydrothermally at 300°-400°C (Siegel *et al.*, 1972). The water content has been reported to vary considerably from $UO_3 \cdot 1/3H_2O$ to $UO_3 \cdot 1/2H_2O$ (Urbanec, 1966; Debets and Loopstra, 1963; Blomeke, 1955; Vier, 1944), although no solid solution has been attributed to this phase (Hoekstra and Siegel, 1973). $U_3O_8(OH)_2$ is structurally equivalent to $UO_3 \cdot 1/2H_2O$ (Smith *et al.*, 1982).

A distinctive feature of all the uranyl oxide hydrates discussed by Hoekstra and Siegel (1973) is the persistence of the $(UO_2)^{2+}$ unit in these structures. The U-O(1) (apical oxygen) bond is 0.18 nm (approximately 0.01 nm greater than the U-O bond in the $(UO_2)^{2+}$ complex in solution). The U-O(2) bond (equatorial oxygen) is significantly larger and varies from 0.225 nm to 0.250 nm (Evans, 1963). The coherence of the $(UO_2)^{2+}$ unit in these structures explains the lack of substitution for uranium by elements such as Th and lanthanides, common in pegmatitic uraninite, into the uranyl minerals. For example, Hoekstra and Siegel (1973) report less than 0.05 weight percent La present in schoepite when synthesized using $La(OH)_3$ in solution. The lack of significant Th and lanthanide content in uraninite and coffinite formed by reduction of U^{6+} in low temperature environments (e.g. sandstone-type deposits) is also explained by the markedly different chemistries of the U^{4+} and $(UO_2)^{2+}$ ions in solution. The $(UO_2)^{2+}$ ion has also been reported in a pegmatitic microlite where it occupies a cation site in the microlite structure (Lumpkin *et al.*, 1986)

Natural Uranyl Oxide-Hydrates

The continued alteration of the uranyl oxide hydrates in contact with natural groundwater is accomplished through ion exchange as schoepite (and related phases) alter to the alkali and alkaline-earth uranyl oxide hydrates. These phases form a mèlange of phases surrounding weathered uraninite. The generic term for the generally yellow-orange, fine-grained, waxy rims of corrosion products found on weathered uraninite crystals is "gummite" because of difficulties in distinguishing individual phases. These rims, or alteration haloes, are typically one or two centimeters wide. Frondel (1956) conducted the first comprehensive analysis of alteration haloes on uraninite samples from several localities (Mitchell Co., NC, USA; Jachymov and Johanngeorgenstadt, Czechoslovakia; Kambove

and Luiwishi, Shaba, Zaire; Morogoro, Tanganyika; Alto do Tibiri, Araiba, Brazil; and Cordoba, Argentina). Frondel's survey of these samples showed that gummite consists predominantly of uranyl oxide hydrates, lead-uranyl oxide hydrates, and uranyl silicates. The alteration haloes are often zoned with respect to the dominant anions or cations present. Table 2 lists the zonation as described by Frondel (1956). Appendix A lists the chemical formulas for the known uranyl minerals. Figure 8 illustrates a typical alteration rim around an oxidized uraninite crystal.

The uraninite in the core (zone 1) is usually brown to dark brown or black and commonly veined with the alteration products occurring in zone 2. The composition of uraninite in contact with the zone 2 minerals closely approximates $UO_{2.25}$ (Frondel, 1956, 1958) and generally shows a sharp x-ray diffraction pattern (Fig. 9; Smith *et al.*, 1982, Finch and Ewing, in press). The uraninite in this zone is also commonly hydrated to some degree and it may contain domains of uranyl oxide hydrates within the structure.

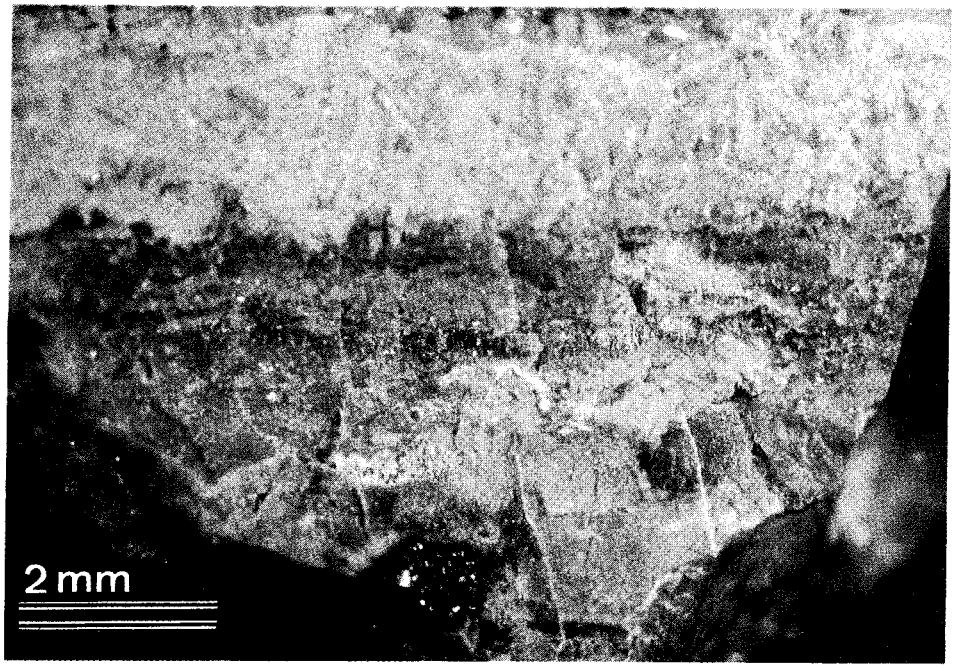

Figure 8 Photomicrograph of typical alteration rim on uraninite. Yellow material is schoepite (top), and orange material is predominantly vandendriesscheite and fourmarierite. Remnant uraninite is evident in bottom center.

Table 2 **Zonation of Uraninite Alteration**

ZONE	MINERALOGY	DOMINANT CATIONS (decreasing order of abundance)
Zone 1 (core)	uraninite	U^{4+}, U^{6+}, Pb
Zone 2	U oxide hydrates	U^{6+}, Pb, Ca, K, Na, Si, Ba
Zone 3	uranyl silicates	U^{6+}, Ca, Si, K, Na, Pb

after Frondel (1956)

The most common minerals in zone 2 are fourmarierite ($Pb[(UO_2)_4O_3(OH)_4]\cdot 4H_2O$), vandendriesscheite ($PbO\cdot 7UO_3\cdot 12H_2O$), wölsendorfite ($(Pb,Ca)O\cdot 2UO_3\cdot 2H_2O$), calciouranoite ($(Ca,Ba,Pb)O\cdot 2UO_3\cdot 5H_2O$), clarkeite ($(Na,Ca,Pb)0\cdot 2U(O,OH)_3$?), becquerelite ($Ca[(UO_2)_6O_4(OH)_6]\cdot 8H_2O$), curite ($Pb_3[(UO_2)_8O_8(OH)_6]\cdot 2H_2O$), and schoepite. Compreignacite ($K_2[(UO_2)_6O_4(OH)_6]\cdot 8H_2O$) is a less common alteration product of uraninite

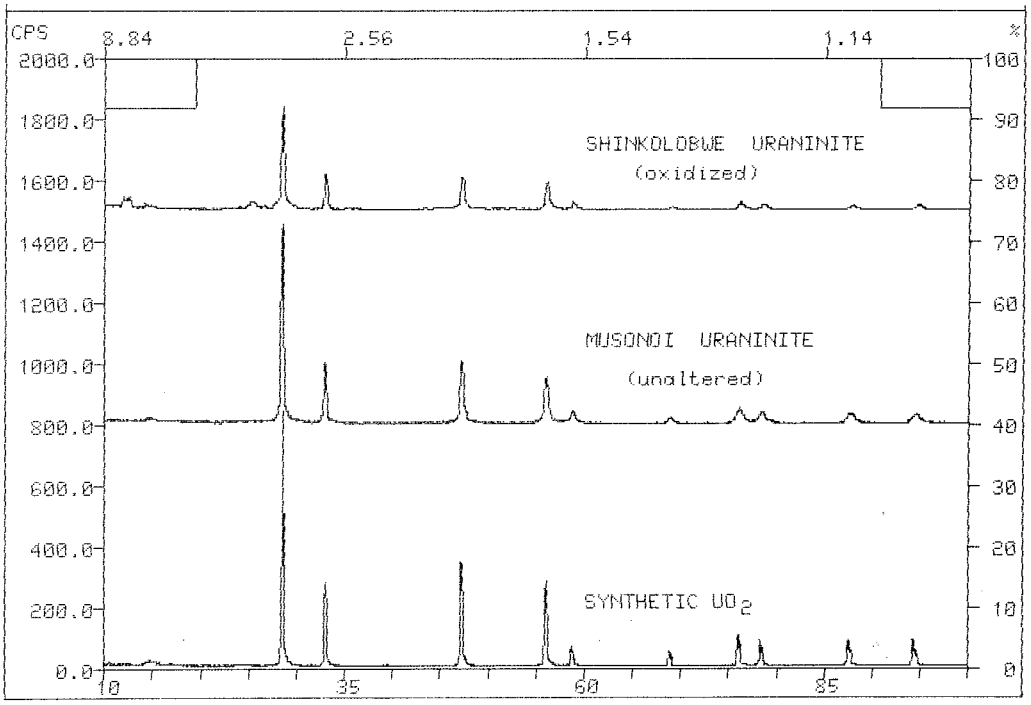

Figure 9 X-ray diffraction patterns of **a**) synthetic UO_2, **b**) unaltered uraninite from the Musonoi mine, Shaba, and **c**) altered uraninite from the Shinkolobwe mine, Shaba, Zaire. Patterns all show sharp diffraction maxima, suggesting a high degree of crystallinity. Extra peak at low 2θ represents a uranyl phase present (schoepite - ?).

described since Frondel's study (Smith, 1984). The lead in the Pb-uranyl oxide hydrates is radiogenic lead derived from the primary uraninite. Lead is enriched in zone 2 minerals with respect to the zone 1 uraninite. All the uranyl oxide hydrates and alkaline and alkaline-earth uranyl oxide hydrates listed in Appendix A are known to occur in contact with primary uraninite undergoing alteration by weathering reactions at various localities (see Appendices A and B).

Zone 3 consists most commonly of uranyl silicates. The most common uranyl silicates in gummite are uranophane and beta-uranophane (both $(H_3O)_2Ca(UO_2)_2(SiO_4)_2{\cdot}3H_2O$). In fact, uranophane is probably the most common uranyl mineral in nature (Smith, 1984). Also reported as constituents of gummite by Frondel (1956), but occurring less commonly, are kasolite ($Pb_2(UO_2)_2(SiO_4)_2{\cdot}2H_2O$), sklodowskite ($(H_3O)_2Mg_2(UO_2)_2(SiO_4)_2{\cdot}4H_2O$), and soddyite ($(UO_2)_2(SiO_4){\cdot}2H_2O$). Cuprosklodowskite ($(H_3O)_2Cu(UO_2)_2(SiO_4)_2{\cdot}4H_2O$) has been reported as a direct alteration product in several copper-bearing localities (Smith, 1984). Additional uranyl silicates are listed in appendix A.

Lead content decreases sharply in zone 3 with respect to the zone 2 minerals. Thorium and lanthinide concentrations decrease from the core outward and are virtually absent from the silicate phases in zone 3 (Smith, 1984; Frondel, 1956). Calcium is the most common cation after lead in zone 2 and is the predominant cation in the zone 3 silicates. Kasolite is the only known Pb-bearing uranyl silicate. Sodium and potassium generally occur as minor constituents in the uranyl oxide hydrates and uranyl silicates except in saline environments (Langmuir, 1978).

Frondel noted that in some cases, the zonation of the uraninite alteration haloes may vary from that listed in table 2. For example, clarkeite may replace the uraninite completely at the core (zone 1), as in some pegmatitic occurrences; or, the uraninite may be pseudomorphously replaced by uranyl silicates, presumably by the alteration of uranyl oxide hydrates formed earlier. The type of alteration associated with gummite formation is consistent with weathering, although late-stage oxidizing hydrothermal fluids have been postulated as a possible mechanism of alteration in some deposits. For example, clarkeite and other (unspecified) uranyl oxide hydrates replace uraninite in fresh, unweathered pegmatite at Spruce Pine, Mitchell Co., NC (Ross *et al.*, 1931).

Other minerals found in the samples studied by Frondel include rutherfordine (UO_2CO_3) from a pegmatite in Morogoro, Tanganyika, in which the rutherfordine surrounds the zone 2 oxide-hydrates and is admixed with uranophane and kasolite. Similar occur-

rences of rutherfordine are at Newry, Maine, USA and Beryl Mountain, New Hampshire, USA. Phosphuranylite ($(H_3O)_2Ca(UO_2)_3(PO_4)_2(OH)_4 \cdot 4H_2O$) was described by Frondel from pegmatites at Spruce Pine, Mitchell Co., NC, USA and at the Ruggles mine, Grafton Center, NH, USA, in which the phosphuranylite occurs with uranophane on the surface of altered uraninite crystals.

The uranyl minerals discussed above constitute only a small portion of the known uranyl minerals (more than 160 have been described). With the occasional exception of the uranyl phosphates, most uranyl minerals are not found as constituents of the alteration haloes surrounding oxidized uraninite, but instead usually occur remote from the uraninite and commonly as large (up to cm-sized), euhedral crystals. Many uranyl minerals occur as powdery coatings in cavities or efflorescences on mine adit walls or at the surface where evaporation may be high. The uranyl minerals discussed below are organized according to their structural similarities and their dominant oxyanion groups.

The uranyl carbonates and sulfates are extremely soluble (Langmuir, 1978), and their presence usually indicates arid conditions and/or high alkalinities (Fig. 10). These minerals are stable only in the absence of substantial V, P, or As. Rutherfordine (UO_2CO_3) and schroeckengerite ($NaCa_3(UO_2)(CO_3)_3(SO_4)F \cdot 10H_2O$) are the most common uranyl carbonates and frequently occur in contact with uraninite or uranyl oxide hydrates as powdery coatings. Other carbonates associated with uranium ore are liebigite ($Ca_2(UO_2)(CO_3)_3 \cdot 11H_2O$), voglite ($Ca_2Cu(UO_2)(CO_3)_4 \cdot 6H_2O$), bayleyite

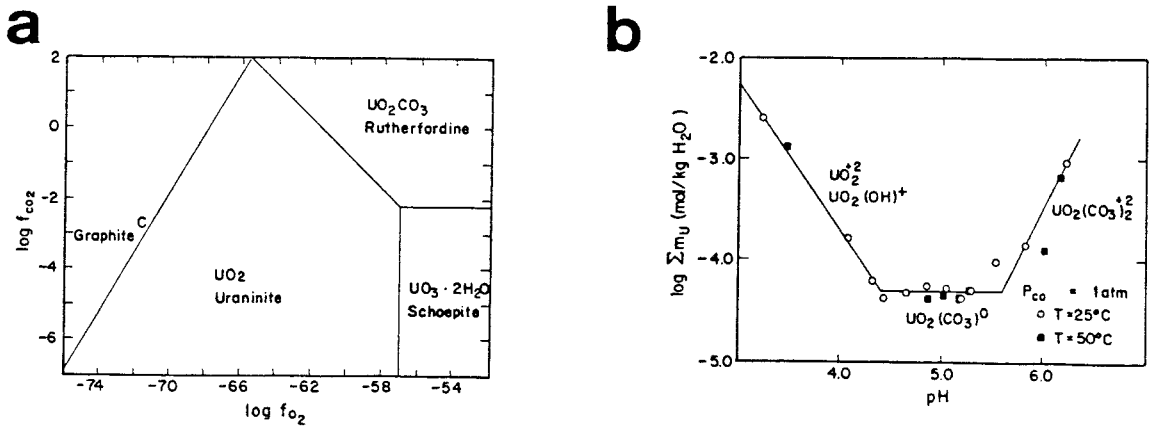

Figure 10 Uranium-carbonate solutions. **a)** Log fO_2-log fCO_2 diagram for relevant solid phases in the system U-O-C-H at 25°C. **b)** Uranium concentration as a function of pH in solutions saturated with respect to rutherfordine (UO_2CO_3) at 25°C, PCO_2 = 1 atm (Sergeyeva *et al.*, 1972).

($Mg_2(UO_2)(CO_3)_3 \cdot 18H_2O$), and andersonite ($Na_2Ca((UO_2)(CO_3)_3 \cdot 6H_2O$). Johannite ($Cu(UO_2)_2(SO_4)_2(OH)_2 \cdot 8H_2O$) and the zippeite group (e.g. $K_4(UO_2)_6(SO_4)_3(OH)_{10} \cdot 16H_2O$) are generally associated with uranium ore bodies, but almost exclusively as efflorescences on mine adit walls. The rare mineral roubaultite ($Cu_2(UO_2)_3(CO_3)_2O_2(OH)_2 \cdot 4H_2O$) was originally described as a uranyl oxide hydrate. The uranyl sulfates, though widespread, rarely occur in significant quantities.

The vanadates are the least soluble of the complex uranyl oxides. According to Langmuir (1978), carnotite ($K_2(UO_2)_2(VO_4)_2 \cdot 8H_2O$) is the stable phase in contact with $UO_{2.25}$ over a wide range of intermediate pH values when groundwater vanadium and uranium concentrations both exceed 10^{-6} mol·kg^{-1} (Fig. 11). Carnotite, however, is not reported as a pseudomorphous replacement product of uraninite in nature. Instead, carnotite usually occurs far removed from U(IV) mineralization, usually at the surface. Tyuyamunite ($Ca(UO_2)_2(VO_4)_2 \cdot 8H_2O$) and meta·tyuyamunite ($Ca(UO_2)_2(VO_4)_2 \cdot 3\text{-}5H_2O$) are commonly associated with oxidation of a uranium ore body (perhaps due to the presence of Ca in the structure), but neither of these two minerals has been reported pseudomorphously replacing

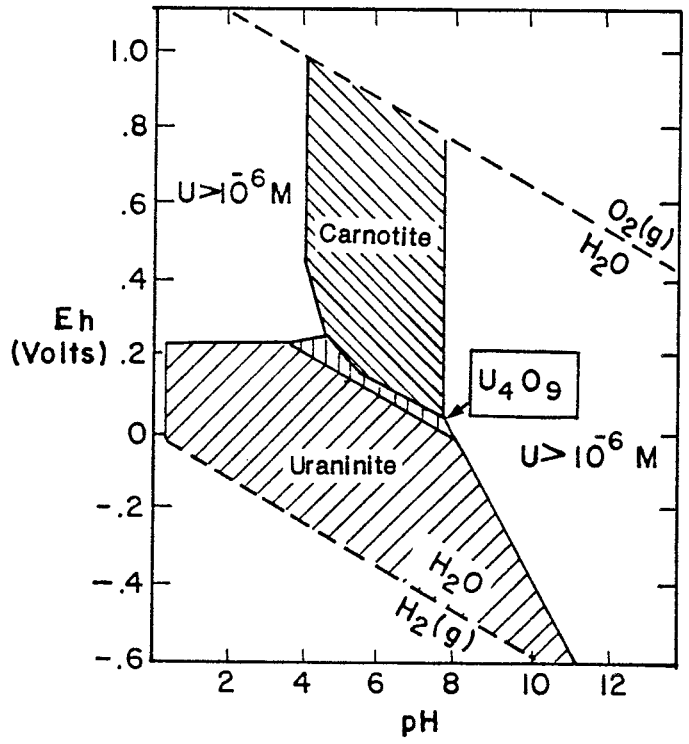

Figure 11 Eh-pH diagram showing stable solid phases for the system K-U-V-O_2-H_2O-CO_2 at 25°C. Solid/solution boundaries drawn for [U] = 10^{-6} mol·kg^{-1}, [K] = 10^{-13} mol·kg, [V] = 10^{-6} mol·kg^{-1}, P_{CO_2} = 10^{-2}atm (Langmuir, 1978).

uraninite either.

The uranyl phosphates are an important group of uranium minerals. Langmuir (1978) indicates that these are only moderately soluble and should be stable in the absence of any significant vanadium concentrations (< 10^{-6} mol·kg^{-1}). Garisto and Garisto (1986) also predict the presence of Na-autunite in contact with uraninite (Fig. 12) over a broad range of Eh-pH values. Several uranyl phosphates have been reported with uraninite and are common constituents of the outermost zone of the alteration haloes known as gummite. Common uranyl phosphates occurring in close proximity to uraninite are torbernite and meta·torbernite, autunite and meta·autunite ($Ca(UO_2)_2(PO_4)_2$•$6H_2O$), salèeite ($Mg(UO_2)_2(PO_4)_2$•$10H_2O$), uranospathite ($Ca(UO_2)_2(PO_4)_4$•$40H_2O$), sabugalite ($HAl(UO_2)_4(PO_4)_4$•$16H_2O$), phosphuranylite ($(H_3O)_2Ca(UO_2)_3(PO_4)_2(OH)_4$•$4H_2O$), and parsonsite ($Pb(UO_2)(PO_4)_2$•$nH_2O$).

The uranyl arsenates, like the uranyl phosphates, are insoluble and tend to occur under conditions similar to those of uranyl phosphate formation, although they are much less common than the uranyl phosphates. Additionally, many uranyl phosphates and uranyl

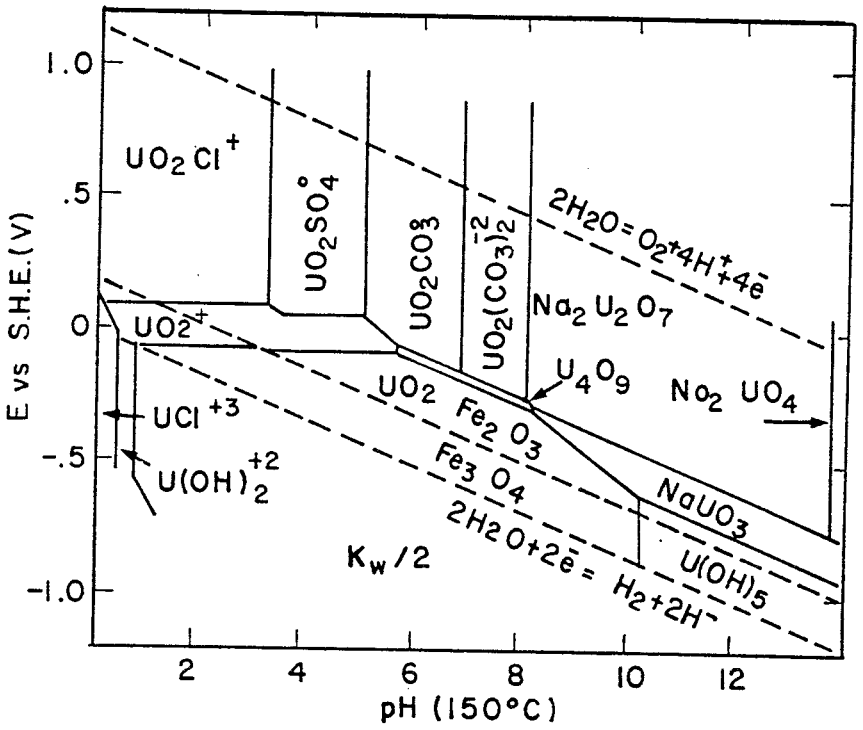

Figure 12 Eh-pH diagram showing stable solid phases for the system Na-U-P-O_2-H_2O. [PO_4] = 10^{-6} mol·kg^{-1}, [Na] = 1.0 mol·kg^{-1}. The composition $Na_2U_2O_7$ has been removed from the calculations (Garisto and Garisto, 1986).

arsenates form solid solutions between end-member compositions (see Appendix A). Though thought to form most commonly by precipitation from uranium-rich groundwaters, the paragenesis of the uranyl arsenates is not well understood. For example, troegerite ($UO_2(UO_2)_2(AsO_4)_2 \cdot 8H_2O$)) has been reported with uraninite in the Bald Mountains mining district, South Dakota, USA, but the exact nature of the relationship is unclear (Dana, 1892).

The uranyl molybdates are relatively rare and are not well researched. The uranous and uranyl molybdates are potential solid phases in a spent fuel repository because Mo is a fission product of uranium. Uranium and molybdenum commonly coexist in nature, especially in sandstone-hosted roll-front ore bodies. Moluranite ($H_4U^{4+}(UO_2)_3(MoO_4)_7 \cdot 18H_2O$), is a uranous/uranyl molybdate reported from a granulated albitite in the U.S.S.R. (Epstein, 1959). Moluranite is either amorphous or metamict. Umohoite ($UO_2MoO_2(OH)_4 \cdot 2H_2O$), a poorly characterized phase (despite several x-ray studies, see Smith, 1984) has been reported at Shinkolobwe, Katanga, Zaire (Piret and Deliens, 1976), Marysvale, Utah, USA (Brophy and Kerr, 1953), and several sandstone deposits (Coleman and Appleman, 1957). Umohoite occurs at the edge of the oxidized zone and is probably one of the first oxidized compounds to form when Mo is present (Smith, 1984). Umohoite is often difficult to identify due to its dark color and the fact that it is intergrown with uraninite and other reduced uranium minerals. Umohoite may be quite common as an alteration product of uraninite (Smith, 1984).

Because of their potential importance in a geologic repository exposed to oxygenated groundwaters, some minerals deserve special note. Several minerals contain both reduced and oxidized uranium, possibly due to incomplete oxidation. These partially reduced phases may be especially important under reducing conditions expected in a spent fuel repository. Ianthinite ($UO_2 \cdot 5UO_3 \cdot 10H_2O$) is a rare mineral found in contact with uraninite, reported at Shinkolobwe, Zaire; Wölsendorf, Germany; Bigay, France; La Crouzille, France; and Bois Noir, France. Ianthinite was discussed in the previous section on U(IV) minerals. Wyartite ($Ca_3U^{4+}(UO_2)_6(CO_3)_2(OH)_{18} \cdot 3\text{-}5H_2O$), a rare mineral, is reported from Katanga, Zaire (Guillemin and Protas, 1959) where it had been mistaken for ianthinite. Wyartite occurs in several hydration states with resultant variations in the x-ray diffraction pattern. Clark (1960) verified two forms of wyartite. Moluranite ($H_4U^{4+}(UO_2)_3(MoO_4)_7 \cdot 18H_2O$) is only reported from a single locality and contains both reduced and oxidized uranium (Epstein, 1959).

Clarkeite is found as an alteration product of pegmatitic uraninite. Although chemically similar to wölsendorfite and calciouranoite, clarkeite can incorporate Th, Na, and lanthanides into its structure. Clarkeite may be formed due to the reaction of late-stage hydrothermal solutions with primary uraninite (Ross *et al.*, 1931). Clarkeite has not been reported from uraninite localities undergoing normal weathering reactions. The relatively high temperatures and high salinities of hydrothermal solutions may be required for the formation of clarkeite. Clarkeite is poorly characterized, but Gruner (1954) demonstrated that it is structurally similar to $Na_2U_2O_7$. Thomas and Till (1984) postulate that a sodium uranyl oxide ($NaUO_3$ or $Na_2U_2O_7$) is the solubility controlling phase in dissolution experiments on UO_2 fuel pellets exposed to granite groundwater (the granite groundwater is reported to be representative of typical groundwater in the Canadian Shield; the composition is not given).

Studtite ($UO_4 \cdot 4H_2O$) and meta·studtite ($UO_4 \cdot 2H_2O$), first reported at Shinkolobwe, Zaire (Walenta, 1974; Deliens and Piret, 1983), are rare minerals indicative of highly oxidizing conditions. Studtite and meta·studtite are the only known natural peroxide minerals (Walenta, 1974). Debets (1963) synthetically prepared studtite and meta·studtite prior to reports of their natural occurrences. Studtite dehydrates irreversibly to produce meta·studtite. The presence of uranium peroxides may be due to the production of highly oxidizing phases (e.g. H_2O_2, HO_2, O_2-) by the radiolysis of water. Radiolysis has been proposed as a potentially important source of locally oxidizing conditions at the UO_2-water interface in spent fuel studies (Sunder *et al.*, 1989; Johnson and Shoesmith, 1988; Means *et al.*, 1987; Forsyth et *al.*, 1986; Bailey *et al.*, 1985; Nichol and Needes, 1975, 1977).

The stability of the uranyl minerals in an oxidizing environment is important to understanding the potential behavior of uranium near a spent fuel reposiory breached by oxidizing groundwater. The formation sequence of minerals and their genetic relationships among one another are collectively known as their paragenesis. The phase relationships observed in nature are a manifestation of the paragenesis of those phases.

Deliens (1977) described uranium mineral relationships from the Shinkolobwe mine in Shaba, Zaire. Several minerals described by him were unknown prior to his study. Deliens used a "spider" diagram to illustrate the mineral associations at Shinkolobwe (Fig. 13). Uraninite is associated directly with the uranyl oxide hydrates: schoepite, ianthinite, and studtite ($UO_4 \cdot 4H_2O$); the alkali oxide hydrates: becquerelite, masuyite, fourmarierite, vandendriesscheite, wyartite, curite and billietite; the carbonates: wyartite and rutherfordine; and the silicate uranophane (epi-ianthinite has since been shown to be equivalent to

schoepite; Smith, 1984). The most common uranyl mineral associations with uraninite (> 80%) are schoepite, fourmarierite, vandendriesscheite, masuyite, and wyartite. If interpreted as a paragenetic description, curite (associated with becquerelite, uraninite and, most commonly, with schoepite) appears to be the precursor to all the phosphates and to the silicates kasolite and soddyite. Curite can be synthetically transformed into the phosphates meta·autunite and meta·torbernite (Vochten and Deliens, 1980; Vochten *et al.*, 1979).

In nature, schoepite always coexists with the alkali and alkaline-earth uranyl oxide hydrates, and schoepite alters readily to these phases, depending on groundwater chemistry. Vochten (1990) synthesized several alkaline-earth uranyl oxide hydrates by the reaction of alkaline-earth-bearing solutions. The phases synthesized by Vochten were: $CaO{\cdot}6UO_3{\cdot}11H_2O$ (= becquerelite); $BaO{\cdot}6UO_3{\cdot}11H_2O$ (= billietite); $PbO{\cdot}2UO_3{\cdot}2H_2O$ (= wölsendorfite); $MgO{\cdot}6UO_3{\cdot}13H_2O$; $NiO{\cdot}3UO_3{\cdot}6H_2O$. Only the first three species are known to occur in nature. In addition to cation exchange, dehydration is an important

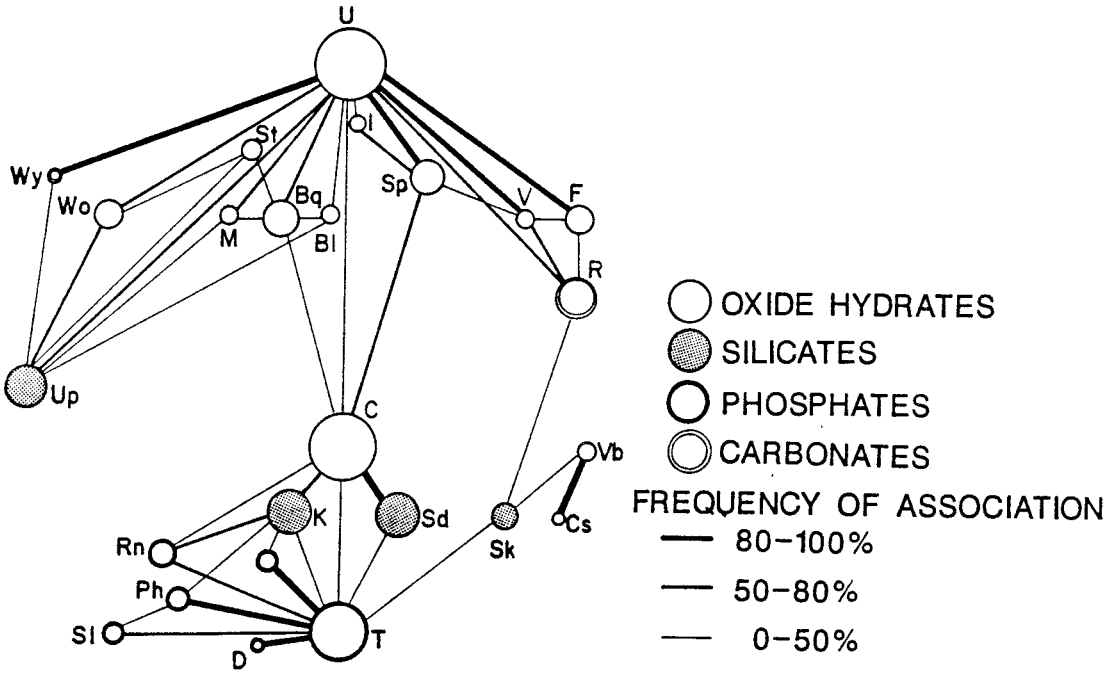

Figure 13 Observed uranium mineral associations at the Shinkolobwe mine, Shaba, Zaire (Deliens, 1977) **U** = uraninite, **I** = ianthinite, **Sp** = schoepite, **St** = studtite, **Wo** = wölsendorfite, **M** = masuyite, **Bq** = becquerelite, **Bl** = billietite, **V** = vandendriesscheite, **F** = fourmarierite, **R** = rutherfordine, **Up** = uranophane, **C** = curite, **K** = kasolite, **Sd** = soddyite, **Sk** = sklodowskite, **Vb** = vandenbrandeite, **Cs** = cuprosklodowskite, **Rn** = renardite, **Pr** = parsonsite, **Ph** = phosphuranylite, **Sl** = saleeite, **T** = torbernite, **D** = dumontite

mechanism for alteration of these phases. Water may be lost most easily by the ejection of interlayer water molecules. Two possible formation sequences are postulated by Finch and Ewing (in press) to explain the phase associations observed in nature. The general formula for the alkaline-earth uranyl oxide hydrates is:

$$M_x[(UO_2)_6O_{2+2x}(OH)_{8-2x}\bullet(8\text{-}n)H_2O \quad (x = 0,1,2,3,\cdots;\ n = 0,1,2,3,\cdots)$$

And the formula for the Pb-bearing uranyl oxide hydrates is:

$$Pb_x[(UO_2)_{6+x}O_{2+2x+m}(OH)_{8-2m}\bullet(8+m\text{-}n)H_2O \quad (x = 0,1,2,3,\cdots;\ n = 0,1,2,3,\cdots;\ m = 0,1,2)$$

As *n* increases, interlayer water is lost and *m* depends on the type of sheet structure (higher values of m correspond to decreasing states of hydration within the structural sheets). As x increases, the pH increases. By plotting phase compositions for the uranyl oxide hydrates on a ternary diagram with the apices H_2O-UO_3-MO (M = Ca, Pb, Ba, K_2, and other exchangeable cations) the compositions of the known uranyl oxide hydrates are seen

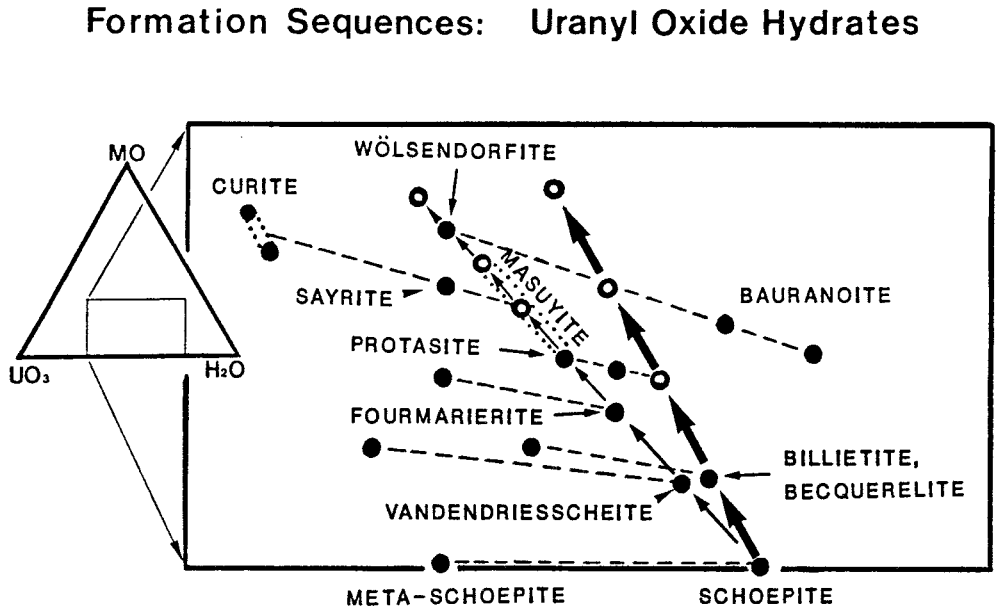

Figure 14 Portion of ternary diagram with apices MO-H_2O-UO_3 showing reaction paths for the uranyl oxide hydrates (Finch and Ewing, *in press.*).
● Known compositions ○ Unknown compositions ⋯⋯ compositional ranges
→ Pb-uranyl minerals ➡ Alkaline-earth minerals - - - - dehydration reactions

to plot on compositions predicted by these two formation sequences (Fig. 14). The formation sequence of the alkali and alkaline-earth uranyl oxide hydrates from schoepite can follow several potential paths depending on the availability of exchangeable cations. In most ancient uranium deposits, radiogenic lead is abundant, and the Pb-uranyl oxide hydrates are expected. Ca is also common in most groundwaters, and becquerelite and calciouranoite may be expected. Among any series (e.g. Pb-bearing phases or Ca-bearing phases), the stable phase will depend largely on the groundwater pH, although kinetics may govern short-term phase formation.

Based on observations in nature, the uranyl phosphates perform a crucial role as the long-term solubility-controlling phases for uranium near an oxidized uranium ore body. The paragenesis of the uranyl phosphates may be important in understanding the long-term behavior of uranium around a repository exposed to oxygenated groundwater. Yet, the parameters governing uranyl phosphate formation are poorly understood. Langmuir (1978) has shown that uranophane should be unstable with respect to K-autunite ($K_2(UO_2)_2(PO_4)_2 \cdot 8\text{-}12H_2O$) and carnotite when P or V are present in concentrations common in most groundwaters. Langmuir estimated the stability field of uranophane empirically by using measured groundwater compositions in contact with uranophane (the solubility minimum occurs at 120 ppm SiO_2, pH = 8.5). The oxidation potential is also important, and the uranyl phosphates are stable at higher oxidation potentials than the uranyl silicates. The apparent lack of uranyl phosphates or uranyl vanadates as pseudomorphous alteration products of weathered uraninite indicates that at lower oxidation potentials the uranyl phosphates and vanadates are not stable with respect to uranophane, or perhaps their formation is inhibited by kinetic factors. Modelling the precipitation of uranyl phosphates such as salèeite from solution requires anomalously high concentrations of U and P (Sverjensky, 1990). Langmuir (1978) used thermodynamic data for anhydrous solids, and this may be a source of error. In fact, autunite has been reported to precipitate when groundwater uranium concentrations are low (approx. 10^{-9} mol·kg^{-1}; Dall'aglio *et al.*, 1974). The observation that uranyl phosphates within oxidized uranium ore bodies are commonly associated with curite suggests an important paragenetic relationship between curite and the uranyl phosphates (see Deliens, 1977; Vochten *et al.*, 1979; Vochten and Deliens, 1980). The potential role of curite as a "catalyst" for overcoming a possible kinetic barrier to uranyl phosphate formation is a factor not addressed in geochemical models. Further study of the paragenesis of the uranyl phosphates is needed.

RADIATION EFFECTS

Uraninite contains approximately 88 percent uranium in its structure. The dominant radiation effects are structural damage caused by the alpha-recoil nucleus, and the radiolysis of the water by the production of reactive oxidants at the uraninite/water interface.

Alpha Recoil Damage

The spontaneous decay of a radionuclide during an alpha-decay event produces an alpha particle (^{4}He nucleus, 4.5 - 5.0 MeV) and an alpha recoil nucleus (0.07 MeV). Though the range of the recoil nucleus (10 nm) is much shorter than that of the alpha particle (10^4 nm), the atomic displacements caused by the recoil nucleus are much greater than that of the alpha particle (on the order of 1500 displacements per event; Weber *et al.*, 1982; Eyal and Fleischer, 1985). The alpha particle loses most of its energy through ionization events and electronic excitations. High cumulative doses can render a crystalline structure x-ray diffraction amorphous. Structural damage in minerals is often recovered through natural annealing of the recoil tracks in the mineral. The final effect of alpha-decay damage varies among different minerals due to variations in natural annealing rates (Lumpkin and Ewing, 1989).

Uraninite remains crystalline, despite high alpha-decay doses ($>10^{27}$ alpha-decay events$\cdot$m^{-3}) due to relatively rapid annealing rates (Lumpkin and Ewing, 1989). Uraninites do show significant evidence of radiation-induced structural damage (Stout *et al.*, 1988). Annealing natural samples by heat treatment above 800°C will decrease structural damage (Stout *et al.*, 1988; Berner, 1956).

The long-term effect of radiation damage on the structure of uraninite is not well understood. The presence of structurally damaged areas may increase dissolution rates and cause selective leaching of radionuclides (Fleischer, 1988; Eyal and Fleischer, 1985). However, the rapid annealing of damaged areas in natural samples may help to offset this effect.

Alpha Radiolysis of Water

Another possible effect of radiation from UO_2 in contact with groundwater is the production of oxidizing species (e.g. H_2O_2, O_2^-, HO_2) from the radiolysis of water at the surface. The production of oxidizing species could raise the local oxidizing potential at the surface well above the bulk solution. Alpha particles are the most effective ionizing particles (Burns and Sims, 1981), and produce relatively high yields of radiolysis products (Bailey *et al.*, 1985). The oxidation potential can be raised to +0.70 V within about 30 mm of the alpha source, but falls off to an ambient potential at 70 mm (Shoesmith *et al.*, 1989; Bailey *et al.*, 1985).

Numerous authors have addressed the subject of radiolysis on the dissolution of spent fuel (e.g. Sunder *et al.*, 1989; Sunder *et al.*, 1987; Christensen and Bjerbakke, 1987; Forsyth *et al., 1986*). Experimental results indicate that the effect of alpha and gamma radiolysis on the dissolution of spent UO_2 fuel in reducing aqueous solutions is not significant (Sunder *et al.*, 1989; Forsyth *et al.*, 1986). The production of oxidizing reactants by radiolysis is accompanied by the production of an equal number of reducing species. The overall effect of radiolysis therefore depends on the relative reactivity of the reactants in the solution of interest. For instance, oxidation by H_2O_2 depends on the pH and the concentration of H_2O_2 ($<10^{-9}$ mol·kg^{-1}; Sunder *et al.*, 1987), whereas H_2 is expected to be relatively inert. The presence of reducing conditions away from the alpha source may also limit the effective overall solubility, although the reprecipitation of reduced uranium phases would be fine-grained, making them susceptible to subsequent attack by the solution. The production of radicals by radiolysis proceeds faster than the rate of change in the corrosion potential on the spent fuel surface, indicating that another, slower reaction, is corrosion rate controlling (Sunder *et al.*, 1989). The rate controlling step may be the breaking of the O-O bond in adsorbed oxygen (Posey-Dowty *et al.*, 1988) if this is the predominant species participating in the oxidative dissolution of UO_2. No studies known to this author address the significance of radiolysis on uraninite. However, the presence of the uranium peroxides studtite and meta·studtite may indicate the existence of highly oxidizing conditions resulting from the radiolysis of water in nature.

NATURAL UO_{2+X} AS AN ANALOGUE FOR SPENT FUEL

The corrosion of spent UO_2 fuel in a geologic repository should be similar to the natural alteration of uraninite because of their similar structures and chemistries. The literature on uranium chemistry is voluminous, but relatively little is directly applicable to understanding the behavior of spent fuel in a geologic repository. Many early studies on uraninite dissolution were conducted for the purpose of concentrating uranium from uranium ore under conditions unlikely to be found in a repository. Numerous studies have also been conducted on the corrosion of synthetic UO_2, unused fuel, and spent fuel under various conditions ranging from strongly oxidizing to strongly reducing in water chemistries ranging from deionized water to concentrated brines. More recently, efforts to model UO_2 dissolution under conditions expected in a spent fuel repository (e.g. using synthetic groundwaters) have increased. However, the focus of such studies is primarily on solution chemistry. The identification and characterization of solubility-controlling secondary phases, such as surface films or colloidal particles, has received detailed study only in the last few years. Unfortunately, the restrictions imposed by conducting experiments in a hot cell make detailed analysis of material difficult. Also, the duration of any laboratory study (as long as 8-10 years) is miniscule compared to the geologic time periods required for long-term waste disposal (>10,000 years). Phases precipitated on a UO_2 surface exposed to water for several months, or even years, may not represent a true equilibrium phase assemblage.

In contrast to laboratory studies, there is a substantial amount of literature describing uranium-bearing solid phases which have been present for thousands or millions of years and which occur in a wide range of geologic settings. However, the emphasis has often been on the cursory identification of minerals for the purpose of ore exploration, and uranyl phases at some localities have been identified simply as "bright yellow and green minerals". Data on groundwater chemistries associated with the formation of the alteration products is virtually absent. Indeed, characterizing groundwater compositions is of only minor (or no) interest to the exploration geologist. Additionally, the characterization of current groundwater chemistry in an ore body may provide little insight into the conditions prevailing at the time of ore formation or alteration. The complexity of natural systems, and the spatial and temporal variability of groundwater compositions make unambiguous interpretation of such data difficult or impossible. Water-rock interactions may cause variations in solution composition by orders of magnitude over small distances (< 1 m). Furthermore, the crystal structures, crystal chemistry, thermodynamic stabilities, and the paragenesis of most uranium minerals are not well understood, as discussed in previous

sections. The stability and evolution of uranyl phases, however, will have significant impact on the long-term behavior of a spent fuel repository.

Still, with all the stated difficulties, the alteration of uraninite in a large-scale, hydrologically complex system over long periods perhaps provides the best picture of the state of spent fuel after thousands of years of storage and exposure to flowing groundwater. Public perception of predictions concerning the behavior of spent fuel as a waste form will rest in part on the ability to understand the behavior of uranium in the natural geochemical environment. The current research program attempts to bridge the gap between the observed alteration phases associated with uraninite and the evolution of solution chemistries associated with the corrosion of spent fuel. The next section outlines some important laboratory studies on the corrosion of synthetic UO_2 and UO_2 fuel, followed by a summary of on-going natural analogue studies.

Laboratory Studies

Nicol and Needes (1975, 1977) conducted dissolution experiments using UO_{2+x} electrodes (x = 0.01, 0.03, 0.14) in perchlorate (two solutions: 1] $HClO_4$ = 1.0 mol·kg^{-1} and 2] $NaClO_4$ = 1.0 mol·kg^{-1} with $HClO_4$ = 0.1 mol·kg^{-1}) and carbonate solutions (two solutions: 1] Na_2CO_3 = 0.4 mol·kg^{-1} and 2] Na_2CO_3 = 0.4 mol·kg^{-1} with Na_2SO_4 = 0.4 mol·kg^{-1}) at 25°C. Potentiostatic measurements in the perchlorate solutions indicate that at low pH (< 2.0), no evidence of a U(VI) layer is found. At higher pH values (up to pH = 5.0), the electric potential is independent of pH, indicating the formation of an insulating U(VI) layer. The phase produced under these conditions is either $UO_2(OH)_2$ or UO_3. Carbonate solutions (pH = 9.8) showed no evidence of a surface layer until moderately high carbonate concentrations. The solid phase formed in a solution of Na_2CO_3 with Na_2SO_4 is UO_2CO_3 (rutherfordine); whereas the solid phase formed in a solution containing only Na_2CO_3 is amorphous UO_3 rather than a carbonate solid.

Taylor and others (1980) studied surface oxidation of UO_2 pellets using x-ray diffraction. Polished UO_2 pellets were exposed to air at temperatures ranging from 175°C to 325°C. β-$UO_{2.33}$ is a significant intermediate oxidation product formed at the surface. The oxidation reaction $UO_2 \rightarrow \beta$-$UO_{2.33}$ was monitored to 97% conversion of the upper 3 μm of the UO_2 surface. β-$UO_{2.33}$ forms initially as a uniform surface layer, but the growth of the β-$UO_{2.33}$ layer occurs preferentially along grain boundaries and microcracks in the fuel

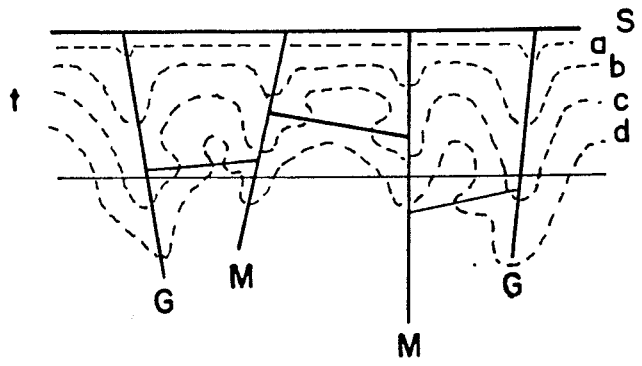

Figure 15 Schematic representation of the progression of a UO_2/β-$UO_{2.33}$ interface into a UO_2 pellet. *S* is the pellet surface, and *t* is the thickness of the layer observable by x-ray diffraction. During the early stages of oxidation, (*a*), the β-$UO_{2.33}$ forms a uniform surface layer, with some enhanced oxidation at grain boundaries, *G*. As oxidation proceeds, preferential oxidation at grain boundaries and possibly at microcracks, *M*, results in increasing convolution of the oxidation front (*b*,*c*). This process continues until virtually all of the UO_2 in the observable region (*t*) has been oxidized (*d*) (Taylor *et al.*, 1980).

pellets (Fig. 15).

Wang and Katayama (1981) studied the dissolution of spent UO_2 fuel single crystals in oxygenated waters (P_{O2} = 6 atm) using deionized water, synthetic groundwater, and sodium chloride-rich brine. Runs were conducted at temperatures of 25°C, 75°C, and 150°C. Wang and Katayama report that large quantities of $UO_2(OH)_2 \cdot H_2O$ precipitated in deionized water while $Na_2U_2O_7$ precipitated in the granite groundwater. These phases controlled the uranium solubility. The UO_2 exposed to the sodium chloride brine formed only a thin surface layer of $UO_2(OH)_2$ (analyzed by XPS), which apparently passivated the UO_2 fuel from further dissolution.

Johnson and others (1982) describe the mechanisms for the dissolution of irradiated UO_2 fuel under oxidizing and reducing conditions at 25°C and 150°C. They used two types of synthetic groundwater, a carbonate groundwater and a granite groundwater. The groundwater compositions are given in table 3. The experimental results were compared to thermodynamic data for several species (Fig. 16.) The uranium concentration assumed in figure 16 is 10^{-9} mol·kg^{-1}. This is probably low for solutions containing the uranyl ion. The uranium concentration may be two or three orders of magnitude higher under oxidizing conditions.). The U(VI) complexes reported for the oxidizing runs are UO_2F^+, UO_2Cl^+, $UO_2SO_4^0$, $UO_2CO_3^0$, $UO_2(CO_3)_2^{2-}$, and $UO_2(CO_3)_4^{4-}$. The presence of a surface film was postulated due to solubility (10^{-6} mol·kg^{-1} uranium) and electrochemical behavior at the

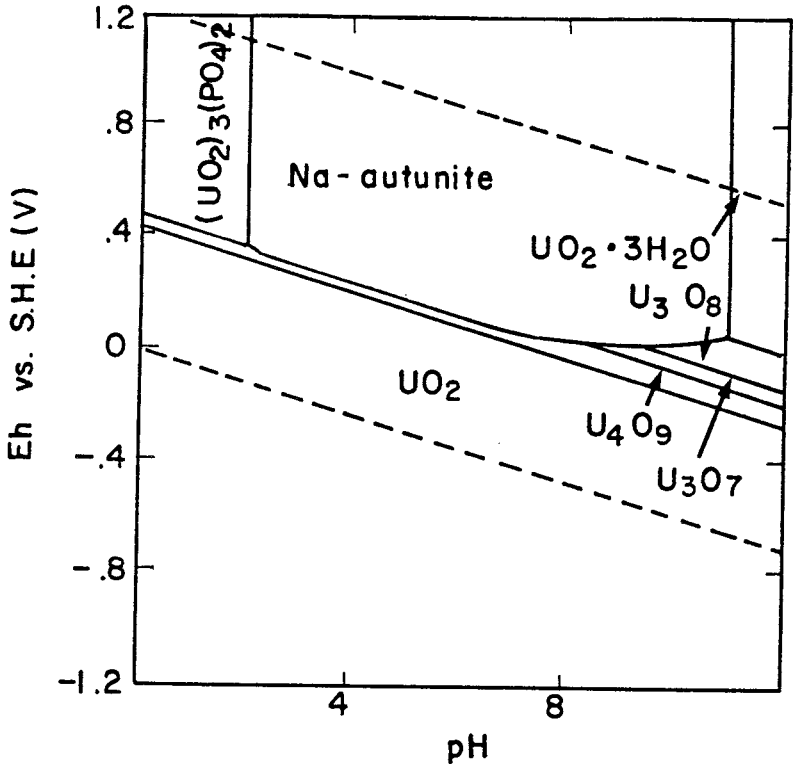

Figure 16 Eh-pH diagram for uranium species in synthetic granite groundwater (Table 3) at 150°C. Solid/solution boundaries are drawn at [U] = 10^{-9} mol·kg^{-1} (Johnson and Joling, 1982).

electrode. At high temperatures (approx. 150°C) and high alkalinities, the formation of $NaUO_3$ or $Na_2U_2O_7$ solids at the surface may control uranium concentrations in solution (see also Thomas and Till, 1984). No evidence for surface film formation was reported for the runs conducted in the carbonate groundwater. This is due to the highly soluble carbonate complexes (Langmuir, 1978).

Johnson and Joling (1982) conducted experiments on the dissolution of irradiated UO_2

TABLE 3 **Synthetic Groundwater Compositions (x10^{-4} mol·kg^{-1})**

	Carbonate GW	Granite GW		Carbonate GW	Granite GW
SiO_2	--	3.05	CO_2	50.0	10.0
Ca	1.5	3.1	SO_4	1.2	1.0
Mg	1.2	1.6	Cl	3.5	8.6
Na	51.7	88.0	F	--	0.10
K	0.5	0.8	NO_3	--	0.10
pH	8.4	7.0			

(Johnson *et al.*, 1982; Johnson and Joling, 1982)

fuel using the low ionic strength granite groundwater of Johnson and others (1982, table 3) under both oxidizing and reducing conditions at 150°C. The oxidizing runs were conducted on approximately 70 g fuel pellets in 500 ml of air-saturated granite groundwater ($CO_2 = 10^{-3}$ mol·kg^{-1}, pH = 7.0; table 3). The uranium concentration in the oxidizing runs is 10^{-7} to 10^{-6} mol·kg^{-1}. The formation of a solubility-controlling U(VI) phase is postulated, the composition of which is probably $UO_3 \cdot 0.8H_2O$ or $UO_2(OH)_2$, based on the study by Hoekstra and Siegel (1973).

Thomas and Till (1984) studied the dissolution of unirradiated UO_2 fuel pellets under mildly oxidizing conditions in deionized water and granite groundwater (composition listed in Vandergraaf, 1980). The formation of a solubility controlling phase such as $NaUO_3$ or $Na_2U_2O_7$ is postulated (Fig. 16, see also Johnson *et al.*, 1982) because of the reduced rate of UO_2 dissolution in the granite groundwater with increasing temperature as compared to the deionized water, in which dissolution rate increases with temperature. Thomas and Till (1984) do not state explicitly if their samples showed evidence of a U(VI)-phase on the surface.

Forsyth and others (1986) used a synthetic groundwater (table 4) and deionized water to study UO_2 fuel corrosion. Thermodynamic data were used to model the dissolution of the fuel for comparison to the experimental results. No surface film is reported in the experimental runs, though the uranium concentrations in the groundwater in the pH range 4.0 to 8.5 agree with the calculated solubilities using $UO_2(OH)_2(s)$ as the solubility controlling phase with a pH = 8.1. The lack of a surface film is probably due to the moderately high carbonate content in the groundwater used in the Forsyth and others (1984) study as compared to the granite groundwater used in the studies by Johnson and others (1982) and Johnson and Joling (1982)

TABLE 4 **Synthetic Groundwater Composition (x10^{-4} mol·kg^{-1})**

HCO_3^-	20.16	SiO_2	2.0
SO_4^{2-}	1.0	Cl^-	19.75
Ca^{2+}	4.49	Mg^{2+}	1.77
K^+	0.10	Na^+	28.27
pH	8.0 to 8.2		
Eh	-0.2 to +0.3		
Ionic strength	0.0085		

(Forsyth *et al.*, 1986; Ollilia, 1989- GW 1)

Uziemblo and others (1987) report the formation of a uranyl silicate (coffinite, a U(IV) phase) on spent UO_2 fuel in natural groundwater at 200°C and 25 MPa pressure. The tests were conducted under moderately reducing conditions, with water in contact with basalt and steel fuel cladding. Unfortunately, the water composition, pH, and Eh were not reported. Similarly, due to the limitations of Energy Dispersive X-ray Spectroscopy (EDS), the stoichiometry of the uranium silicate is not reported. Additionally, the formation of a uranium hydroxide is common at elevated temperatures (150°C to 300°C), and the UO_2 fuel dissolved completely. The uranium hydroxide formed at these temperatures may be α-$UO_2(OH)_2$ (Hoekstra and Siegel, 1973), although ianthinite ($UO_{2.83}$•$10H_2O$) may be a possible phase.

Taylor and others (1989) exposed unused CANDU™ fuel to air-steam mixtures at approximately 200°C. Below approximately 50% saturation of the air, oxidation proceeded in a manner similar to that seen during dry air oxidation experiments (see Taylor *et al.*, 1980 cited above). Between 50% and 100% saturation the most common product formed at the surface was dehydrated schoepite (α-UO_3•$0.8H_2O$) although schoepite was also detected in some runs. Runs conducted with excess water (>100% sat.) showed coexisting anhydrous U_3O_8 and α-UO_3•$0.8H_2O$ at the surface. At high moisture levels (> 50% sat.), the reaction appears to occur within a "liquid-like" surface film of adsorbed moisture whereby UO_2 dissolves, followed by precipitation of the UO_3-hydrate, a process similar to the rusting of steel. Phases were identified using XRD and SEM (w/EDS).

Thomas and others (1989) performed a TEM study of oxidized spent pressurized-water-reactor (PWR) fuel. The fuel was oxidized in air at 155°C and 175°C. Internal oxidation proceeded by the formation of γ-U_4O_9 ($UO_{2.25}$) along grain boundaries and by an advancing, coherent $UO_{2.25}/UO_2$ interface within the UO_2 grains. The unit cell for $UO_{2.25}$ is smaller (by 0.4%) than the unit cell of UO_2. The reduced volume resulting from oxidation was accommodated by expansion of cracks at grain boundaries within the fuel. No change in crystal orientation between coexisting UO_2 and $UO_{2.25}$ was observed, although some mismatch across the interface exists. Observed defects were not common. However, most UO_2 grains contained one or two microcracks. Such microcracks did not generally intersect grain boundaries. The γ-U_4O_9 in the fuel lacked long-range order. The oxidation of the UO_2 fuel resulted in embrittlement as grain boundary cracking proceeded. Rapid internal oxidation was attributed to the presence of closely-spaced fission gas micro-bubbles along grain boundaries. These bubbles provide for rapid diffusion of oxygen into the fuel. Higher oxides, such as $UO_{2.33}$ or $UO_{2.67}$ were not detected.

Ollila (1989) compared calculated and experimental results of UO_2 dissolution under oxidizing and reducing conditions using deionized water, a sodium carbonate water ($NaCO_3$: 60 mg/l, = 7.14 x10^{-4} mol·kg^{-1}; 120 mg/l, = 14.28 x10^{-4} mol·kg^{-1}; 275 mg/l, = 32.74 x10^{-4} mol·kg^{-1}; 600 mg/l = 71.42 x10^{-4} mol·kg^{-1}), and two synthetic groundwaters. The two groundwaters simulate granite groundwater (GW 1, table 4) and granite groundwater with bentonite present (GW 2, table 5). The granite groundwater composition used by Ollilia is identical to the granite groundwater of Forsyth and others (1986; table 4). The bentonite/granite groundwater is significantly higher in silica, sulfate, fluoride, and sodium. The chloride and phosphate concentrations are moderately increased with respect to the granite groundwater.

TABLE 5 **Synthetic Groundwater Composition: GW 2 granite/bentonite (x10^{-4} mol·kg^{-1})**

SiO_2	3.33	Ca^{2+}	4.49
Mg^{2+}	1.77	Na^{+}	118.75
K^{+}	0.10	Fe	0.05
HCO_3^{-}	99.85	SO_4^{2-}	6.24
Cl^{-}	22.56	F^{-}	3.95
PO_4^{3-}	0.001	HPO_4^{2-}	0.05
pH	8.6 to 9.2		
Eh (V)	-0.3 to +0.3		

(Ollilia, 1989)

Under oxidizing conditions, the formation of a uranyl hydroxide at the UO_2 surface is reported in the deionized water. The phases used for comparison to the experimental concentrations are $UO_2(OH)_2 \cdot H_2O$ and $UO_2(OH)_2$. The experimental uranium concentrations differed from the calculated solubilities of these uranyl hydroxides by an order of magnitude. In the sodium carbonate water, under oxidizing conditions, the formation of a uranyl phase is postulated to explain solubility control, but no uranyl phase is reported on the surface. The calculated solubilities are based on formation of U_4O_9 ($UO_{2.25}$), U_3O_8 ($UO_{2.67}$), $UO_2(OH)_2$, or $UO_2(OH)_2 \cdot H_2O$. The calculations of Garisto and Garisto (1986) indicate that ($UO_2(OH)_2 \cdot H_2O$) forms at all pH values only in the absence of carbonate (table 1a). The only other uranyl phase may be rutherfordine (UO_2CO_3) which is only stable in carbonate solutions at neutral pH (pH = 7.0; table 1a). The increased solubility of U(VI) in carbonate solutions is due to complex formation between UO_2^{2+} and

CO_3^{2-}. However, the experimental solubilities in the carbonate solutions are lower by as much as two and one half orders of magnitude as compared to the calculated solubilities. $UO_{2.33}$ could form in these carbonate solutions as per the calculations of Garisto and Garisto (1986).

The phases used by Ollila to compare the experimental uranium concentrations to the calculated solubilities in the synthetic groundwaters (I and II) are: $(UO_2(OH)_2 \cdot H_2O)$, $UO_2(OH)_2$, U_3O_8, $Na_2U_2O_7$, and $CaUO_4$. Again, the calculated solubilities were significantly higher than the experimental concentrations. The formation of precipitates is noted only on the UO_2 surface exposed to the bentonite/granite groundwater.

Franco and others (1989) analyzed surface films on leached UO_2 pellets using rutherford backscattering spectroscopy (RBS), SEM, and x-ray photoelectron spectroscopy (XPS). Leaching runs were conducted in deionized water and synthetic groundwater (table 6) at 25°C, 60°C, and 90°C. The uranium concentration in the groundwater decreased with increasing temperature, especially at 90°C, whereas, in the deionized water, the uranium concentration increased with temperature. Also, except at 90°C, the uranium concentrations in the deionized water were lower than the uranium concentrations in the synthetic groundwater. The presence of a surface layer is emphasized in the 90°C runs. The surface layer composition is that of a hydrated Mg-Si-uranyl oxide. Film thicknesses are 100 nm to 400 nm thick. The dominant complexing anions present in the groundwater are HCO_3^-, Cl^-, and SO_4^{2-}. These are not present in concentrations high enough to precipitate uranyl carbonate or uranyl sulfate solids (table 6; Langmuir, 1978). An important Mg-Si-uranyl phase found in nature is haiweeite $((Ca,Mg)(UO_2)_2Si_6O_{15} \cdot 5\text{-}9H_2O)$.

Lahalle and others (1989) studied single crystals of UO_2 by XPS surface analysis after leaching them in deionized water and synthetic groundwater (table 6) at 60°C and 90°C. The uranium concentrations in the groundwater runs were lower than comparable runs in

TABLE 6 **Synthetic Groundwater Composition ($x10^4$ mol·kg^{-1})**

SiO_2	5.46	Ca^{2+}	2.60
Mg^{2+}	2.47	Na^+	3.48
K^+	1.38	HCO_3^-	10.66
Cl^-	2.12	SO_4^{2-}	0.73
NO_3^-	0.65		

(Franco *et al.*, 1989; Lahalle *et al.*, 1989)

deionized water. A double layer approximately 100 nm thick is present at the UO_2 surface (Fig. 17). A hydrated UO_3 layer, in contact with the UO_2 surface, underlies a hydrated Mg-Si oxide which is similar to a synthetic $MgSi_3O_8$ used for comparison with XPS. This upper layer, in contact with the leachate, does not contain uranium.

Wilson (1988) and Wilson and Bruton (1989) exposed spent fuel particles, along with split fuel cladding hulls, to natural well water from the Yucca Mountain repository site in Nevada, USA (J-13 well water, table 7) at 25°C and 85°C for periods up to 240 days. Experiments were conducted on both unsealed, fused silica (25°C) and sealed, stainless steel (25° and 85°C) test vessels. Dissolved (particle size <0.4 μm) actinide concentrations (U, Np, Am, Pu, Cm) in the water were measured and compared to predicted values using the EQ3/6 geochemical code (with version 3270R13 of the thermodynamic database). Solid phase precipitates obtained by filtration were also analyzed with XRD and EDS.

Measured actinide concentrations were consistently higher than those predicted by modelling. Uranium concentrations at 85°C were lower than in the 25°C runs. This is in agreement with results reported by Franco (1989) and Lahalle and others (1989). The calcium uranyl silicates uranophane, $(H_3O)_2Ca(UO_2)_2(SiO_4)_2 \cdot 3H_2O$, and haiweeite, $Ca(UO_2)_2Si_6O_{15} \cdot 5H_2O$, (reported as $3CaO \cdot 4UO_3 \cdot 10SiO_2 \cdot 24H_2O$ = $Ca_3(UO_2)_4Si_{10}O_{27} \cdot 24H_2O$), and possibly the uranyl silicate soddyite, $(UO_2)(SiO_4)_2 \cdot 2H_2O$, were

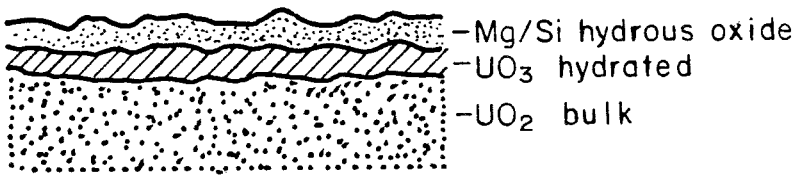

Figure 17 Diagrammatic representation of the UO_2 surface after exposure to mineral water (table 6) at 90°C for six weeks (Lahalle *et al.*, 1989).

detected in the 85°C tests. These phases are presumed to be responsible for the reduced uranium concentrations in the 85° tests (approx. 0.15 μg/ml) as compared to the 25° tests (approx. 0.3 μg/ml). The phases used in the modelling calculation were haiweeite, soddyite and schoepite. No thermodynamic data for uranophane are included in the database used. Schoepite is not reported in any of the tests. The composition of the haiweeite reported in the Wilson and Bruton (1989) study differs from the accepted composition of natural haiweeite. WILSON AND GRAY (1990) discuss the advantages and disadvantages of semi-static and flow-through tests on spent fuel.

TABLE 7 **J-13 Well Water Composition (μg/ml)**

Si	27.0	Ca	12.5
Mg	1.92	Na	43.9
K	5.11	Li	0.042
Sr	0.035	Al	0.012
Fe	0.006	HCO_3	125.3
Cl	6.9	F	2.2
SO_4	18.7	NO_3	9.6
pH	7.6		

(Delany, 1985)

Bates and others (1990) conducted a corrosion study on UO_2 pellets and UO_2 powders at undersaturated conditions using EJ-13 water (i.e. J-13 water that had been equilibrated with tuff at 90°C: table 8). Three test configurations were used: (1) a stack of eleven as-cut pellet discs (13.7 mm diameter, 1.75 mm thick); (2) approximately 19 mm high column of crushed UO_2 (60 - 80 mesh), vertically sandwiched between two 1.75 mm discs; and (3) approximately 30 mm high stack of three 13.7 mm diameter UO_2 pellets. The specimens were encased in Zircaloy cladding and placed on a Teflon stand sealed in an air-tight stainless steel vessel. All tests were perfomed at 90°C. 0.075 mL of EJ-13 water was dripped on the specimens at 3.5 day intervals. Solution U concentrations were measured and correlated to corrosion products formed on the UO_2 pellet surfaces. The pH decreased slightly, followed by a gradual increase (minimum pH values were only slightly lower than the starting water pH). After 182.5 days, Ca, Mg, and Si concentrations in the sampled solutions decreased substantially, while HCO_3^-, NO_3^-, SO_4^{2-} and Cl^- increased substantially compared to the starting water composition.

TABLE 8 EJ-13 Water Composition (mg/L)

Si	34.4	Ca	9.1
Mg	1.0	Na	46.5
K	N.R.	Li	N.R.
Sr	N.R.	Al	N.R.
Fe	N.R.	HCO_3	135
Cl	7.2	F	2.4
SO_4	17.0	NO_3	7.6
U	0.0024		
pH	8.1		

(Bates *et al.*, 1990) N.R. = not reported

The samples exhibited a significant build up of corrosion products. The corrosion products identified are given in Table 9. The initial "pulse" of uranium release is due to the initial formation of schoepite, which has a relatively high solubility. Subsequent formation of the more complex uranyl oxide hydrates and uranyl silicates (with lower solubilities) resulted in a decreased release of uranium in solution. Bates and others note that restricted water flow aided in the formation of the complex uranyl minerals having lower solubilities due to the evaporative concentration of cations. Samples for which water was allowed to drip down the sides did not tend to form the complex uranyl oxide hydrates and uranyl silicates Instead, dehydrated schoepite usually formed on the sides and bottoms of these samples.

TABLE 9 Corrosion Products of UO_2/EJ-13 water reaction

schoepite	$UO_3 \cdot 2H_2O$	uranophane	$Ca(UO_2)_2(SiO_3)_2(OH)_2 \cdot 5H_2O$
dehydrated schoepite	$UO_3 \cdot 0.8H_2O$	boltwoodite	$K(H_3O)UO_2(SiO_4) \cdot nH_2O$
becquerelite	$CaU_6O_{19} \cdot 10H_2O$	sklodowskite	$Mg(UO_2)_2(SiO_3OH)_2 \cdot 5H_2O$
compriegnacite*	$K_2U_6O_{19} \cdot 11H_2O$		
*tentative identification			

(Bates *et al.*, 1990)

Natural Analogue Studies

Natural analogue studies attempt to correlate the long-term behavior of naturally occurring elements to the expected behavior of elements in a man-made environment such as a spent fuel or high-level waste repository. The natural occurrence of the same or geochemically similar radionuclides as those expected in a nuclear waste repository makes natural analogue studies vital to the long-term performance assessment of a proposed repository site. Several problems arise when comparing natural systems to experimental studies on UO_2 fuel. The focus of the vast majority of laboratory studies address the corrosion of spent fuel, that is, near-field behavior, while most natural analogue studies is on the migration of actinides in the far-field. The long-term processes operating in the near field which affect the ultimate release of elements to the environment are often unclear in many natural analogue studies. The effectiveness of natural analogue studies varies with the site, and no single analogue site is a perfectly representative of a radioactive waste repository. Therefore, one must evaluate several analogue sites in order to address any single process. This section summarizes pertinent aspects of several important natural analogue studies.

Cigar Lake, Saskatchewan, Canada

The Cigar Lake uranium deposit, located in the Athabasca Basin of northern Saskatchewan, has been extensively studied as an analogue for a radioactive waste disposal vault under water-saturated, reducing conditions. This deposit shows substantial promise as a useful analogue for radionuclide migration under the conditions proposed for the deep burial of spent nuclear fuel.

The Athabasca Basin in northern Saskatchewan contains several unconformity-type uranium deposits (Fig. 18). These deposits form at the base of the Phanerozoic Athabasca sandstones and conglomerates associated with faulting in the basement metamorphic rocks (schists and gneisses). The base of the Athabasca Formation constitutes a paleo-surface due to the erosion of the pre-existing metamorphic terrain. Some deposits extend into the basement rocks along fault zones (e.g. Key Lake, Rabbit Lake), although formation is considered syn-depositional with the sandstone or due to post-depositional hydrothermal fluids derived from the basement rocks (perhaps during metamorphic reactions) and

percolated up along the fracture zones. This latter mode of formationseems to best explain the genesis of the 1300 million year old Cigar Lake deposit. Cramer (1986) summarizes the geology of the Cigar Lake deposit. More thorough descriptions of the geology are provided by Bruneton (1986) and by Fouques and others (1986).

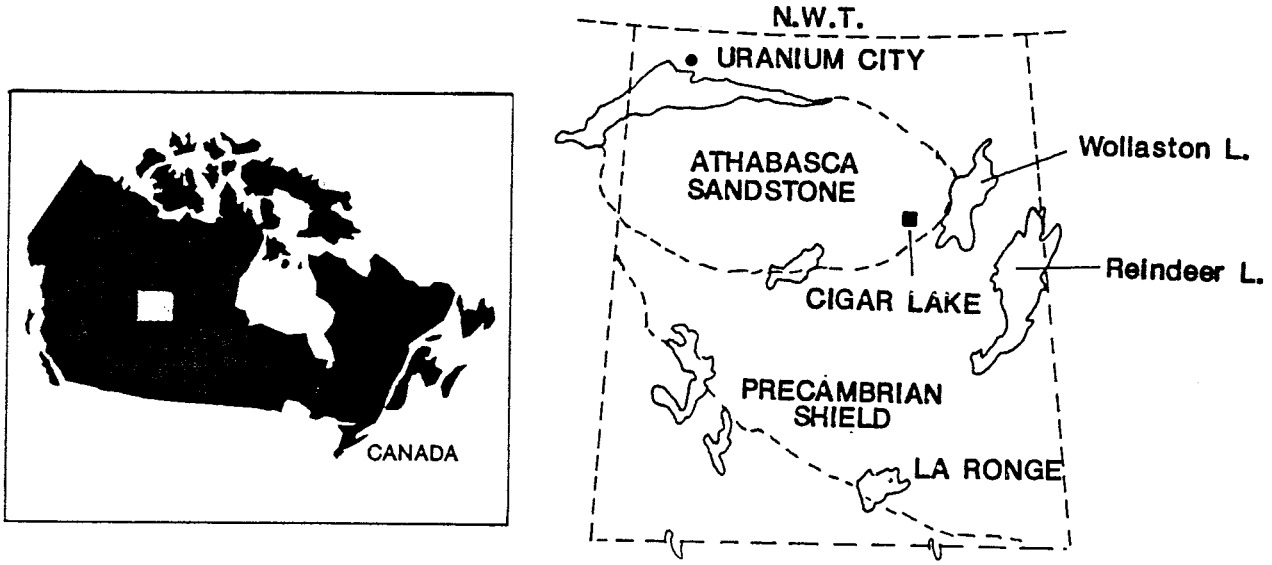

Figure 18 Location map showing the Cigar Lake uranium deposit in the Athabasca Sandstone Formation in northern Saskatchewan (after Cramer *et al.*, 1987).

Located at the southwestern tip of Waterbury Lake, the Cigar Lake ore body lies 450 m below the surface, where it straddles a ridge in the basement rocks and overlies a fracture zone (Fig. 19). The ore is surrounded by a clay-rich halo (5-30 m thick), an area substantially depleted in silica and consisting predominantly (>80 vol. %) of kaolinite and illite. At the contact between the ore and clay halo, there is a narrow band (1-10 m thick) of amorphous iron oxides which coat the clays. Above the clay halo, the Athabasca sandstone is altered, being enriched in kaolinite, illite, and other clay minerals and depleted in quartz relative to the unaltered sandstone. Above this altered zone is a band of silica-rich sandstone, the "quartz cap", in which secondary silica fills fractures in the sandstone. Above the quartz cap the sandstone is relatively unaltered.

Present groundwater flow is south to north along the unconformity (Fig. 19). Groundwaters are derived from surface waters, although flow is slow (the basal unit has a hydraulic conductivity of 10^{-6} m·s^{-1}, Vilks *et al.*, 1988). The uranium was apparently transported upwards to the base of the unconformity along the fracture zone by hydrothermal solutions and deposited as uraninite at the unconformity when these solutions came into contact with groundwater in the sandstone. These hydrothermal solutions are also responsible for the alteration of the sandstone surrounding the ore body, dissolving quartz and feldspar, and replacing them with clay minerals. The ore body is high grade, containing an average U_3O_8 concentration of 14 weight percent with zones of enrichment up to 65 weight percent.

Cramer (1986) and Cramer and others (1987) discuss the analogue features of the Cigar Lake deposit. The ore has a relatively low concentration of Th and lanthanides. The oxidation state of the ore is at or below $UO_{2.33}$ (the U^{6+}/U^{4+} ratio ranges from 0.24 to 0.57) indicating reducing conditions. Within the ore body, the Eh is estimated to be -0.21 to -0.4 volts and the pH is 7.03 to 7.35. The phases identified include UO_2, $UO_{2.25}$, coffinite

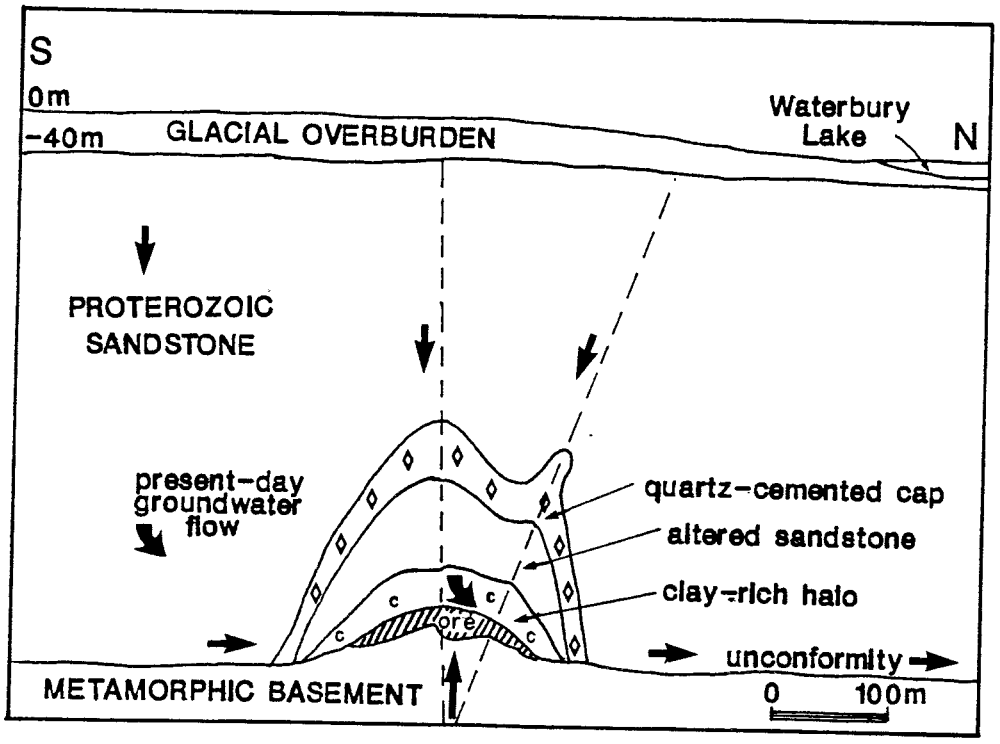

Figure 19 A schematic cross-section for the Cigar Lake uranium deposit. Arrows represent groundwater flow. (courtesy of D. Curtis).

($USiO_4$), and perhaps α-$UO_{2.33}$ (Sunder et al., 1988). No uranyl minerals are reported. The system is water-saturated and open to groundwater flow. Uranium concentrations of the groundwater range from 2.5 to 11.9 $\mu g \cdot l^{-1}$ within the ore body. Vilks and others (1988) studied particulate and colloid matter in groundwater and showed that half or more of the uranium in the water is carried in suspension associated with particulate matter. Radiolysis of the groundwater within the ore zone may be the cause of locally oxidizing conditions causing formation of the Fe-oxides (e.g. goethite) at the top of the ore body. Perhaps due to the presence of the Fe-oxides at the ore/clay interface, uranium concentrations in the surrounding sandstone are depleted with resect to the ore body water. Also, the filtration of particulate matter by the clay minerals plays a role in reducing groundwater uranium activity (Vilks *et al.*, 1988). Vilks and others also oxidized a sample of the groundwater by letting it sit overnight prior to testing. The precipitation of amorphous Fe-Si-hydroxides was noted. These precipitates act as scavengers for the uranium in solution. Reactions such as this would tend to buffer uranium migration in the event of exposure of uranium-rich groundwater to oxidizing conditions. As Cramer and others (1987) point out, there are no surface indicators of the deposit. Uranium mobility has been substantially restricted.

Koongarra, Northern Territories, Australia

Several uranium deposits have been described in the Alligator Rivers region of northern Australia (Fig. 20). A number of these has been analyzed for use as natural analogue studies for a spent fuel repository (Airey, 1986; Shirvington, 1988). The Koongarra deposit has received the most attention recently and appears to be a promising analogue for spent fuel exposed to oxidizing groundwater. Numerous reports and papers discussing the analogue characteristics and project goals have been published (e.g. Duerden and Hardy, 1990; Duerden *et al.*, 1988, 1987; Airey *et al.*, 1987, 1985; Airey, 1986)

The regional geology of the Alligator Rivers area has been briefly summarized by Wilde and Wall (1987) and more completely by Needham and others (1980) and Stuart-Smith and others (1980). The geology of the Koongarra deposit was described by Foy and Pederson (1975) and Pederson (1978). The Koongarra deposit, like the other Alligator Rivers uranium deposits, is an unconformity-type deposit similar to the occurrences in the Athabasca Basin in northern Saskatchewan, Canada. Koongarra consists of two stratibound ore bodies separated by a barren gap. The primary ore bodies consist of partially coalescing

lenses of uraninite veins which are approximately conformable with the schistosity of the host rocks, steeply dipping quartz-chlorite schists known as the Cahill Formation. The host schists are exposed to the surface, brought up along a steeply dipping reverse fault which juxtaposes the approximately 1800 million year old Cahill Formation against the approximately 1650 million year old Komboglie Formation Sandstone (Fig. 21).

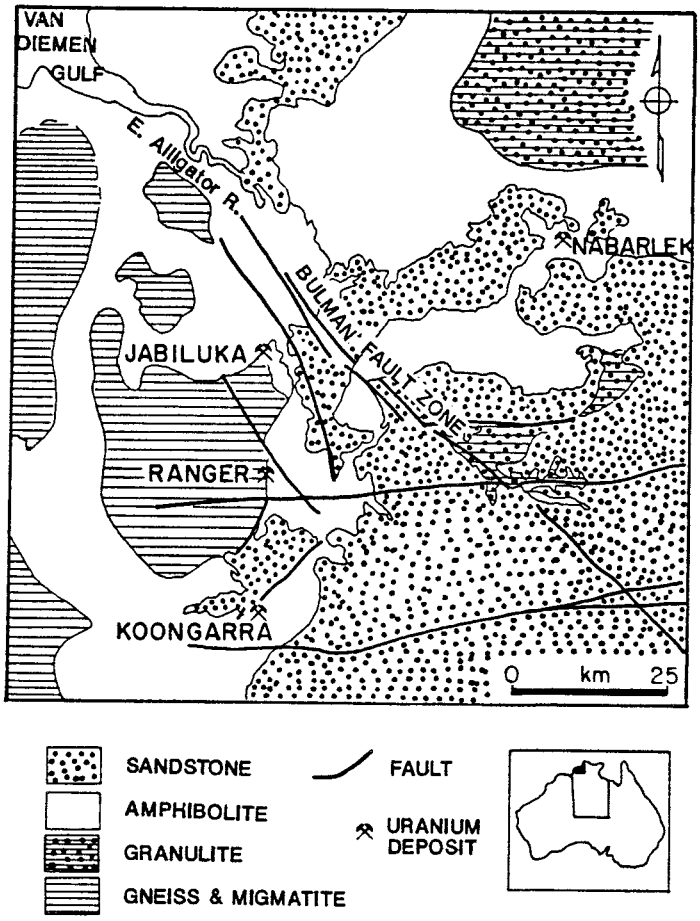

Figure 20 Regional geology of the east Alligator River uranium field (Wilde and Wall, 1987)

The uranium mineralogy of Koongarra was described by Snelling (1980). The primary ore is uraninite. Two distinct types of uraninite can be identified: low Ca (1-3 wt. %) vein-type uraninite, forming small disseminated sub- to euhedral grains, thin veinlets, spherules and botryoidal masses, and high Ca (3-5 wt. %) hydrothermal uraninite, forming colloform fracture and cavity infillings and occurring along grain boundaries in the host rock. The vein-type uraninites are more oxidized than the hydrothermal uraninites. Two

periods of remobilization are apparent from the uraninite in the ore zone. The first remobilization event partially dissolved much of the originally euhedral uraninite grains, redepositing them as veinlets and botryoidal masses, but without any significant change in their chemistry. The second remobilization resulted in the precipitation of low temperature, supergene uraninite with increased Si, P, Ca, and O, and decreased U and Pb relative to the vein-type uraninites. Alteration of the primary ore zone also produced uranyl oxide-hydrates and uranyl silicates at depth. Often uraninite grains or entire veins were pseudomorphously replaced by the Pb-uranyl minerals vandendriesscheite, fourmarierite, and curite. The uranyl oxide hydrates showed continuously variable compositions from the uraninite core outwards, suggesting some degree of solid solution among them. The uranyl oxide hydrates were, in turn, replaced by the uranyl silicates uranophane, sklodowskite, and kasolite. In several instances, uraninite is completely altered to uranyl silicates. Uranophane and sklodowskite also occur commonly as fracture fillings and are intergrown along chlorite cleavage planes.

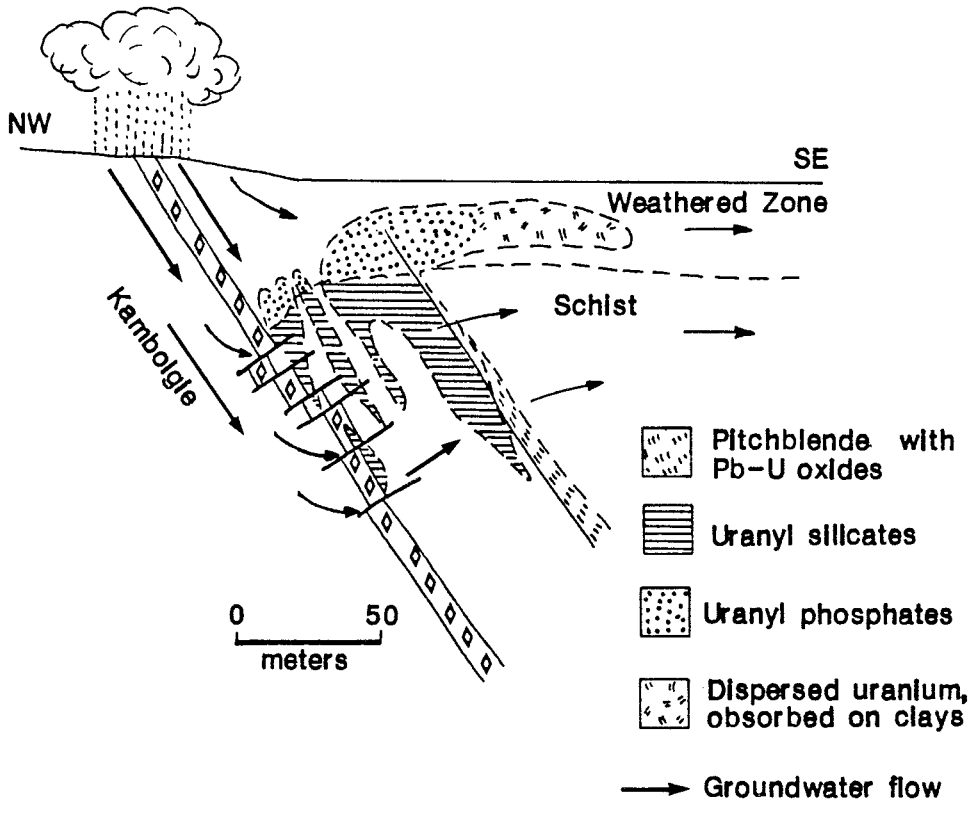

Figure 21 Simplified cross-section through the Koongarra No. 1 Orebody. The distribution of the various uranium minerals and the paths of groundwater circulation at the present time are shown schematically (Snelling, 1980).

The No. 1 ore body has been exposed to the surface where it has undergone extensive oxidation through interaction with meteorically derived groundwater. This has resulted in a secondary uranium ore zone in the form of a dispersion fan extending 80 meters downslope from the primary ore zone (Fig. 21). The upstream portion of the dispersion fan consists predominantly of uranyl phosphates (salèeite, sabugalite, torbernite-metatorbernite, and renardite-dewindtite), while the uranium in the downstream portion is associated with clay minerals and iron oxides. The uranyl phosphates are derived predominantly from alteration of the uranyl silicates by reaction with phosphate-containing meteoric waters in the uppermost weathered zone. Apparently, phosphate-rich waters do not penetrate into the primary ore zone at depth because no uranyl phosphates occur within this zone. Langmuir (1978) showed that phosphates are more stable than silicates except at high silica concentrations and a pH of approximately 6.0. The pH in the primary ore zone is 6.0 to 6.5 (Snelling, 1980).

Three distinctive zones of relative weathering exist at Koongarra. The uppermost zone (above approx. 20 m) is the most weathered. Chlorite has been altered to kaolinite, minor smectite, hematite, and various iron oxy-hydroxides. A transitional zone (20-25 m) of less weathered rock consists predominantly of vermiculite derived from primary chlorite (present below approx. 24 m) and altering to kaolinite and iron oxides. The highest uranium concentrations in the dispersion fan are associated with the lower part of the kaolinite zone (Isobe and Murakami, in press).

Edghill (in press) described uranium redistribution associated with weathering. All uranium activity in the unweathered schists is associated with uranium minerals. In the slightly weathered rocks (vermiculite zone of Isobe and Murakami, in press), uranium activity is associated with iron-oxide "staining" and with altered biotite and chlorite. Uranium activity closely follows oxidation fronts in this weathering zone and advances most readily along cracks and fissures in which percolation of oxidizing groundwater is most enhanced. The Si and P content of the uraninite in the slightly weathered rocks is higher than that of the uraninite in the unweathered rocks. Alteration of the high Si-P uraninite simultaneously produces salèeite and sklodowskite. Snelling (1980) found that salèeite and sklodowskite show limited solid solution through substitution of $(SiO_4)^{2-}$, $(PO_4)^{3-}$, $(AsO_4)^{3-}$ in their structures.

In the most strongly weathered rocks (kaolinite zone of Isobe and Murakami, in press), uranium activities are highest on the manganese and iron oxy-hydroxides which act as scavengers for uranium in solution. Uranium distribution in the most strongly weathered

rocks depends only on the mineralogy present and is not controlled by the presence of fissures, as is the case for the more moderately weathered rocks. The form in which the iron oxides occur (e.g. goethite vs. ferrihydrite) may also play a role in their relative effectiveness in retaining uranium (Edghill, in press).

Koongarra shows significant alteration of primary uraninite. The uraninite alteration products are as follows (Fig. 22):

(1) Supergene uraninite with significantly increased Si, Ca, P, and O.

(2) Pb-uranyl oxide hydrates, perhaps displaying significant solid solution.

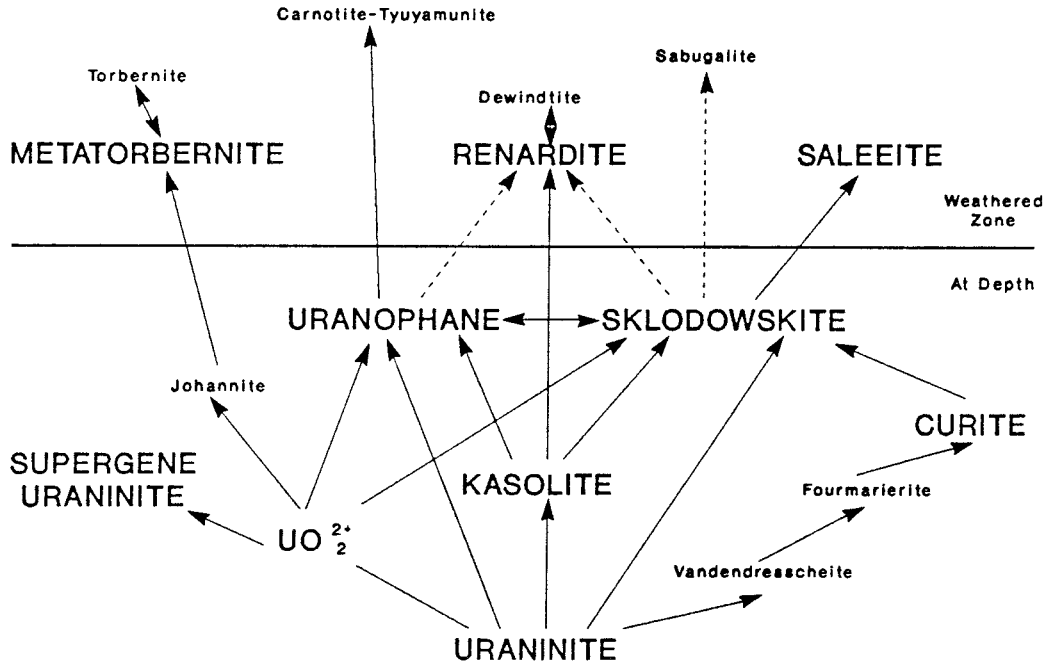

Figure 22 Schematic diagram showing proposed paths of secondary uranium mineral formation from uraninite at Koongarra (Snelling, 1980).

(3) Ca-, Mg- and Pb-uranyl silicates, with uranophane (Ca) and sklodowskite (Mg) showing substantial solid solution. The silicates may pseudomorphously replace uraninite in the slightly weathered zone, replace the Pb-uranyl oxide hydrates, or precipitate from solution in fissures and cracks.

(4) , the Mg-, Al-, Cu-, and Pb-uranyl phosphates, which are present only in the upper 20 m of the ore deposit, are derived from alteration of the uranyl silicates or from the sulfate johannite (Snelling, 1980), derived directly from weathered uraninite (Edghill, in press), derived from curite (cf. Vochten *et al.*, 1979) or are precipitated from solution.

(5) Uranium is associated with Fe- and Mn-oxides (Fe-oxides being most common) at the furthest extent of the dispersion fan, .

Poços de Caldas, Minas Gerais, Brazil

The Osamu Utsumi uranium mine and the Morro do Ferro Th/lanthanide prospect in the Poços de Caldas caldera of Minas Gerais, Brazil are the sites of a multi-disciplinary analogue study of radionuclide migration around a spent fuel or high level waste repository. The Poços de Caldas project is a joint venture of Brazil, Sweden, Switzerland, UK, and the USA. The project's background and site information is discussed in detail by Smellie and others (1987). The project has four main objectives, which are discussed in some detail by Smellie and others (1989):

1. Assist in the validation of thermodynamic models, codes, and databases used to evaluate water/rock interactions, solubilities, and speciation of elements in an environment rich in natural radionuclides and lanthanides.

2. Establish the interactions of natural groundwater colloids, radionuclides, and mineral surfaces with respect to radionuclide transport processes and colloid stability.

3. To model geochemical transport across redox fronts in order to understand the long-term, large scale behavior of redox-sensitive natural series radionuclides.

4. To model the migration of lanthanides/U-Th series radionuclides during hydrothermal activity similar to that anticipated in a spent fuel repository.

The Poços de Caldas caldera (Fig. 23) is a Cretaceous (65-130 x 10^6 years ago) alkaline volcanic complex consisting of phonolites and carbonotites which, due to the tropical climate, have been intensely weathered near the surface. The Osamu Utsumi mine is a roll-front uranium deposit, and the movement of radionuclides across the redox front is being monitored. The Osamu Utsumi mine consists of an upper weathered zone (laterite soil, top 40 m) which is completely argillized, depleted in Si and K, and enriched in alumina. The underlying oxidized zone is approximately 150 meters thick and consists of alternating areas of oxidized and reduced bedrock. The reduced zone consists of essentially unaltered phonolites (62% K-feldspar, 37% clay minerals, with accessory pyrite, fluorite, and barite). The primary mineralogical difference between the oxidized and reduced rocks is the presence of pyrite in the reduced rocks (Smellie *et al.*, 1989).

The groundwater flow at the Osamu Utsumi mine is upward from depth, except for the upper 10 - 15 meters, where lateral surface flow predominates (Fig. 24). Smellie and

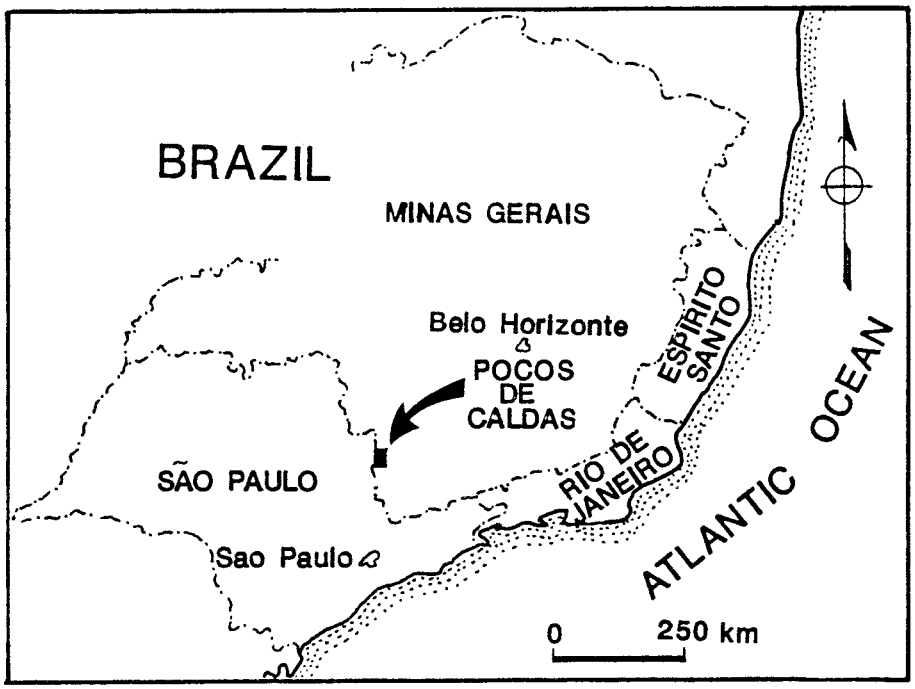

Figure 23 Location map showing Poços de Caldas area in Minas Gerais, Brazil.

others (1987) describe the groundwater as "K-Fe-SO_4-type" of moderately reducing capacity. The groundwater chemistry is the result of intense weathering of the potassium-rich igneous rocks. Low concentrations of dissolved organic carbon (DOC) are due to the scarcity of vegetative cover at the mine. Typical groundwater parameters are given in Table 9. Groundwaters in the upper 10 - 15 meters of the Osamu Utsumi mine are oxidizing and relatively acidic and have high concentrations of U, Fe, F, and SO_4.

Miekeley and others (1989) report on the study of colloidal characteristics and transport at Poços de Caldas. Interestingly, the colloidal concentration at the Osamu Utsumi mine is relatively low (typically <1 ppm), in spite of the advanced weathering of the rocks. The dominant colloidal chemistry is due to Fe-hydroxides, DOC, K, Ca, and minor Si. Though the proportions are not stoichiometric, the Si, Ca, and K may be due to clay minerals in the colloidal fraction. Also, relatively high concentrations of Ba and SO_4 detected in the groundwater from the Osamu Utsumi mine may be important since microcrystalline barite can act as a scavenger for several important radionuclides. The groundwater at the Osamu Utsumi mine is apparently supersaturated with respect to barite.

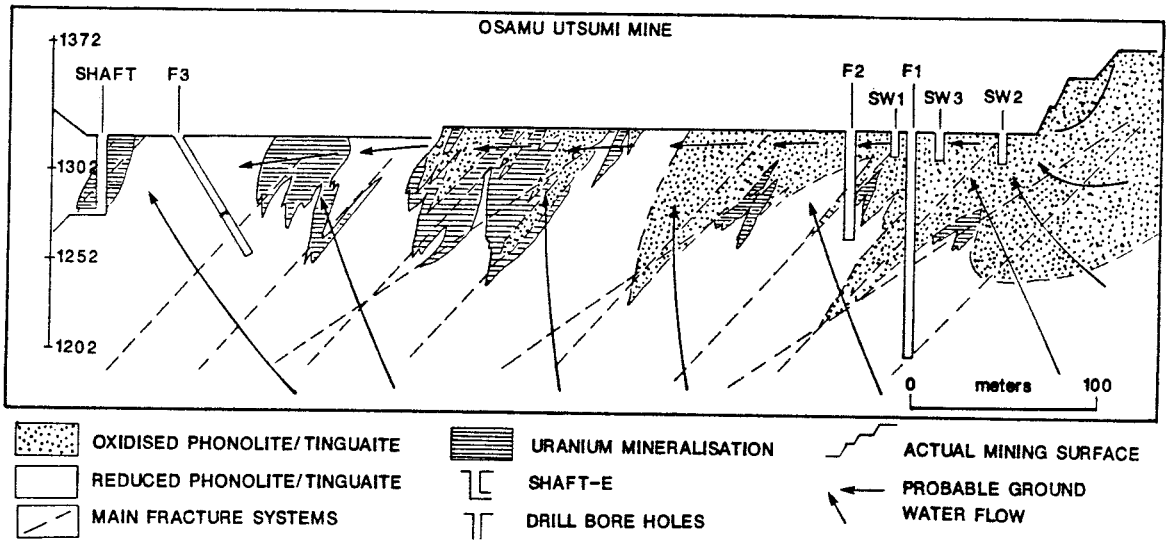

Figure 24 Cross-section through the Osamu Utsumi mine, Poços de Caldas, showing location of boreholes and illustrating groundwater flow

$^{234}U/^{238}U$ isotopic ratios from boreholes F1 and F2 (Fig. 24) are significantly different from each other and are indicative of more oxidizing conditions in borehole F2. Borehole F1 $^{234}U/^{238}U$ isotopic ratios are typically near 2.4, whereas, $^{234}U/^{238}U$ isotopic ratios in borehole F2 are close to 1.7. $^{234}U/^{238}U$ isotopic ratios in colloids and in the "dissolved" fraction (<1 nm) are generally identical, indicating equilibrium between the two phases.

The dissolved uranium in borehole F1 is higher than that of F2 (F1: 1.5 - 3.5 ppb, F2: 2.5 - 8.2 ppb), but both boreholes exhibit high percentages of uranium in the dissolved fraction (F1: 97%, F2: 75%). The proportion of uranium in colloids is not apparently

TABLE 9 **Typical Groundwater Composition Ranges, Osamu Utsumi mine, Poços de Caldas, Minas Gerais, Brazil**

Si	13-15	ppm	K	10-13	ppm
Na	0.1-1	ppm	Ca	0.5-2	ppm
Ba	0.10-0.15	ppm	(Sr,Mg)	<0.1	ppm
Fe(total)	0.6-2	ppm	Mn	0.1-0.3	ppm
U	4-15	ppb	Th	0.03-0.07	ppb
Lanthanides	5-8	ppb	SO_4	13-19	ppm
HCO_3	8-13	ppm	F	0.3-1.9	ppm
HPO_4	<0.05	ppm	DOC	1-4	ppm
pH	5.6-6.1				
Eh	200-400 mV				

(Miekeley, *et al.*, 1989)

correlated to total [U] or to colloidal [DOC], but seems to be correlated to colloidal iron.

West and others (1989) studied the influence of microbial activity on uranium transport at the Osamu Utsumi mine. They note that the redox front is moving faster than would be expected from dissolved oxygen inventory alone. Also, no sulfur oxidizing bacteria are found in the rocks at the redox front itself and a rapid pH drop (5.5 to 1.5) occurs in the surface water although the sulfide concentration is low. At the surface, sulfur oxidizers are present which consume sulfide, producing sulfuric acid and, therefore, high sulfate levels. In the oxidized zone, uraninite and pyrite are dissolving and iron oxy-hydroxides are forming. Sulfate is low and sulfide is absent. This may be due to bacteria

which catalyze pyrite oxidation without oxidation of sulfide to sulfate. Instead, sulfide may be converted to polysulfide or colloidal sulfur which may then be utilized at the surface by the sulfur oxidizing bacteria. At depth, within the reducing zone, sulfur-reducing bacteria may be important for the precipitation of pyrite and uraninite, as is suggested by the nodular forms of these minerals. Hence, microbial activity is important for the oxidation of pyrite and may be responsible for the mobilization and reprecipitation of uraninite at the redox front. West and others suggest that microbial activity will tend to encourage uranium immobilization rather than the formation of mobile colloids or complexes.

The Morro do Ferro thorium/lanthanide prospect is in a much more pronounced stage of weathering than the Osamu Utsumi mine. Morro do Ferro is characterized by high concentrations of Th and lanthanides in soils and weathered rocks (usually >1%). Uranium concentrations are relatively low. Miekeley and others (1989) suggest that secondary enrichment of Th and the lanthanides is because of weathering processes. Leaching of uranium is due to percolating, oxidizing groundwaters. Distinct from groundwater flow at the Osamu Utsumi mine, the groundwater flow at Morro do Ferro is more "homogeneous" (Fig. 25).

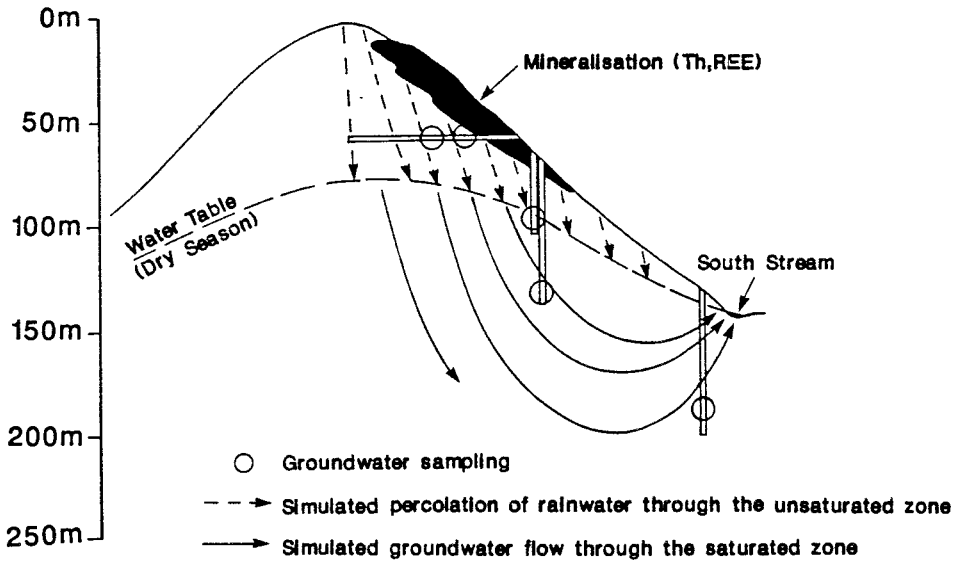

Figure 25 Cross-section through Morro do Ferro showing boreholes and groundwater flow (Smellie et al., 1989).

Groundwater chemistry at Morro do Ferro is difficult to obtain, but preliminary evidence suggests much lower major and trace element concentrations at Morro do Ferro than at the Osamu Utsumi mine (e.g., [F] < 0.2 ppm, [SO_4] < 10 ppm, see table 9) (Miekeley *et al.*, 1989). However, high concentrations of Mn are an exception and are due to the presence of nodular Mn-oxides. As with the Osamu Utsumi mine, DOC is low (1-4 ppm), owing to a lack of substantial vegetation, high rainfall, and the presence, at depth, of adsorptive species (e.g., clays and Fe-hydroxides).

Similar to the Osamu Utsumi mine, colloid concentrations are low, a low fraction of the DOC is in the size fraction of humic acids (<10%), a large amount of the Fe present is colloidal (10 - 20%), The $^{234}U/^{238}U$ isotopic ratios of the colloidal fraction and the dissolved fraction are the same (1.0 - 2.0), implying equilibrium. The tendency to form colloids increases in the order U < Ce < Th (Miekeley and others, 1989).

Due to the stability of Mn(II) species, Mn colloids do not form as readily as Fe(III) colloids in these groundwaters. Colloidal humic acids are the principle carriers of the major and trace elements studied. Since concentrations of colloidal organic carbon species are so low, Th migration is not significant (see also Eisenbud, *et al.*, 1982).

No secondary uranyl minerals are discussed in any studies on the Poços de Caldas project. The low concentrations of uranium in the colloidal fraction of the groundwaters indicates that uranyl phases do not play an important role in colloidal transport of uranium at Poços de Caldas. The concentration of uranium in the dissolved fraction (< 1 nm) is lower than that expected to be in equilibrium with the solid uranyl phases. No evidence for the presence of uranyl minerals is cited in the work on Poços de Caldas.

Oklo, Gabon

The only known examples of naturally occurring fission reactions lasting for several thousands of years are the fission reactors in eastern Gabon. Fourteen reactor zones have been identified among three uranium deposits in the Franceville Basin (Gauthier-Lafaye *et al.*, 1989). Numerous studies have been carried out on these natural reactors, which occur within approximately 2000 million year old uranium deposits. The age of the reactions is still uncertain, although the reactions probably occurred either contemporaneously with, or immediately subsequent to, ore deposition. Two symposium proceedings have been

published on the reactors in Gabon: *The Oklo Phenomenon* (1975) and *Natural Fission Reactors* (1978). Much of the geology of the area is summarized by Gauthier-Lafaye and Weber (1989) as well the effects on the rocks surrounding the reactor zones. The Franceville Basin consists predominantly of deltaic sandstones, conglomerates and marine black shales with interbedded dolomites, cherts, and some rhyolitic tuffs in the upper strata. The uranium mineralization most commonly occurs near the base of the Francevillian and occurs adjacent to sandstone-shale interfaces in rocks laid down in a deltaic environment.

Two grades of ore are distinguished in the Franceville Basin: the low-grade ore contains 0.1 to 1.0 percent U_3O_8 and the high grade ore (> 1.0 percent) commonly contains up to 10 percent U_3O_8. The most common (low-grade) ore occurs within black silicified sandstones containing secondary silica, chlorite, illite, and this ore is always associated with hydrocarbon material having a high catagenetic rank (Gauthier-Lafaye and Weber, 1989). Common sulfides include pyrite and galena. The uranium exists predominantly as fine-grained botryoidal uraninite (pitchblende) with sporadic coffinite surrounding the pitchblende. Uranyl minerals are rare or absent, but when present these minerals are always associated with recent alteration.

The high-grade ore occurs within fractured sandstones which have been interpreted as hydraulic breccias, and these are associated with faults or joints in the sandstone. As with the low-grade ore, uranium occurs as pitchblende with rare coffinite, but the high-grade ore usually occurs within secondary porosity caused by the dissolution of detrital quartz. The formation of the high grade ore is attributed to the remobilization of low-grade ore by oxidizing hydrothermal fluids, which transport the uranium along the faults, followed by precipitation within the fracture zones when conditions became more reducing. The origin of the ores in the Franceville Basin probably closely resembles the origin of the Grants district sandstone-hosted uranium deposits in New Mexico, U.S.A. (Brookins, 1980).

Uranium content within the reactor zones exceeds 20 percent and is reported as high as 60 percent U_3O_8. The reactor zones commonly contain well crystallized, cubic uraninite with depleted $^{235}U/^{238}U$ ratios. The gangue material within the reactors is generally a clay matrix without quartz. The loss of quartz is due to heat generated by the reactions (temperatures to 350°C). The type of clay mineralization within the reactor zones is related to the temperature regime (Gauthier-Lafaye *et al.*, 1989).

The reactions were possible because the $^{235}U/^{238}U$ ratio 2000 million years ago was approximately 3.5 percent (a value similar to ^{235}U enrichment for modern nuclear fuel). The

conditions leading up to spontaneous nuclear fission were discussed by Naudet (1978), who showed that criticality and subsequent nuclear reaction may occur spontaneously if the uranium content reaches 10 percent within a two centimeter-thick layer. Such concentrations occur within the high-grade ores at Oklo. The fission reactions probably occurred spontaneously in relatively small volumes within the high-grade ore. Heat generated by these fission reactions would have resulted in local convective circulation of groundwater as well as inducing uranium migration to some of the reactors zones, thereby sustaining these reactions for several thousands of years. There exist areas around the reactor zones in which isotopically normal uranium is depleted.

Fission products generated during the reactions either remained within the reactor zones or were transported by means of local circulation. Of course, since the reactions ended nearly 2000 million years ago, the short-lived radionuclides have decayed to more stable daughters. Analysis of the behavior of these short-lived radionuclide is problematic. Brookins (1978) has discussed the application of Eh-pH diagrams for addressing the retention/migration of fission products at Oklo. He maintains that thermodynamic data (25°C, 1 atm) indicate that the oxyphile elements (Y, Zr, Nb, Rh, Sn) and most chalcophile elements (Pd, Ag, Tc, Ru, In, Sb, Te) were retained within the reactor zones. Only Mo and Cd are predicted to have migrated under sulfate-stable conditions. Brookins agues that the geochemical similarity of most lanthinides to U^{4+} indicates that these, too, were retained "nearly" completely. Plutonium, Np, and Am were likely retained, while Bi and Pb would be redistributed locally without substantial migration. Most geochemical observations at Oklo support these predictions to varying degrees. The alkalis and alkaline-earths, while not adequately addressed by Eh-pH considerations only, probably experienced significant migration, although data are lacking on the behavior of these radionuclides at Oklo.

Palmottu, Finland

A small Precambrian uranium ore deposit (approx. 1800 m.y.) in southwest Finland is being studied as a potential analogue site. The host rocks consist of mica gneisses. Two types of uraniferous veins are described (Jaakkola *et al.*, 1989; Ruskeeniemi *et al.*, 1989): (1) a coarse-grained feldspar-quartz-biotite pegmatite, and (2) a sheared granitic rock rich in quartz and biotite. Average ore grade is approximately 0.1 weight percent U_3O_8. Primary ore minerals are uraninite and coffinite

The mineralogy and groundwater within the deposit are described by Jaakkola and others (1989). Groundwater redox conditions were measured by Pt electrode (dissolved oxygen was measure as well). Oxidizing conditions exist in the upper 100 meters of the deposit. Below 160 meters reducing conditions prevail. The pH increases from 7.4 close to the surface to approximately 9.0 at the drill hole bottom (195 m). Tritium values also decreased with depth to below detectable limits, indicating a lack of meteoric water infiltration at depth. Uranium concentrations were measured in groundwater from several depths, and uranium associated with particulate matter (0.45 μm filter) was compared to dissolved uranium. Uranium activity above 100 meters is in the dissolved fraction (173 $\mu g \cdot l^{-1}$ above 21 m to 83 $\mu g \cdot l^{-1}$ at 84 - 104 m). At depth (>150 m) uranium concentrations in solution decrease substantially (<10 $\mu g \cdot l^{-1}$ below 145 m). The opposite trend is observed with regard to particulate matter. The upper 100 meters show that most particulate matter contains little or no uranium, whereas uranium at depth is associated predominantly with particulate matter (the identification or composition of the particulate matter is not provided). Additionally, isotopic ratios $^{234}U/^{238}U$ were measured in the groundwater. $^{234}U/^{238}U$ in the dissolved fraction increased with depth from a value of nearly 1.0 while $^{234}U/^{238}U$ in the particulate fraction showed a slight (though less significant) decrease with depth.

Uranium is contained in primary uraninite, coffinite, monazite and is associated with Fe-oxides and clay minerals in the more altered areas. Uraninite occurs as predominantly euhedral to subhedral grains disseminated through the host rock. Uraninite is often altered to coffinite. Coffinite is precipitated along fractures and cracks short distances (<1 m) from the uraninite grains. The Fe-oxides associated with high uranium activities occur as fracture coatings in the host rock. The centers of plagioclase grains are commonly altered to "sericite" clay. The interiors of such grains show high uranium activities.

Significant dissolution of uraninite has occurred regardless of depth or the current measured oxidation potential. Jaakkola and others (1989) suggest that the oxidation potential at depth was higher in the past, perhaps due to infiltration of meteoric waters to greater depths. Giblin and Appleyard (1987), however, cite experimental evidence and evidence from natural occurrences for the dissolution of uraninite and for the mobility of uranium under strictly reducing conditions, especially in saline brines. Groundwaters at depth (>250 m) in the Palmottu deposit contain large amounts of total dissolved solids (TDS = 0.6), the dominant ions being Ca^{2+}, Na^{+}, SO_4^{2-}, Cl^{-}, HCO_3^{-}.

Krunkelbach mine, Menzenschwand, Germany

Hofmann (1989) and Dearlove and others (1989) studied the Krunkelbach mine in Menzenschwand, Germany. The groundwater composition is given in table 9. Ca^{2+}, Na^{+}, HCO_3^{-}, and SiO_2 constitute 86 percent of the total dissolved matter (Hofmann, 1989). Uranium is fixed in Fe-oxy-hydroxides (0.6 to 3.3 wt. % UO_3), gorciexite-kaolinite aggregates and "a large suite of secondary uranyl minerals" including uranocircite ($Ba(UO_2)_2(PO_4)_2 \cdot 12H_2O$), autunite ($Ca(UO_2)_2(PO_4)_2 \cdot 8\text{-}12H_2O$), heinrichite ($Ba(UO_2)_2(AsO_4)_2 \cdot 8H_2O$), uranospinite ($Ca(UO_2)_2(AsO_4)_2 \cdot 10H_2O$), and unidentified uranyl sulfates. Of significant importance is that the Ba-uranyl minerals (uranocircite and heinrichite) are much more common than their Ca equivalents (autunite and uranospinite). Although the barite is up to four times as radioactive as the pitchblende ore, it contains no microprobe-measurable uranium. The radioactivity is attributed to the incorporation of ^{226}Ra into the barite during oxidation. A late Tertiary or early Quaternary hydrothermal (approx. 150°C) event mobilized SO_4^{2-} (S derived from pyrite). The increased SO_4^{2-} dissolved the primary barite, increasing the Ba concentration in solution, thereby precipitating the Ba-uranyl phosphates.

Dearlove and others (1989) studied uranium transport and partitioning of uranium, thorium, and radium isotopes in the Krunkelbach mine. Relatively high uranium concentrations within the ore zone (1 ppm U = 4.2 $x10^{-6}$ mol·kg-1, to 4 ppm U = 16.8 $x10^{-6}$ $mol \cdot kg^{-1}$) are due to CO_2-rich waters in the ore body. Higher pH values correspond to higher uranium concentrations. The dominant uranium species in solution changes within "a few meters" from carbonate complexes (e.g. $(UO_2CO_3)^0$, $(UO_2)(CO_3)_2^{2-}$, etc) to phosphate complexes (predominantly $UO_2(HPO_4)_2^{2-}$).

TABLE 10 **Groundwater Composition, Krunkelbach mine, Germany ($x10^4 mol \cdot kg^{-1}$)**

Cl^-	0.25	SO_4^{2-}	0.52
SO_4^{2-}(ore zone)	3.1	NO_3^-	0.23
SiO_2	Na^+	86% of dissolved solids	
Ca^{2+}	HCO_3^-		
pH	6.4 to 7.3		

(Hofmann, 1989; Dearlove *et al.*, 1989)

Needle's Eye, Scotland

Roberts and others (1989) report on a geochemical study at Needle's Eye in southwest Scotland (Fig. 26). Groundwater chemistries are given in terms of depth profiles. Uranium concentrations are governed largely by changing redox conditions and U adsorption. A humic layer at the surface induces strongly reducing conditions and uranium concentrations are low at the surface (approx 5.8 $x10^{-8}$ $mol \cdot kg^{-1}$). The uranium concentration is also low at depth due to adsorption on iron-oxyhydroxides (approx. 1.3 $x10^{-7}$ $mol \cdot kg^{-1}$). Uranium concentrations reach a maximum near 107 m below the surface. This is in a relatively oxidizing zone and approximately ten meters below the phosphate concentration maximum (1.06 $x10^{-2}$ $mol \cdot kg^{-1}$) at 97 m. The phosphate concentration at 107 m is approximately 0.9 $x10^{-2}$ $mol \cdot kg^{-1}$. No mineralogical description of uranyl minerals at the Needle's Eye site is given by Roberts and others (1989).

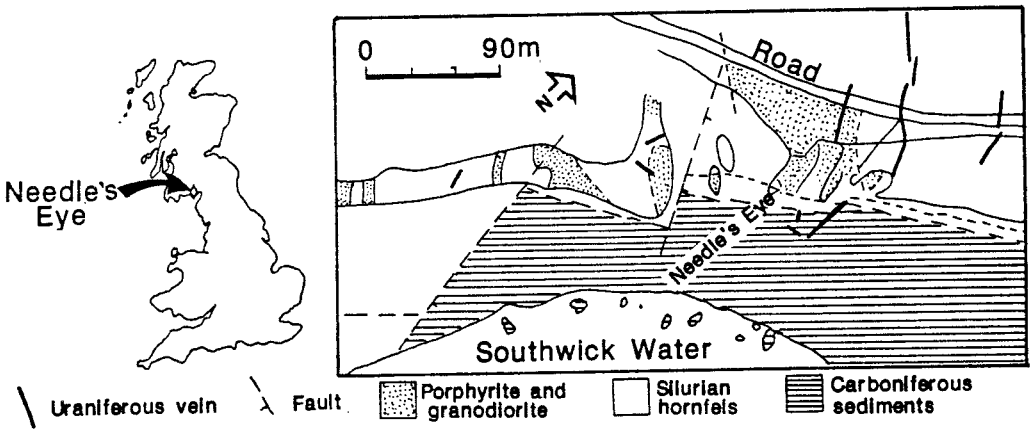

Figure 26 Geologic map of the Needle's Eye site and vicinity showing location in southern Scotland (after Hooker *et al.*, 1987).

Shinkolobwe mine, Shaba, Zaire

Finch and Ewing (in press) studied uraninite alteration products at the 1800 million year old Shinkolobwe deposit located in the Shaba province of southern Zaire (Fig. 27). The host rocks at Shinkolobwe are dolomitic shales, siliceous dolostones and chloritic siltstones (Gauthier, *et al*, 1989; Cahen *et al.*, 1984). The host rocks contribute to significant concentrations of silica, carbonate, and sulfate in the groundwater. Common uranyl complexes in solution at Shinkolobwe are therefore expected to be $[UO_2(CO_3)_2]^{2-}$, $[UO_2(CO_3)_3]^{4-}$, $[UO_2(SO_4]^{2-}$, and $[UO_2(SiO_4)]^{2-}$. Metal cations present are Ca^{2+}, Ba^{2+}, Mg^{2+}, Cu^{2+}, Pb^{2+}, Mo^{6+}, V^{5+}, and lanthanides (Ce^{3+}, La^{3+}, Y^{3+}, Gd^{3+}, Dy^{3+}). Leaching of radiogenic lead occurred 600 to 720 million years ago due to hydrothermal fluids and some alteration may have occurred at that time (Cahen *et al.*, 1984).

The uraninite at Shinkolobwe lacks many impurities (e.g. Th, lanthanides) common in uraninite. The lack of impurities suggests that the thermodynamic stability of the Shinkolobwe ore may approximate that of spent fuel. The composition of "pure" Shinkolobwe uraninite is given by Davis (1926) as (wt. %): UO_2 = 37.52, UO_3 = 52.77, PbO = 7.02, He = 0.159, N = 0.076, Ce_2O_3 = 0.22, ZrO_2 = 0.14, $(Y,Er)_2O_3$ = 0.35, $(La,Dy)_2O_3$ = 0.153 (total: 98.408). The lead is radiogenic, so that uranium and its decay products constitute over 99 weight percent of the analytical total. The uraninite alteration occurs

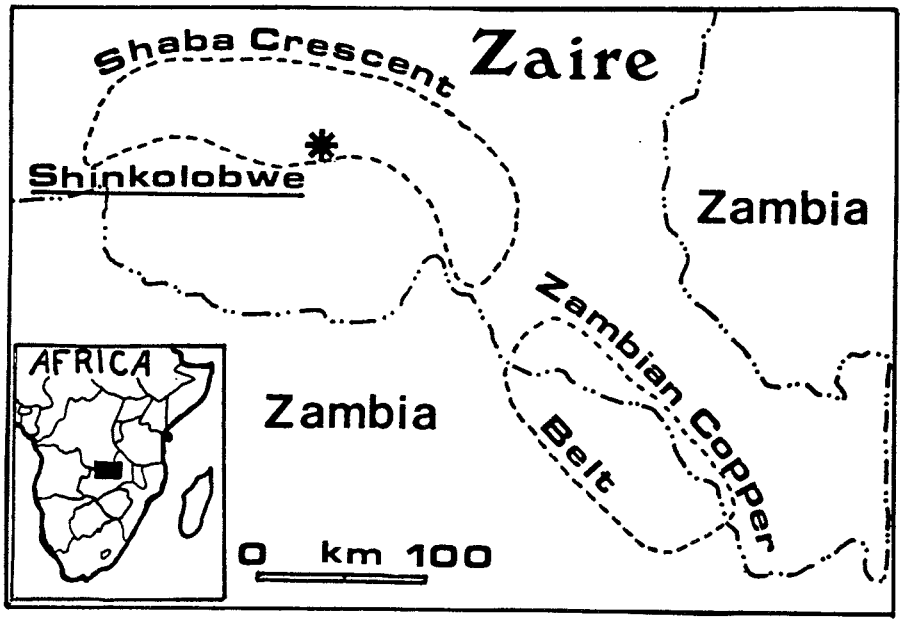

Figure 27 Location map of Shinkolobwe in the Shaba Crescent, Katanga, Zaire (after Gauthier *et al.*, 1989).

under highly oxidizing conditions. The deposit has been exposed at the surface since Tertiary time (<60 million years) and extensive weathering has significantly altered or replaced the uraninite. Uranium mineralization occurs along fracture zones in which meteoric waters have penetrated 80 meters or more.

Scanning electron microscopy, x-ray diffraction, and optical microscopy showed that the phases comprising the corrosion haloes surrounding the uraninite were undergoing further alteration. This alteration proceeded along small (approx. 1 - 2 mm) veins, and consisted of two types of alteration-related veining: 1) an increase in lead content of the minerals within a vein compared to the minerals comprising the matrix with a concomitant decrease of grain size within these veins; and 2) alteration of the uranyl oxides hydrates to uranyl silicates, and this also occurred as veins of silicates within the uranyl oxide hydrates matrix (Fig. 28). The uranyl silicate veins cross-cut the Pb-rich veins, indicating later formation. The following conclusions are presented on the alteration of uraninite from Shinkolobwe (Finch and Ewing, in press):

Figure 28 Backscattered electron image of uranyl silicate (*dark*) replacing becquerelite (*light*). Scale bar equals 100 microns.

1) Becquerelite, vandendriesscheite, fourmarierite, schoepite, billietite, and compriegnacite, are most commonly the first formed phases at the surface of the uraninite. These phases have similar structures and significant solid-solution may exist among them.

2) The earliest formed phases are often replaced by much finer-grained phases such as curite, wölsendorfite, and masuyite. Fourmarierite and vandendriesscheite are also common fine-grained constituents. These replacement minerals are generally higher in Pb than the coarser-grained minerals. The fine-grained areas occur as veins within the coarser grained matrix (Fig. 29).

3) Uranyl silicates (uranophane and cuprosklodowskite) vein the uraninite and the alteration mantle. The uranyl silicates replace the Pb-uranyl oxide hydrates and perhaps the uraninite through reaction of silica-rich groundwater with the Pb minerals. Uranyl silicates also occur as intimately intergrown crystals within the oxide hydrates. These inclusions appear to be formed concurrently with the oxide hydrates and not by replacement. The uranyl silicates appear to be the last formed phases in these samples.

4) A reduction in grain size occurs as alteration proceeds. This alteration occurs most commonly along veins rather than as concentric zones. The apparent sequence of formation for the uranium minerals studied is:
uraninite → becquerelite + billietite + compriegnacite (+ schoepite) + vandendriesscheite + fourmarierite → masuyite → curite + wölsendorfite → uranyl silicates

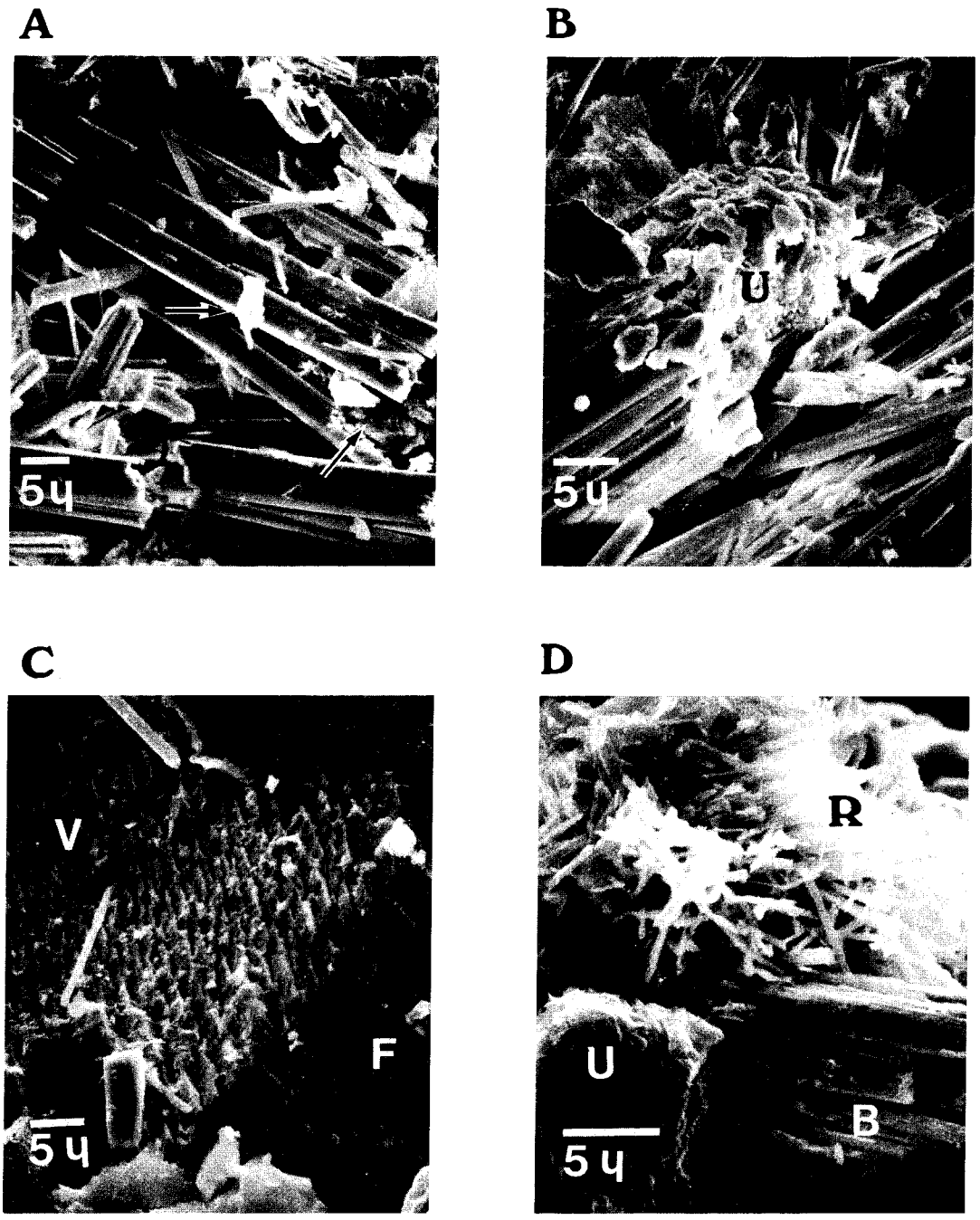

Figure 29 SEM micrographs of uraninite alteration. **A)** Euhedral becquerelite crystals with fine-grained rutherfordine (*arrows*). **B)** Becquerelite crystal being replaced by uranophane (*U*). **C)** Fourmarierite (*F*) veined by and being replaced by finer-grained Pb-uranyl oxide hydrates (*V*). The becquerelite shows a pitted surface characteristic of dissolution at the surface. Mats of an unidentified uranyl silicate are seen at the top and bottom of the image. **D)** Rutherfordine (*R*) and uranophane (*U*) with embayed crystals of becquerelite (*B*). The becquerelite is being replaced by uranophane (Finch and Ewing, in press).

SUMMARY

Uraninite is stable over a wide range of pH in reducing to moderately oxidizing environments. Uraninite consists of two coexisting oxygen-excess phases UO_{2+x} ($0.01 < x < 0.04$); and $UO_{2.25-y}$ ($0.0 < y < 0.02$). Both phases are cubic (fluorite structure type), but $UO_{2.25-y}$ shows evidence of a 4**a** x 4**a** x 4**a** superstructure (**a** = 0.5441 nm).

$UO_{2.33}$ may be stable as α-U_3O_7 under a narrow range of moderately reducing conditions (Eh = -100 mV), and α-U_3O_7 may exist as a short-lived intermediate phase prior to the dissolution or hydration of uraninite, but its existence in nature is uncertain. Higher anhydrous oxides of uranium have never been reported in nature. This may be due to a kinetic barrier to the reconstructive phase transformation between $UO_{2.25}$ (cubic) and U_3O_8 (orthorhombic).

The uranyl oxide hydrates are based on layers of uranyl polyhedra which share edges to form sheets similar to the structures of the U_3O_8 polymorphs. The uranyl oxide hydrates contain exchangeable interlayer water and cations between the structural sheets (Pagoaga *et al.*, 1987; Pagoaga, 1983). These phases are probably metastable under most geochemical conditions and alter readily to more complex uranyl phases.

Pseudomorphous replacement of uraninite by the uranyl oxide hydrates and the uranyl silicates indicates that these phases are formed early in a uranium ore body in contact with oxidizing groundwater. The phosphates may form as pseudomorphous replacement products after the Pb-uranyl oxide hydrates, or they may precipitate from groundwater solutions. The arsenates and vanadates, which are generally much less soluble than the uranyl oxide hydrates and uranyl silicates, are not reported as pseudomorphous replacement products of weathered uraninite. Instead, such phases most often occur quite removed from the source of uranium.

The stability of the UO_2 matrix, exposed to the geochemical conditions of a repository, will determine the release of radionuclides from spent fuel. Under oxidizing conditions, spent fuel will corrode and uranyl phases will be produced. The uranyl phases may form protective coatings on oxidized fuel surfaces, inhibiting further decomposition of the spent fuel, especially if they act to suppress diffusion of radionuclides from the fuel matrix to the groundwater. This would most likely be the case with the pseudomorphous replacement products such as the uranyl oxide hydrates. Conversely, the precipitation of uranyl phases may provide a "sink" for uranium in solution, thereby enhancing dissolution of the spent fuel. Subsequent alteration of the earliest formed phases will also affect the

solubility of uranium and certain fission products. The exact role of the uranyl phases on the long-term stability of spent fuel may vary with environment.

Two approaches are employed for assessing the behavior of spent fuel under oxidizing conditions: laboratory studies on fuel and UO_2, which are generally conducted from known initial conditions using a controlled environment, and natural analogue studies, which can only observe existing geochemical parameters, from which earlier conditions must be inferred. Laboratory-based studies generally provide insight into the earliest state of spent fuel corrosion, while natural analogue studies may represent a much later state of corrosion (> 10,000 years). These two methods are at the extremes of the temporal spectrum; hence, both types of study must be integrated in order to assess the performance of spent fuel over time. However, as illustrated in this report, numerous differences exist between laboratory studies and natural analogue studies, and the current level of knowledge concerning uranium solubility-controlling phases makes the correlation of these two approaches all the more important.

Laboratory-based studies are necessarily short-term experiments compared to the time required for the performance assessment of a spent fuel repository. The long-term extrapolation of the behavior of spent fuel exposed to groundwater under oxidizing conditions requires the identification of the solid phase alteration products. The only means at our disposal for "observing" the behavior of spent fuel in contact with groundwater after geologically significant periods is to examine the behavior of uraninite, because it is a natural analogue for spent fuel. Furthermore, the low radioactivity of natural samples means that they can be more easily examined by a full range of analytical techniques (e.g. EMPA, XRD, SEM, AEM). Thus, natural uranium-bearing phases may be explicitly identified, characterized, and their paragenesis determined. Unfortunately, natural analogue studies often fail to properly describe the uranium phases at the analogue site and tend to focus on current groundwater chemistry. Nevertheless, the evolution of the uranium-bearing phase assemblage and the geochemical conditions leading to the formation of these phases must be understood in order to ascertain the relevance of a natural analogue site to the future behavior of spent fuel within a repository. Without understanding the conditions under which the observed solubility-controlling phases formed, the significance of data obtained from a natural analogue study may easily be misconstrued.

A common aim of many natural analogue studies is to verify geochemical models of spent fuel corrosion and the subsequent migration or retention of important radionuclides. In this respect, natural analogue sites serve to demonstrate the major solubility-controlling

phases which must be accounted for in any geochemical model. Yet, without the proper mineralogical descriptions of the phases present, some of the most important information available from a natural analogue site is lost. Moreover, determination of the paragenesis of the alteration products observed at a natural analogue site provides invaluable information on projected reaction paths postulated by geochemical models. Finally, important differences exist between spent fuel (and its corrosion products) and analogous natural phases. These differences must be understood and quantified in order to explain dissimilarities between the results of natural analogue studies and studies on spent fuel. For these reasons, the complete characterization of uranium phases, both natural and synthetic, is critical. Proper characterization of the uranium-bearing phases is difficult and subjects which still need to be addressed include:

- Thermodynamic Stability
  solubilities, free energies
- Kinetics of Formation
  crystallinity and "aging" effects
- Paragenesis
  formation sequences, phase assemblages
- Crystal Chemistry
  structures, ion exchange, hydration, redox conditions

The number of known uranyl phases occurring in nature is staggering; over 160 have been identified. Laboratory studies which have examined the corrosion of spent fuel and synthetic UO_2 under a variety of conditions have identified only a limited number of uranium oxides, uranyl oxide hydrates, and uranyl silicates (Table 10). However, oxidizing groundwater in contact with spent fuel during the life of a repository will also promote the formation of many more complex uranyl oxide hydrates and other uranyl minerals found in nature (Appendix A). Given such complexity, the lack of adequate mineralogical data on these phases is understandable. Nonetheless, such information is critical in order to use natural analogues for the confident assessment of the long-term behavior of spent fuel under the geochemical conditions in a geologic repository.

TABLE 10 Corrosion Products Identified in Experimental Studies with Spent Fuel and Synthetic UO_2

Anhydrous oxides			
$UO_{2.25}$	β-U_3O_7	α-U_3O_8	amorphous UO_3

Uranyl Oxide Hydrates		Uranyl Silicates	
"UO_3-hydrate"		$3CaO{\cdot}4UO_3{\cdot}10SiO_2{\cdot}24H_2O$	(haiweeite-?)
$UO_3{\cdot}2H_2O$	(schoepite)	$(UO_2)(SiO_4)_2{\cdot}2H_2O$	(soddyite)
$UO_3{\cdot}0.8H_2O$	(dehydrated schoepite)	$Ca(UO_2)_2(SiO_3OH)_2{\cdot}5H_2O$	(uranophane)
$CaU_6O_{19}{\cdot}10H_2O$	(becquerelite)	$K(H_3O)UO_2(SiO_4){\cdot}nH_2O$	(boltwoodite)
$^*K_2U_6O_{19}{\cdot}11H_2O$	(compriegnacite)	$Mg(UO_2)_2(SiO_3OH)_2{\cdot}5H_2O$	(sklodowskite)
$^*Na_2U_2O_7$		"hydrated Mg-Si-uranyl oxide"	

*tentative identification

REFERENCES

AIREY, P. L. (1987) Application of natural analogue studies to the long-term prediction of far field migration at repository sites. In: *Natural Analogues in Radioactive Waste Disposal* (B. Côme and N. A. Chapman, eds.) Radioactive Waste Management Series, Graham and Trotman, 32-41.

AIREY, P. L. (1986) Radionuclide migration around uranium ore bodies in the Alligator region of the Northern Territory of Australia - Analogue of radioactive waste repositories - A review. *Chem. Geol.*, **55**, 255-268.

AIREY, P. L., P. DUERDEN, D. ROMAN, C. GOLIAN, T. NIGHTINGALE, T. PAYNE, B. G. DAVEY, D. GRAY, J. FABRYKA-MARTIN, D. B. CURTIS, A. SNELLING, D. A. LEVER, P. J. SHIRVINGTON (1987) *Radionuclide migration around uranium ore bodies -- Analogue of radioactive waste repositories*, Annual Rept.: NUREG/CR-5040, U.S.NRC

AIREY, P. L., D. ROMAN, C. GOLIAN, S. SHORT, T. NIGHTINGALE, T. PAYNE, R. T. LOWSON, P. DUERDEN, B. G. DAVEY, D. GRAY, J. ELLIS, P. J. SHIRVINGTON, M. IVANOVICH (1985) *Radionuclide migration around uranium ore bodies -- Analogue of radioactive waste repositories*, Annual Rept.: AAEC/C45, Australian Atomic Energy Commission.

AIREY, P. L. AND M. IVANOVICH (1986) Geochemical analogues of high-level radioactive waste repositories. *Chem. Geol.*, **55**, 203-213.

AIREY, P. L., D. ROMAN, C. GOLIAN, S. SHORT, T. NIGHTINGALE, T. PAYNE, R. T. LOWSON, P. DUERDEN, B. G. DAVEY, D. GRAY, J. ELLIS, P. J. SHIRVINGTON, M. IVANOVICH (1985) *Radionuclide migration around uranium ore bodies -- Analogue of radioactive waste repositories*, Annual Rept.: AAEC/C45, Australian Atomic Energy Commission.

ALLEN, G. C., P. A. TEMPEST AND J. W. TYLER (1987) Oxidation of polycrystalline UO_2 studied by using x-ray photoelectron spectroscopy. *Journ. Phys. Chem.*, **86**, 224-228.

ALLEN, G. C., P. M. TUCKER, AND J. W. TYLER (1982) Oxidation of uranium dioxide at 298 K studied by using x-ray photoelectron spectroscopy. *Journ. Phys. Chem.*, **86**, 224-228.

APT, K. E. (1976) Investigations of the Oklo natural fission reactor (July 1975 - June 1976). Los Alamos Laboratory Progress Report LA-6575-PR, 69p.

BAILEY, M. G., L. H. JOHNSON, AND D. W. SHOESMITH (1985) The effects of the alpha-radiolysis on the corrosion of UO_2. *Corr. Sci.*, **25**, 233.

BAIN, G. W. (1982) Formation of veins. In: *Vein-Type and Similar Uranium Deposits in Rocks Younger Than Proterozoic*, IAEA, Vienna, 23-33.

BARRETTO,, P. M. C., AND K. FUJIMORI (1986) Natural analogue studies: geology and mineralogy of Morro do Ferro, Brazil. *Chem. Geol.*, **55**, 297-312.

BATES, J. K., T. J. GERDING, E. VELECKIS, D. J. WRONKIEWICZ, AND B. S. TANI (1990) Leaching action of EJ-13 water on unirradiated UO_2 under unsaturated conditions at 90°C: interim report, April, 1990. Chemical Technology Division, Argonne National Laboratories, Argonne, IL, U.S.A., 81p.

BATES, J. K., B. S. TANI, E. VELECKIS, AND D. J. WRONKIEWICZ (1990) Identification of secondary phases formed during unsaturated reaction of UO_2 with EJ-13 water. In: *Scientific Basis for Nuclear Waste Management XIII* (V. M. Oversby and P. W. Brown, eds.), Mat. Res. Soc. Symp. Proc. Vol. 176, MRS, Pittsburgh, 499-506.

BELBEOCH, B., J. C. BOIVINEAU, AND P. PERIO (1967) Changements de structure de l'oxyde U_4O_9. *J. Phys. Chem. Solids*, **28**, 1267.

BELL, K. (1981) A review of the geochronology of the precambrian of Sakatchewan -- some clues to uranium mineralization. *Mineral. Mag.*, **44**, 371-378.

BELLE, J. (1961) Uranium dioxide properties and nuclear applications. U.S. Govt. Printing Office, Washington D.C.

BENNETT, M. J., J. B. PRICE AND P. WOOD (1987) Influence of manufacturing route and burnup on the oxidation and fission gas release behaviour of irradiated uranium dioxide in air at 175-400°C. In: *Proceedings from Chemical Reactivity of Oxide Fuel and Fission Product Release*, Berkeley Nuclear Laboratories, Berkeley, CA, 157-174.

BERGSTROM, G., AND G. LUNDGREN (1956) X-ray investigations of uranyl hydroxides I: Crystal structure of -$UO_2(OH)_2$. *Acta Chem. Scand.*, **10**, 673.

BERMAN, R. M. (1957) The role of lead and excess oxygen in uraninite. *Am. Min.*, **42**, 705.

BJURSTRÖM, S. AND J. LEFEVRE (1990) Waste management approaches in Europe. In: *Proceedings of the Seventh Pacific Basin Nuclear Conference*, San Diego, CA, March 4-8, 1990. *Trans Am. Nucl. Soc.*, 118-129.

BLOMEKE, J. O.(1955) ORNL-1904.

BROOKER, E. J. AND E. W. NUFFIELD (1952) Studies of radioactive compounds: IV -- pitchblende from Lake Athabasca, Canada. *Am. Min.*, **37**, 363-385.

BROOKINS, D. G. (1988) Revised Eh-pH diagrams (25°C, one bar) for uranium and transuranic elements: application to radioactive waste studies. In: *Materials Stability and Environmental Degradation* (A. Barkatt, L. R. Smith, E. Verink, eds.), Mat. Res. Soc. Symp. Proc. Vol. 125, MRS, Pittsburgh, 161-168.

BROOKINS, D. G. (1980) Syngenetic model for some early proterozoic uranium deposits: some evidence from Oklo. In: *Uranium in the Pine Creek Geosyncline* (J. Ferguson and A. B. Goleby, eds.), IAEA, Vienna, 709-719.

BROOKINS, D. G. (1978) Applications of Eh-pH diagrams to problems of retention and/or migration of fissionogenic elements at Oklo. In: *Natural Fission Reactors*, IAEC, Vienna, 243-265.

BROPHY, G. P. AND P. F. KERR (1953) Hydrous uranium molybdate in Marysvale [Utah] ore, a preliminary report. In: Annual report for June 30, 1952, to April 1 1953, U.S.Atomic Energy Comm. Tech. Inf. Service Extension, Oak Ridge, TN, U.S.

BRUNO, J., R. S. FORSYTH AND L. O. WERME (1985) Spent UO_2-fuel dissolution. Tentative modelling of experimental apparent solubilities. In: *Scientific Basis for Nuclear Waste Management VIII* (C. M. Jantzen, J. A. Stone, R. C. Ewing, eds.), Mat. Res. Soc. Symp. Proc. Vol. 44, MRS, Pittsburgh, 413-420.

BRUNO, J. AND I. PUIGDOMENECH (1989) Validation of the SKBU1 data base for its use in geochemical calculations with EQ3/6. In: *Scientific Basis for Nuclear Waste Management XII* (W. Lutze and R. C. Ewing, eds.), Mat. Res. Soc. Symp. Proc. Vol. 127, MRS, Pittsburgh, 887-896.

BRUNO, J. AND A. SANDINO (1989) The solubility of amorphous and crystalline schoepite in neutral to alkaline aqueous solutions. In: *Scientific Basis for Nuclear Waste Management XII* (W. Lutze and R. C. Ewing, eds.), Mat. Res. Soc. Symp. Proc. Vol. 127. MRS, Pittsburgh, 871-878.

BRUNO, J., I. CASAS, B. LAGERMAN, M. MUNOZ (1987) The determination of the solubility of amorphous $UO_{2(s)}$ and the mononuclear hydrolysis constants of uranium(IV) at 25°C. In: *Scientific Basis for Nuclear Waste Management X*, (J. K. Bates and W. S. Seefelt, eds.), Mat. Res. Soc. Symp. Proc. Vol. 84, MRS, Pittsburgh, 153-160.

BRUSH, L. H. (1980) The solubility of some phases in the system UO_3-Na_2O-H_2O in aqueous solutions at 60 and 90°C. Ph.D dissertation, Harvard University, Cambridge, Mass.

CADELLI, N. (1987) Natural analogues and performance assessments. A point of view based on the PAGIS experience.. In: *Natural Analogues in Radioactive Waste Disposal* (B. Côme and N. A. Chapman, eds.) Radioactive Waste Management Series, Graham and Trotman, 3-11.

CAHEN, L., N. J. SNELLING, J. DELHAL, AND J. R. VAIL (1984) *The Geochronology and Evolution of Africa*, Clarendon Press, Oxford, 512p.

CATHELINEAU, M., AND M. VERGNEAUD (1989) U-Th-REE mobility and diffusion in granitic environments during alteration of accessory minerals and U-ores: a geochemical analogue to radioactive waste disposal. In: *Scientific Basis for Nuclear Waste Management XII* (W. Lutze and R. C. Ewing, eds.), Mat. Res. Soc. Symp. Proc. Vol. 127. MRS, Pittsburgh, 941-947.

CAMPBELL, T. K., E. R. GILBERT, C. A. KNOX, G. WHITE, G. F. PIEPEL, C. W. GRIFFIN (1987) Interim Results from UO_2 Fuel Oxidation Tests in Air. PNL-6201, Pacific Northwest Laboratory, Richland, WA.

CESBRON, F., W. L. BROWN AND P. BARIAND (1972) Rameauite and agrinierite, two new hydrated complex uranyl oxides from Margnac, France. *Mineral. Mag.*, **299**, 781-789.

CHEN, Z., AND Y. HUANG (1990) A new uranium mineral - Yingjiangite. In: ABSTRACTS, vol. 2, The 15th General Meeting of the IMA, 28 June to 3 July, 1990, Beijing, China.

CHOPPIN, G. R. (1990) Actinide speciation in spent fuel leaching studies. In: *Scientific Basis for Nuclear Waste Management XIII* (V. M. Oversby and P. W. Brown, eds.), Mat. Res. Soc. Symp. Proc. Vol. 176, MRS, Pittsburgh, 449-456.

CHRIST, C. L., AND J. R. CLARK (1960) Crystal chemical studies of some uranyl oxide hydrates. *Am. Min.*, **45**, 1026-1061.

CHRISTENSEN, H., AND A. BJERBAKKE (1987) Radiation induced dissolution of UO_2. In: *Scientific Basis for Nuclear Waste Management X*, (J. K. Bates and W. S. Seefelt, eds.), Mat. Res. Soc. Symp. Proc. Vol. 84, MRS, Pittsburgh, 115-122.

CLARK, J. R. (1960) X-ray study of alteration in the uranium mineral wyartite. *Am. Min.*, **45**, 200-208.

COLEMAN,R. G., AND D. E. APPLEMAN (1957) Umohoite from the Lucky Mc mine, Wyoming. *Am. Min.*, **42**, 657-660

CORDFUNKE, E. H. P. (1969) *The Chemistry of Uranium.* Elsevier, 256p.

CORDFUNKE, E. H. P., AND P. C. DEBETS (1964) Preparation and properties of a new monohydrate of uranium trioxide - $UO_3 \cdot H_2O$. *J. Inorg. Nucl. Chem.*, **26**, p1671.

CRAMER, J. J. (1986a) Sandstone-hosted uranium deposits in northern Saskatchewan as natural analogs to nuclear fuel waste disposal vaults. *Chem. Geol.*, **55**, 269-279.

CRAMER, J. J. (1986b) A natural analogue for a fuel waste disposal vault. In: *Proceedings of 2nd Int. Conf. Radioactive Waste Management*, Can. Nucl. Soc., Winnipeg, Canada, Sept. 7-11, 1986, 697-702.

CRAMER, J. J., P. VILKS, AND J. P. A. LAROCQUE (1987) Near field analog features from the Cigar Lake uranium deposit. In: *CEC Symposium "Natural Analogs in Radioactive Waste Disposal"*, Brussels, April 28-30, 1987, Proceedings.

CRICK, I. H. AND M. D. MUIR (1980) Evaporites and uranium mineralization in the Pine Creek Geosyncline. In: *Uranium in the Pine Creek Geosyncline* (J. Ferguson and A. B. Goleby, eds.), IAEA, Vienna, 531-542.

CURTIS, D., T. BENJAMIN, A. GANCARZ, R. LOSS, K. ROSSMAN, J. DELAETER, J. E. DELMORE, W. J. MAECK (1989) Fission product retention in the Oklo natural fission reactors. *Appl. Geochem.*, **4**, 42-69.

CURTIS, D., T. BENJAMIN, A. GANCARZ, R. LOSS, K. ROSSMAN, J. DELAETER, J. E. DELMORE, W. J. MAECK (1987) Geochemical controls on the retention of fission products at the Oklo natural fission reactors. In: *Natural Analogues in Radioactive Waste Disposal* (B. Côme and N. A. Chapman, eds.) Radioactive Waste Management Series, CEC, Graham and Trotman, London, 140-141.

DAHLKAMP, F. (1978) Geologic appraisal of the Key Lake U-Ni deposits, northern Saskatchewan, Canada. *Econ. Geol.*, **73(8)**, 1430-1449

DALL'AGLIO, M., R. GRAGNANI AND E. LOCARDI (1974) Geochemical factors controlling the formation of the secondary minerals of uranium. In: *Formation of Uranium Ore Deposits.* Internat. Atomic Energy Agency, Vienna, 33-48.

DANA, E. S. (1892) *System of Mineralogy, 6th Edition.* Wiley and Sons, New York.

DAVIDSON, G. I., AND S. S. GANDHI (1989) Unconformity-related U-Au mineralization in the Middle Protoerozoic Thelon Sandstone, Boomerang Lake Prospect, Northwest Territories, Canada. *Econ. Geol.*, **84**, 143-157.

DAVIS, C. W. (1926) The composition and [illegible] of uranium minerals from Katanga, South Dakota, and Utah. *Amer. Journ. Sci.*, **11**, 201.

DEARLOVE, J. P. L., D. C. GREEN AND M. IVANOVICH (1989) Uranium transport and the partitioning of U, Th and Ra isotpes between solid and aqueous phases in the Krunkelbach mine, Federal Republic of Germany. In: *Scientific Basis for Nuclear Waste Management XII* (W. Lutze and R. C. Ewing, eds.), Mat. Res. Soc. Symp. Proc. Vol. 127. MRS, Pittsburgh, 927-932.

DEBETS, P. G., AND B. O. LOOPSTRA (1963) Uranates of ammonium.II. X-ray investigations of the compounds in the system NH_3-UO_3-H_2O. *J. Inorg. Nucl. Chem.*, **25**, 945.

DELANEY, J. M. (1985) Reaction of Topopah Spring Tuff with J-13 water: a geochemical modeling approach using the EQ3/6 reaction path code. Lawrence Livermore National Laboratory, UCRL-53631.

DELIENS, M. (1977) Associations de Minèraux secondaires d'uranium à Shinkolobwe (règion du Shaba, Zaïre). *Soc. fr. Minèr. Crystallogr.*, **100**, 32-38.

DELIENS, M. (1977) Review of the hydrated oxides of U and Pb, with new x-ray powder data. *Mineral. Mag.*, **41**, 51-57.

DELIENS, M., AND P. PIRET (1989) Shabaite-(Nd), $Ca(REE)_2(UO_2)(CO_3)_4(OH)_2 \cdot 6H_2O$, new mineral species from Kamoto, Shaba, Zaire. *Eur. J. Mineral.*, **1**, 85.

DELIENS, M., P. PIRET AND G. COMBLAIN (1981) *Les Mineraux Secondaires d'Uranium du Zaïre.* Musèe Royal de l'Afrique Centrale, Tervuren, Belgique, 113p.

DELIENS, M., P. PIRET AND G. COMBLAIN (1984) *Les Mineraux Secondaires d'Uranium du Zaïre -- Complement.* Musèe Royal de l'Afrique Centrale, Tervuren, Belgique, 37p.

DELIENS, M., AND P. PIRET (1983) Metastudtite, $UO_4 \cdot 2H_2O$, a new mineral from Shinkolobwe, Shaba, Zaire. *Am. Min.*, **68**, p456.

DEVIVO, B., F. IPPOLITO, G. CAPALDI,, AND P. R. SIMPSON, (eds.) (1985) *Uranium Geochemistry, Mineralogy, Geology, Exploration and Resources.* Institute of Mining and Metallurgy, London, 201p.

DICKSON, B. L. AND A. A. SNELLING (1980) Movement of uranium and daughter isotopes in the Koongarra uranium deposit. In: *Uranium in the Pine Creek Geosyncline* (J. Ferguson and A. B. Goleby, eds.), IAEA, Vienna, 499-507.

DUERDEN, P., G. GOLIAN, C. J. HARDY, T NIGHTINGALE, T. PAYNE (1987) Alligator rivers analogue project. Review of research and its implications for model validation. In: *Natural Analogues in Radioactive Waste Disposal* (B. Côme and N. A. Chapman, eds.) Radioactive Waste Management Series, CEC, Graham and Trotman, London, 82-91.

DUERDEN, P., AND C. J. HARDY (1990) The international Alligator Rivers Natural Analogue Project progress and future plans. In: *Proceedings of the Seventh Pacific Basin Nuclear Conference*, San Diego, CA, March 4-8, 1990. *Trans. Am. Nucl. Soc.*, 309-313.

DUERDEN, P., D. ROMAN, C. GOLIAN, T. NIGHTINGALE, T. PAYNE, R. T. LOWSON, B. G. DAVEY, R. EDGHILL, D. GRAY, S. N. DAVIS, J. FABRYKA-MARTIN, D. B. CURTIS, A. SNELLING (1988) *Radionuclide migration around uranium ore bodies -- Analogue of radioactive waste repositories,* Annual Rept.: ANSTO/C72, Australian Nuclear Science and Technology Organisation.

EDGHILL, R. (in press) The redistribution of uranium with weathering in the Koongarra uranium deposit. *Radiochim. Acta*

EINZIGER, R. E. AND R. V. STRAIN (1986) Oxidation of spent fuel between 250 and 360°C. EPRI NP-4524, Electric Power Research Institute, Palo Alto, CA.

EPSTEIN, G. Yu. (1959) On molybdates of uranium — moluranite and iriginite. *Zap. Vses. Miner. Obshch.*, **88**, 564-570.

EVANS, H. T. (1963) Uranyl ion coordination. *Science*, **141**, 154.

EWERS, G. R. AND J. FERGUSON (1980) Mineralogy of the Jabiluka, Koongarra, and Nabarlek uranium deposits. In: *Uranium in the Pine Creek Geosyncline* (J. Ferguson and A. B. Goleby, eds.), IAEA, Vienna, 363-374..

EYAL, Y., AND R. L. FLEISCHER (1985) Preferential leaching and the age of radiation damage from alpha decay in minerals. *Geochim. cosmochim. Acta*, **49**, 1155

FABRYKA-MARTIN, J. T., D. ROMAN, P. L. AIREY, D. ELMORE, P. W. KUBIC (1987) Distribution of natural ^{129}I among mineral phases and groundwater in the Koongarra uranium ore deposit, N. T., Australia. In: *Natural Analogues in Radioactive Waste Disposal* (B. Côme and N. A. Chapman, eds.) Radioactive Waste Management Series, CEC, Graham and Trotman, London, 374-385.

FERGUSON, J. AND J. C. ROWNTREE (1982) The uranium cycle and the development of vein-type deposits. In: *Vein-Type and Similar Uranium Deposits in Rocks Younger Than Proterozoic*, IAEA, Vienna, 3-9.

FINCH, R. J. AND R. C. EWING (in press) Phase relation of the uranyl oxide hydrates and their relevance to the disposal of spent fuel. MRS Proceedings *Scientific Basis for Nuclear Waste Management XIX*, November, 1990.

FINCH, R. J. AND R. C. EWING (in press) Alteration of natural UO_2 under oxidizing conditions from Shinkolobwe, Katanga, Zaire: A natural analogue for the corrosion of spent fuel. *Radiochim. Acta.*

FISHMAN, N. S., R. L. REYNOLDS AND J. F. ROBERTSON (1985) Uranium mineralization in the Smith Lake district of the Grants uranium region, New Mexico. *Econ. Geol.*, **80(5)**, 1348-1364.

FLEISCHER, M. (1989) Additions and corrections to the Glossary of Mineral Species, 5th Edition (1987). *Min. Record.*, **20**, 289-298.

FLEISCHER, M. (1987) *Glossary of Mineral Species, Fifth Edition.* Mineralogical Record, Inc. P.O.Box 35565, Tucson, AZ, 85740.

FLEISCHER, R. L. (1988) Alpha-recoil damage Relation to isotopic disequilibrium and leaching of radionuclides. *Geochim. cosmochim. Acta*, **52**, 1459.

FORSYTH, R. S., L. O. WERME AND J. BRUNO (1986) The corrosion of spent UO_2 fuel in synthetic groundwater. *J. Nucl. Mater.*, **138**, 1.

FORSYTH, R. S., U-B. EKLUND, O. MATTSSON, D. SCHRIRE (1990) Examination of the surface deposit on an irradiated PWR fuel specimen subjected to corrosion in deionized water. SKB Technical Report **90-04**.

FORSYTH, R. S., T. JONSSON, O. MATTSSON (1990) Examination of reaction products on the surface of UO_2 fuel exposed to reactor coolant water during power operation. SKB Technical Report **90-07**.

FOUQUES, J. P., M. FOWLER, H. D. KNIPPING, K. SCHIMANN (1986) Geology of the Cigar Lake uranium deposit - Discovery and general characteristics. *Can. Inst. Mining Bulletin*, **79**, 70-82.

FOY, M. F. AND C. P. PEDERSON (1975) Koongarra uranium deposit. In: *Economic Geology of Australia and Papua New Guinea*, Ausralis Inst. Min. Metall. Monograph Series No. 5,1. Metals, 317-321.

FRANCO, P., P. TROCELLIER, F. MENES (1989) UO_2 corrosion study in mineral water: A surface analysis approach. In: *Scientific Basis for Nuclear Waste Management XII* (W. Lutze and R. C. Ewing, eds.), Mat. Res. Soc. Symp. Proc. Vol. 127, MRS, Pittsburgh, 343-349.

FRANÇOIS, A. (1987) Synthèse gèologique sur l'Arc Cuprifère du Shaba (Rèp. du Zaïre). *Centenaire de la Sociètè Gèologie, Bruxelles, Belgique*, **56**.

FREEBORN, W. P., M. E. ZOLENSKY, B. E. SHEETZ, S. KOMARNENI, G. J. MCCARTHY, W. B. WHITE (1980) Shale rocks as nuclear waste repositories: hydrothermal reactions with glass, caramics and spent fuel waste forms. In: *Scientific Basis for Nuclear Waste Management II* (C. J. M. Northrup, Jr., ed.), Plenum Press, NY, 499.

FRONDEL, C. (1958) Systematic mineralogy of uranium and thorium. *Geol. Soc. Amer. Bulletin* **1064**, 399p.

FRONDEL, C. (1956) Mineral composition of gummite. *Am. Min.*, **41**, 539-568.

FRONDEL, C., AND R. MEYROWITZ (1956) Studies of uranium minerals (XIX): rutherfordine, diderichite, and clarkeite. *Am. Min.*, **41**, 127-133.

FRONDEL, J. W. AND F. CUTTITTA (1953) Studies of uranium minerals (XIV): the status of billietite and becquerelite. *Am. Min.*, **38**, 1019-1024.

FUCHS, L. H., AND E. GEBERT (1958) X-ray studies of coffinite, thorite and uranothorites. *Am. Min.*, **43**, 243-248.

GALKIN, N. P. AND N. A. STEPANOV (1961) Solubility of uranium (IV) hydroxide in sodium hydroxide. *Soviet Journ. Atomic Energy*, **2**, 231-233.

GARLICK, W. G. (1989) Mineralization controls and source of metals in the Lufilian Fold Belt, Shaba (Zaire), Zambia, and Angola - a discussion. *Econ. Geol.*, **84**, 963-973.

GARISTO, N. C. AND F. GARISTO (1986) The dissolution of UO_2: a thermodynamic approach. *Nucl. Chem. Waste Man.*, **6**, 203-211.

GAUTHIER, G., A. FRANÇOIS, M. DELEINS, AND P. PIRET (1989) The uranium deposits of the Shaba Region, Zaire. *Miner. Record*, **20**, 26-288.

GAUTHIER-LAFAYE, F., AND F. WEBER (1989) The Francevillian (Lower Proterozoic) uranium ore deposit of Gabon. *Econ. Geol.*, **84**, 2267-2285.

GAUTHIER-LAFAYE, F., F. WEBER, N. NAUDET, J. P. PFIFFELMAAN, R. CHAUVET, B. MICHEL, J. C. REBOUL (1982) Le Gisement d'Oklo et ses reacteurs de fission naturels. In: *Uranium in the Pine Creek Geosyncline* (J. Ferguson and A. B. Goleby, eds.), IAEA, Vienna, 663-673.

GAUTHIER-LAFAYE, F., F. WEBER AND H. OHMOTO (1989) Natural Fission reactors of Oklo. *Econ. Geol.*, **84**, 2286-2295.

GIBLIN, A. (1982) The role of clay adsorption in genesis of uranium ores. In: *Uranium in the Pine Creek Geosyncline* (J. Ferguson and A. B. Goleby, eds.), IAEA, Vienna, 521-529.

GIBLIN, A., M., AND E. C. APPLEYARD (1987) Uranium mobility in non-oxidizing brines: field and experimental evidence. *Appl. Geochem.*, **2**, 285-295.

GOLIAN, C., AND P. DUERDEN (1987) Application of open system modelling to studies of secondary mineralization (Koongarra) and rock matrix diffusion (Kräkemäla). In: *Natural Analogues in Radioactive Waste Disposal* (B. Côme and N. A. Chapman, eds.) Radioactive Waste Management Series, CEC, Graham and Trotman, London, 328-341.

GRAMBOW, B., R. S. FORSYTH, L. O. WERME, AND J. BRUNO (in press) Fission product release from spent UO_2 fuel under uranium-saturated oxic conditions. *J. Nucl. Tech.*

GRAMBOW, B., L. O. WERME, R. S. FORSYTH, AND J. BRUNO (1990) Constraints by experimental data for modelling of radionuclide release from spent fuel. In: *Scientific Basis for Nuclear Waste Management XIII* (V. M. Oversby and P. W. Brown, eds.), Mat. Res. Soc. Symp. Proc. Vol. 176, MRS, Pittsburgh, 465-474.

GRANDSTAFF, D. E. (1976) A kinetic study of the dissolution of uraninite. *Econ. Geol.*, **71**, 1493.

GRAY, W. J., D. M. STRACHEN, AND M. J. APTED (in press) Grain boundary inventory and UO_2 matrix dissolution studies on spent LWR fuel.

GREEGOR, R. B., F. W. LYTLE, B. C. CHAKOUMAKOS, G. R. LUMPKIN, R. C. EWING (1989) An investigation of uranium L-edges of metamict and annealed betafite. In: *Scientific Basis for Nuclear Waste Management XII* (W. Lutze and R. C. Ewing, eds.), Mat. Res. Soc. Symp. Proc. Vol. 127, MRS, Pittsburgh, 261-268.

GUILLEMIN, C., AND J. PROTAS (1959) Ianthinite et wyartite. *Bull. Soc. fr. Minèr. Crystallogr.*, **82**, p80.

GUTHRIE, V. A. (1989) Fission-track analysis of uranium distribution in granitic rocks. *Chem. Geol.*, **77**, 87-103.

HABASHI, F., AND G. A. THURSTON (1966) Kinetics and mechanism of the dissolution of uranium dioxide. *Energia Nucleare*, **14**, 238.

HANCOX, W. T. (1990) The Canadian approach to safe, permanent disposal of nuclear fuel waste. In: *Proceedings of the Seventh Pacific Basin Nuclear Conference*, San Diego, CA, March 4-8, 1990. *Trans Am. Nucl. Soc.*, 102-110.

HANSULD, J. A. (1966) Eh and pH in geochemical prospecting. In: *Proceedings, Symposium on Geochemical Prospecting, April, 1966, Ottawa*, Geol. Surv. Canada Paper 66-54, 172-187.

HARDING, J. H., AND D. G. MARTIN (1989) A recommendation for the thermal conductivity of UO_2. *Journ. Nucl. Mater.*, **166**, 223-226.

HOEKSTRA, H. R., AND S. SIEGEL (1973) The uranium trioxide-water system. *J. Inor. Nucl. Chem.*, **35**, 761-779.

HOEKSTRA, H. R., S. SIEGEL, L. H. FUCHS, J. J. KATZ (1955) The uranium-oxygen system: $UO_{2.5}$ to U_3O_8. *J. Phys. Chem.*, **59**, 136-138.

HOEKSTRA, H. R., S. SIEGEL AND F. X. GALLAGHER (1970) The uranium-oxygen system at high pressure. *J. Inor. Chem.*, **32**, 3237-3248.

HOEVE, J., AND T. I. I. SIBBALD (1978) On the genesis of Rabbit Lake and other unconformity-type uranium deposits in northern Saskatchewan, Canada. *Econ. Geol.* **73(8)**, 1450-1473.

HOFMANN, B. A. (1989) Geochemical analogue study in the Krunkelbach Mine, Menzenschwand, southern Germany: geology and water-rock interaction. In: *Scientific Basis for Nuclear Waste Management XII* (W. Lutze and R.C. Ewing, eds.), Mater. Res. Soc. Symp. Proc. Vol. 127, MRS, Pittsburgh, 921-926.

HOOKER, P. J., N. A. CHAPMAN, A. B. MACKENZIE, R. D. SCOTT, M. IVANOVICH (1987) Natural analogues of radionuclide migration in sediments in Britain. In: *Natural Analogues in Radioactive Waste Disposal* (B. Côme and N. A. Chapman, eds.) Radioactive Waste Management Series, CEC, Graham and Trotman, London, 104-115.

HOSTETLER, P. B., AND R. M. GARRELS (1962) Transportation and precipitation of uranium and vanadium at low temperatures, with special reference to sandstone-type uranium deposits. *Econ. Geol.*, **57**, 137.

HUSSONNOIS, M., R. GUILLAUMONT, L. BRILLARD, M. FATTAHI (1989) A method for determining the oxidation state of uranium at concentration as low as 10^{-10} M. In: *Scientific Basis for Nuclear Waste Management XII* (W. Lutze and R. C. Ewing, ed.), Mat. Res. Soc. Symp. Proc. Vol. 127. MRS, Pittsburgh, 979-984.

ILGER, J. D., W. A. ILGER, R. A. ZINGARO, M. S. MOHAN (1987) Modes of occurrence of uranium in carbonaceous uranium deposits: characterization of uranium in a south Texas (U.S.A.) lignite. *Chem. Geol.*, **63**, 197-216.

INTERNATIONAL ATOMIC ENERGY AGENCY (1978) *Natural Fission Reactors*. IAEA, Vienna, 754p.

ISOBE, H., AND T. MURAKAMI (in press) Alteration of chlorite in the Koongarra uranium deposit and its implication for uranium migration. *Radiochim. Acta*

IVANOVICH, M., P. DUERDEN, T. PAYNE, T. NIGHTINGALE, G. LONGWORTH, M. A. WILKINS, R. B. EDGHILL, D. J. COCKAYNE, B. C. DAVEY (1987) Natural analogue study of the distribution of uranium series radionuclides between the colloid and solute phases in the hydrogeological system of the Koongarra uranium deposit N. T., Australia. In: *Natural Analogues in Radioactive Waste Disposal* (B. Côme and N. A. Chapman, eds.) Radioactive Waste Management Series, CEC, Graham and Trotman, London, 300-313.

JAAKOLA, T., J. SUKSI, R. SUUTARINEN, H. NIINI, T. RUSKEENIEMI, B. SÖDERHOLM, M. VESTERINEN, R. BLOMQVIST, S. HALONEN, A. LINDBERG (1989) The behavior of natural radionuclides in and around uranium deposits. 2. Results of investigations at the Palmottu analogue site, SW Finland. *Geol Surv. Finland, Nuclear Waste Disposal Research Report* **YST-64**, Espoo, Finland, 60p.

JOHNSON, L. H. AND H. H. JOLING (1982) The dissolution of irradiated fuel under hydrothermal conditions. In: *Scientific Basis for Nuclear Waste Management IV* (S. V. Topp, ed.), Mat. Res. Soc. Symp. Proc. Vol. 6, MRS, Pittsburgh, 321-327.

JOHNSON, L. H., AND D. W. SHOESMITH (1988) Spent fuel. In: *Radioactive Wasteforms for the Future* (W. Lutze and R. C. Ewing, eds.). Elsevier, 635-698.

JOHNSON, L. H., D. W. SHOESMITH, G. E. LUNANSKY, M. G. BAILEY, AND P. R. TREMAIN (1982) *Nucl. Technol.*, **56**, 238.

KNIPPING, H. D. (1974) The concept of supergene versus hypogene emplacement of uranium at Rabbit Lake, Saskatchewan, Canada. In: *Formation of Uranium Deposits*. IAEA, Vienna, 531-549.

KOUL, S. L., A. R. WAILD, V. J. WALL, A. K. TICKOO (1988) Fission track annealing behavior of minerals of the East Alligator River uranium field, N. T. Australia. *Min. Journ.*, **14**(2), 48-55.

KRAUSKOPF, K. B. (1986) Aqueous geochemistry of radioactive waste disposal. *Appl. Geochem.*, **1**, 15-23.

KRUPKA, K. M., D. RAI, R. W. FULTON, R. G. STRICKERT (1985) Solubility data for U(VI) hydroxide and Np(IV) hydrous oxide: application of MCC-3 methodology. In: *Scientific Basis for Nuclear Waste Management VIII* (C. M. Jantzen, J. A. Stone, R. C. Ewing, eds.), Mat. Res. Soc. Symp. Proc. Vol. 44, MRS, Pittsburgh, 753-760.

LAHALLE, M. P., J. C. KRUPPA, R. GUILLAUMONT, M. GENET, G. C. ALLEN, AND N. R. HOLMES (1989) Surface analysis of UO_2 leached in mineral water studied by x-ray photoelectron spectroscopy. In: *Scientific Basis for Nuclear Waste Management XII* (W. Lutze and R. C. Ewing, eds.), Mat. Res. Soc. Symp. Proc. Vol. 127. MRS, Pittsburgh, 351-357.

LANGMUIR, D. (1978) Uranium solution-mineral equilibria at low temperatures with applications to sedimentary ore deposits. *Geochim. cosmochim. Acta*, **42**, 547-569.

LEE, M. J. (1976) Geochemistry of the sedimentary uranium deposits of the Grants Mineral Belt, southern San Juan Basin, New Mexico. Ph.D. dissertaion, Univ. New Mexico, 241p.

LEI, W., P. LINSALATA, E. PENNA FRANCA, M. EISENBUD (1986) Distribution and mobilization of cerium, lanthanum and neodymium in the Morro do Ferro Basin, Brazil. *Chem. Geol.*, **55**, 313-322.

LEVENTHAL, J. S, R. I. GRAUCH, C. N. THRELKELD, F. E. LICHTE, C. T. HARPER (1987) Unusual organic matter associated with uranium from the Claude deposit, Cluff Lake Canada. *Econ. Geol.* **82**(5), 1169-1176.

LEVER, D. A. (1987) Natural analogues and radionuclide transport model validation. In: *Natural Analogues in Radioactive Waste Disposal* (B. Côme and N. A. Chapman, eds.) Radioactive Waste Management Series, CEC, Graham and Trotman, London, 23-31.

LINSALATA, P., E. P. FRANCA, AND M. EISENBUD (1987) Biogeochemical studies of the Ra, U, Th, and REE deposit at Morro do Ferro: A qualitative application to improve confidence in radionuclide immobilization processes. In: *Natural Analogues in Radioactive Waste Disposal* (B. Côme and N. A. Chapman, eds.) Radioactive Waste Management Series, CEC, Graham and Trotman, London, 116-117.

LOOPSTRA, O. (1970) The structure of β-U_3O_8. *Acta Crystallogr.*, **B26**, 656-657.

LOOPSTRA, O. (1964) Neutron diffraction investigation of U_3O_8. *Acta Crystallogr.*, **17**, 651.

LUCUTA, P. G., B. J. PALMER, HJ. MATZKE, D. S. HARTWIG (1989) Preparation and characterization of Simfuel: simulated CANDU high-burnup nuclear fuel. Second International Conf. on CANDU Fuel, October 1-5, 1989.

LUMPKIN, G. R., AND R. C. EWING (1989) Alpha-decay damage and annealing effects in natural pyrochlores: analogues for long-term radiation damage effects in actinide, pyrochlore, structure types. In: *Scientific Basis for Nuclear Waste Management XII* (W. Lutze and R. C. Ewing, eds.), Mat. Res. Soc. Symp. Proc. Vol. 127, MRS, Pittsburgh, 253-260.

LUMPKIN, G. R., AND R. C. EWING (1988) Alpha-decay damage in minerals of the pyrochlore group. *Phys. Chem. Minerals*, **16**, 2-20.

LUMPKIN, G. R. AND R. C. EWING (1987) Transmission electron microscopy of alpha-decay damage and alteration of betafite. In: *Proceedings of the 45th Annual Meeting of the Electron Microscopy Society of America*, G. W. Bailey, ed., San Fransisco Press, 376-377.

LUMPKIN, G. R., B. C. CHAKOUMAKOS, AND R. C. EWING (1986) Mineralogy and radiation effects of microlite from the Harding pegmatite, Taos County, New Mexico. *Am. Min.*, **71**, 569.

MAAS, R. (1989) Nd-Sr isotope constraints on the age and origin of unconformity-type uranium deposits in the Alligator Rivers uranium field, Northern Territory, Australia.. *Econ. Geol.*, **84**, 64-90.

MCCONNEL, D. B., AND J. J. CRAMER (1987) Simulating the movement of radium and lead away from the Cigar Lake uranium deposit. In: *Natural Analogues in Radioactive Waste Disposal* (B. Côme and N. A. Chapman, eds.) Radioactive Waste Management Series, CEC, Graham and Trotman, London, 179-190.

MEANS, J. L., A. J. MARKWORTH, J. K. MCCOY, M. P. FAILEY, M. J. STENHOUSE, R. KOHLI, AND G. C. TAYLOR (1984) Long-term performance of spent fuel waste forms. U.S. Nucl. Reg. Comm. Rept. NUREG/CR-4954.

MEUNIER, J. D., A. TROUILLER, J. BRULHET, M. PAGEL (1989) Uranium and organic matter in a paleodeltaic environment: The Coutras deposit (Gironde, France). *Econ. Geol.*, **84**, 1541-1556.

MIEKELEY, N., H. C. JESUS, C. L. P. SILVEIRA, I. L. KUECHLER (1989) Colliod investigation in the 'Poços de Caldas' natural analogue project. In: *Scientific Basis for Nuclear Waste Management XII* (W. Lutze and R. C. Ewing, eds.), Mat. Res. Soc. Symp. Proc. Vol. 127, MRS, Pittsburgh, 831-842.

MILLER, L.J. (1958) The chemical environment of pitchblende. *Econ. Geol.*, **53**, 521-544.

MUCKE, A., AND H. STRUNZ (1978) Petscheckite and liandratite, two new pegmatite minerals from Madagascar. *Am. Min.*, **63**, 941.

MUENIER, J. D., P. LANDAIS AND M. PAGEL (1990) Experimental evidence of uraninite formation from diagenesis of uranium-rich organic matter. *Geochim. cosmochim. Acta*, **54**, 809-817.

NAITO, K. (1974) Phase transitions of U_4O_9. *J. Nucl. Mater.*, **51**, 126.

NEEDHAM, R. S., I. H. CRICK, P. G. STUART-SMITH (1980) Regional geology of the Pine Creek Geosyncline. In: *Uranium in the Pine Creek Geosyncline* (J. Ferguson and A. B. Golebey, eds.), Uranium Symposium on the Pine Creek Geosyncline, Sydney, Australia, June, 1979. Internat. Atomic Energy Agency, 1980, 1-22.

NEEDHAM, R. S. AND P. G. STUART-SMITH (1980) Geology of the Alligator Rivers uranium field. In: *Uranium in the Pine Creek Geosyncline* (J. Ferguson and A. B. Golebey, eds.), Uranium Symposium on the Pine Creek Geosyncline, Sydney, Australia, June, 1979. Internat. Atomic Energy Agency, 1980, 233-256.

NERETNIEKS, I. (1986) Some uses for natural analogues in assessing the function of a HLW repository. *Chem. Geol.*, **55**, 175-188.

NICHOL, M. J., AND C. R. S. NEEDES (1977) The anodic dissolution of uranium dioxide - II. In carbonate solutions. *Electrochim. Acta*, **22**, 1381.

NICHOL, M. J., AND C. R. S. NEEDES (1975) The anodic dissolution of uranium dioxide - I. In perchlorate solutions. *Electrochim. Acta*, **20**, 585.

NOE-SPIRLET, M. R. AND R. SOBRY (1974) Les uranates hydratès ne forment pas une sèrie continue. *Bull. Soc. Royal Sci. Liège*, **43**, 164-171.

OLLILA, K. (1989) Dissolution of UO_2 at various parametric conditions: A comparison between calculated and experimental results. In: *Scientific Basis for Nuclear Waste Management XII* (W. Lutze and R. C. Ewing, eds.), Mat. Res. Soc. Symp. Proc. Vol. 127, MRS, Pittsburgh, 337-342.

PAGE, R. W., W. COMPSTON, AND R. S. NEEDHAM (1980) Geochronology and evolution of the Late-Archean basement and Proterozoic rocks in the Alligator Rivers uranium field, Northern Territory, Australia. In: *Uranium in the Pine Creek Geosyncline* (J. Ferguson and A. B. Goleby, eds.), IAEA, Vienna, 39-68.

PAGOAGA, M. K., D. E. APPLEMAN AND J. M. STUART (1987) Crystal structures and crystal chemistry of the uranyl oxide hydrates becquerelite, billietite, and protasite. *Am. Min.*, **72**, 1230-1238.

PAGOAGA, M. K., D. E. APPLEMAN AND J. M. STUART (1986) A new barium uranyl oxide hydrate, protasite. *Min. Mag.*, **50**, 125-128.

PAGOAGA, M. K. (1983) The crystal chemistry of the uranyl oxide hydrate minerals. Ph.D. Thesis, University of Maryland, 167p.

PAPP, T. (1987) The role of natural analogues in safety assessment and acceptability. In: *Natural Analogues in Radioactive Waste Disposal* (B. Côme and N. A. Chapman, eds.) Radioactive Waste Management Series, CEC, Graham and Trotman, London, 12-21.

PARKS, G. A., AND D. C. POHL (1988) Hydrothermal solubility of uraninite. *Geochim. cosmochim. Acta*, **52**, 863-875.

PEDERSON, C. P. (1978) The geology of the Koongarra deposits including investigations of contained elements. *In: Koongarra Project: Environmental Impact Statement.* Noranda Australia Ltd., Melbourne, Appendix V.

PIRET, P. (1985) Structure cristalline de la fourmarièrite, $Pb(UO_2)_4O_3(OH)_4 \cdot 4H_2O$. *Bull. Minèral.*, **108**, 659-665..

PIRET, P., AND M. DELIENS (1976) Nouvelles donèes sur une umohoite magnèsienne de Shinkolobwe (region du Shaba, Republique du Zaire). *Annls. Soc. gèol. Belg.*, **99**, 205.

PIRET, P., M. DELIENS, J. PIRET-MEUNIER AND G. GERMAIN (1983) La sayrite, $Pb_2[(UO_2)_5O_6(OH)_2] \cdot 4H_2O$, nouveau minèral; proriètès et structure cristalline. *Bull. Minèral.*, **106**, 299-304..

PIRET, P., M. DELIENS AND J. PIRET-MEUNIER (1988) La françoisite-(Nd), nouveau phosphate d'uranyl et de terres rares; propriètès et structure cristalline. *Bull. Minèral.*, **111**, 443.

PIRET-MEUNIER, J., AND P. PIRET (1982) Nouvelle determination de la structure cristalline de la becquerelite. *Bull. Minèral.*, **105**, 606-610.

POINTER, C. M., J. R. ASHWORTH AND P. R. SIMPSON (1989) Genesis of coffinite and the U-Ti association in Lower Old Red Sandstone sediments, Ousdale, Caithness, Scotland. *Mineral. Deposita*, **24**, 117-123.

POSEY-DOWTY, J., E. AXTMANN, D. CRERAR, M. BORCSIK, A. RONK, AND W. WOODS (1987) Dissolution rate of uraninite and uranium role-front ores. *Econ. Geol.*, **82**, p184.

PUIGDOMENCH, I., I. CASAS, J. BRUNO (1990) Kinetics of $UO_{2(S)}$ dissolution under reducing conditions: numerical modelling. SKB Technical Report **90-25**.

RICH, R. A., H. D. HOLLAND AND U. PETERSON (1977) Hydrothermal uranium deposits. In: *Developments in Economic Geology 6*. Elsevier, 264pp.

RILEY, G. H., R. A. BINNS, AND S. J. CRAVEN (1980) Rb-Sr cronology of micas at Jabiluka. In: *Uranium in the Pine Creek Geosyncline* (J. Ferguson and A. B. Goleby, eds.), IAEA, Vienna, 457-468..

RIMSAITE, J. (1982) Chemical and isotopic evolution of radioactive minerals in remobilized vein-type uranium deposits, Saskatchewan, Canada. In: *Vein-Type and Similar Uranium Deposits in Rocks Younger Than Proterozoic*, IAEA, Vienna, 23-33.

ROMBERGER, S. B. (184) Transport and deposition of uranium in hydrothermal systems at temperatures up to 300°C: geological implications. In: *Uranium Geochemistry, Mineralogy, Geology, Exploration, and Resources* (B. DeVivo, F. Ippolito, G. Capaldi, and P. R. Simpson, eds.). Inst. Min. Metall, 12-22.

ROSENZWEIG, A., AND R. R. RYAN (1977) Kasolite, $Pb(UO_2)(SiO_4)\cdot H_2O$. *Cryst. Struct. Comm.*, **6**, 617-621.

ROSS, C. S., E. P. HENDERSON AND E. POSNJAK (1931) Clarkeite, a new uranium mineral. *Am. Min.*, **16**, 213.

RUSKEENIEMI, T., H. NIINI, B. SÖDERHOLM, M. VESTERINEN, R. BLOMQVIST, S. HALONEN, A. LINDBERG, T. JAAKOLA, J. SUKSI, R. SUUTARINEN (1989) The Palmottu U-Th deposit in SW Finland as a natural analogue to the behavior of spent nuclear fuel in bedrock: A preliminary report. In: *Water-Rock Interaction* (Miles, ed.), Balkema, Rotterdam, 1989, 60p.

RYAN, R. R., AND A. ROSENZWEIG (1977) Sklodowskite, $MgO\cdot 2UO_3\cdot 2SiO_2\cdot 7H_2O$. *Cryst. Struct. Comm.*, **6**, 611-615.

SEGEYEVA, *et al.* (1972) Experimental investigation of equilibria in the system UO_3-CO_2-H_2O in 25-200°C interval. *Geochem. Internat.*, **9**, 900.

SHEA, M. (1987) Marysvale natural analogue study: Feasibility phase analytical results. In: *Natural Analogues in Radioactive Waste Disposal* (B. Côme and N. A. Chapman, eds.) Radioactive Waste Management Series, CEC, Graham and Trotman, London, 275-287.

SHEA, M., AND K. A. FOLAND (1986) The Marysvale natural analog study: preliminary oxygen isotope relations. *Chem. Geol.*, **55**, 281-295.

SHIRVINGTON, P. J. (1983) Fixation of radionuclides in the ^{238}U decay series in the vicinity of mineralized zones: 1. The Austatom Uranium Prospect, Northern Territory, Australia. *Geochim. cosmochim. Acta*, **47**, 403-412.

SHIRVINGTON, P. J. (1980) $^{234}U/^{238}U$ activity ratios in clays as a function of distance from primary ore. In: *Uranium in the Pine Creek Geosyncline* (J. Ferguson and A. B. Goleby, eds.), IAEA, Vienna, 509-519.

SHOESMITH, D. W., S. SUNDER, B. M. IKEDA, AND F. KING (1989) The development of a mechanistic basis for modelling fuel dissolution and container failures under waste vault conditions. In: *Scientific Basis for Nuclear Waste Management XII* (W. Lutze and R. C. Ewing, eds.), Mat. Res. Soc. Symp. Proc. Vol. 127, MRS, Pittsburgh, 279-290.

SIEGEL, S., A. VISTE, H. R. HOEKSTRA, AND B. TANI (1972) *Acta Crystallogr.*, **B28**, p117.

SMELLIE, J., L. BARROSO MAGNO, N. A. CHAPMAN, I. G. MCKINLEY, E. PENNA FRANCA (1987) The Poços de Caldas project feasilbilty study: 1986-7. In: *Natural Analogues in Radioactive Waste Disposal* (B. Côme and N. A. Chapman, eds.), Radioactive Waste Management Series, CEC, Graham and Trotman, London, 118-132.

SMELLIE, J., N. CHAPMAN, I. MCKINLEY, E.P. FRANCA, M. SHEA (1989) Testing safety assesment models using natural analogues in high natural-series groundwaters. The second year of the Poços de Caldas project. In: *Scientific Basis for Nuclear Waste Management XII* (W. Lutze and R. C. Ewing, eds.), Mat. Res. Soc. Symp. Proc. Vol. 127, MRS, Pittsburgh, 863-870.

SMITH, D. K. JR. (1984) Uranium mineralogy. In: *Uranium Geochemistry, Mineralogy, Geology, Exploration, and Resources* (B. DeVivo, F. Ippolito, G. Capaldi, and P. R. Simpson, eds.). Inst. Min. Metall.

SMITH, D. K., B. E. SCHEETZ, C. A. F. ANDERSON, AND K. L. SMITH (1982) Phase relations in the uranium-oxygen-water system and its significance on the stability of nuclear waste forms. *Uranium*, **1**, p79.

SNELLING, A. A. (1980) Uraninite and its alteration products, Koongarra uranium deposit. In: *Uranium in the Pine Creek Geosyncline* (J. Ferguson and A. B. Golebey, eds.), Uranium Symposium on the Pine Creek Geosyncline, Sydney, Australia, June, 1979. Internat. Atomic Energy Agency, 1980, 487-498.

SOBRY, R. (1973) Etude des uranates hydrates - I. Proprietes radiocristallographiques des uranates hydrates de cations bivalents. *J. Inorg. Nucl. Chem.*, **35**, 1515-1524.

SOBRY, R. (1971) Water and interlayer oxonium in hydrated uranates. *Am. Min.*, **56**, 1065-1076.

STERN, T. W., L. R. STIEFF, M. N. GIRHARD, R. MEYROWITZ (1956) The occurrence and properties of meta-tyuyamunite, $Ca(UO_2)_2(VO_4)_2 \cdot 3\text{-}5H_2O$. *Am. Min.*, **41**, 187-201.

STOHL, F. V., AND D. K. SMITH (1981) The crystal chemistry of the uranyl silicate minerals. *Am. Min.*, **66**, 610.

STOUT, P. J., G. R. LUMPKIN, R. C. EWING, AND Y. EYAL (1988) An annealing study of alpha-decay damage in natural UO_2 and ThO_2. In: *Scientific Basis for Nuclear Waste Management XI* (M. J. Apted and R. E. Westerman, eds.), Mater. Res. Soc. Symp. Proc. Vol. 112. MRS, Pittsburgh, 495.

STOUT, R. B., H. F. SHAW, AND R. E. EINZIGER (1990) Statistical model for grain boundary and grain volume oxidation kinetics in UO_2 spent fuel. In: *Scientific Basis for Nuclear Waste Management XIII* (V. M. Oversby and P. W. Brown, eds.), Mat. Res. Soc. Symp. Proc. Vol. 176. MRS, Pittsburgh, 475-488.

STUART-SMITH, P. G., K. WILLS, I. H. CRICK, R. S. NEEDHAM (1980) Evolution of the Pine Creek Geosyncline. In: *Uranium in the Pine Creek Geosyncline* (J. Ferguson and A. B. Golebey, eds.), Uranium Symposium on the Pine Creek Geosyncline, Sydney, Australia, June, 1979. Internat. Atomic Energy Agency, 1980, 23-38.

SUNDER, S., D. W. SHOESMITH, M. G. BAILEY, F. W. STANCHEL, N. S. MCINTYRE (1981) Anodic oxidation of UO_2: Part I. Electrochemical and x-ray photoelectron spectroscopic studies in neutral solutions. *Journ. Electroanal. Chem.*, **130**, 163-179.

SUNDER, S., D. W. SHOESMITH, M. G. BAILEY, F. W. STANCHEL, N. S. MCINTYRE (1981) Anodic oxidation of UO_2: Part II. Electrochemical and photoelectron spectroscopic studies in alkaline solutions. *Journ. Electroanal. Chem.*, **150**, 217-228.

SUNDER, S., D. W. SHOESMITH, H. CHRISTENSEN, N. H. MILLER AND, M. G. BAILEY (1990) Oxidation of UO_2 fuel by radicals formed during the radiolysis of water. In: *Scientific Basis for Nuclear Waste Management XIII* (V. M. Oversby and P. W. Brown, eds.), Mat. Res. Soc. Symp. Proc. Vol. 176. MRS, Pittsburgh, 457-466.

SUNDER, S., D. W. SHOESMITH, H. CHRISTENSEN, M. G. BAILEY, AND N. H. MILLER (1989) Electrochemical and x-ray photoelectron spectroscopic studies of UO_2 fuel oxidation by specific radicals formed during radiolysis of groundwater. In: *Scientific Basis for Nuclear Waste Management XII* (W. Lutze and R. C. Ewing, eds.), Mat. Res. Soc. Symp. Proc., Vol. 127. MRS, Pittsburgh, 317-324.

SUNDER, S., D. W. SHOESMITH, L. H. JOHNSON, G. J. WALLACE, M. G. BAILEY, AND A. P. SNAGLEWSKI (1987) Oxidation of CANDU™ fuel by the products of the alpha radiolysis of groundwater. In: *Scientific Basis for Nuclear Waste Management XI* (M. J. Apted and R. E. Westerman, eds.), Mat. Res. Soc. Symp. Proc. Vol. 112. MRS, Pittsburgh, 465-472.

SUNDER, S., P. TAYLOR, J. J. CRAMER (1988) XPS and XRD studies of uranium rich minerals from Cigar Lake, Saskatchewan. In: *Scientific Basis for Nuclear Waste Management X*, (J. K. Bates and W. S. Seefelt, eds.), Mat. Res. Soc. Symp. Proc. Vol. 84. MRS, Pittsburgh, 103-113.

SVERJENSKY, D. A. (1989) Geochemical modelling of the Koongarra uranium deposit -- Alligator Rivers Analogue Project. In: *Progress report for geochemical investigations of uranium mobility in the Koongarra ore deposit -- a natural analogue for the migration of radionuclides from a nuclear waste repository.* August 31, 1989. 313-326.

SWEENEY, M. A., AND P. L. BINDA (1989) Mineralization controls and source of metals in the Lufilian Fold Belt, Shaba (Zaire), Zambia, and Angola - a discussion. *Econ. Geol.*, **84**, 963-973.

TAYLOR, J. C., W. I. STUART AND I. A. MUMME (1981) The crystal structure of curite. *J. Inorg. Nucl. Chem.*, **43**, 2419-2423.

TAYLOR, J. G. AND H. G. HURST (1971) Hydrogen atom location in the α- and β-forms of uranyl hydroxide. *Acta Cryststallogr.*, **B27**, 1088.

TAYLOR, P., E. A. BURGESS, AND D. G. OWEN (1980) An x-ray diffracion study of the formation of β-$UO_{2.33}$ on UO_2 pellet surfaces in air at 229 to 275°C. *Journ. of Nucl. Mater.*, **88**, 153-160.

TAYLOR, P., D. D. WOOD, A. M. DUCLOS, D. G. OWEN (1989) Formation of uranium trioxide hydrates on UO_2 fuel in air-steam mixtures near 200°C. *Journ. of Nucl. Mater.*, **168**, p70-75.

THOMAS, G. F. AND G. TILL (1984), The dissolution of unirradiated UO_2 fuel pellets under simulated disposal conditions. *Nucl. Chem. Waste Man.*, **5**, 141.

THOMAS, L. E. AND L. A. CHARLOT (1990) Analytical electron microscopy of light-water reactor fuels. In: *Proceedings of the Fourth International Symposium on Ceramics in Nuclear Waste Management* (G. B. Mellinger, ed.). American Ceramic Society, Westerville, OH.

THOMAS, L. E., R. E. EINZIGER, AND R. E. WOODLEY (1989) Microstructural examination of oxidized spent PWR fuel by transmission electron microscopy. *Journ. of Nucl. Materials.*, **166**, 243-251.

THOMAS, L. E., AND R. J. GUENTHER (1989) Characterization of low-gas-release LWR fuels by transmission electron microscopy. In: *Scientific Basis for Nuclear Waste Management XII* (W. Lutze and R. C. Ewing, eds.), Mat. Res. Soc. Symp. Proc. Vol. 127. MRS, Pittsburgh, 293-300.

THOMAS, L. E., AND R. J. GUENTHER (1988) AEM analysis of condensed-phase xenon in UO_2 spent fuel. In: *Proceedings of the 46th Annual Meeting of the Electron Microscopy Society of America* (G. W. Bailey, ed.). San Fransisco Press, San Fransisco, CA, 512-513.

THOMAS, L. E., R. W. KNOLL, L. A. CHARLOT, J. E. COLEMAN, E. R. GILBERT (1989) Storage of LWR spent fuel in air. Volume 2 -- microstructural characterization of low-temperature oxidized LWR spent fuel. PNL-6640, vol.2, UC-812. U.S.DOE/PNL.

THOMAS, L. E., J. M. MCCARTHY AND E. R. GILBERT (1986a) TEM examination of oxidized spent fuel. In: *Proceedings of the Third International Spent Fuel Storage Technology Symposium/Workshop, Vol. 2.* CONF-860417, U. S. Department of Energy, Seattle, WA.

THOMAS, L. E., J. M. MCCARTHY AND E. R. GILBERT (1986b) Transmission electron microscopy of oxidized UO_2 spent fuel. In: *Proceedings of the 44th Annual Meeting of the Electron Microscopy Society of America* (G. W. Bailey, ed.). San Fransisco Press, San Fransisco, CA, 512-513.

THOMPSON, M. E., B. INGRAM AND E. B. GROSS (1956) Abernathyite, a new mineral of the metatorbernite group. *Am. Min.*, **41**, 82-90.

TIMO, J., J. SUKSI, R. SUUTARINEN, H. NIINI, T. RUSKEENIEMI, B. SÖDERHOLM, M. VESTERINEN, R. BLOMQVIST, S. HALONEN, A. LINDBERG (1989) The behavior of natural radionuclides in and around uranium deposits. 2. Results of investigations at the Palmottu analogue site, SW Finland. Geol. Surv. Finland, Nuclear Waste Disposal Research Report YST-64, Espoo, Finland, 60p.

TREMAINE, P. R., J. D. CHEN, G. J. WALLACE, W. A. BOIVIN (1981) Solubility of uranium (IV) oxide in alkaline aqueous solutions to 300°C. *Journ. Solution Chem.*, **10(3)**, 221-230.

TRIPATHI, S. (1984) Uranium (VI) transport modelling: geochemical data and submodels. Ph.D. dissertation, Stanford University, 1984.

TROCKI, L. K., D. B. CURTIS, A. J. GANCARZ, J. C. BANAR (184) Ages of major uranium mineralization and lead loss in Key Lake uranium deposit, northern Saskatchewan, Canada. *Econ. Geol.*, **79(6)**, 1378-1386.

TURNER-PETERSON, C. E., E. S. SANTOS AND N. S. FISMAN (eds.) (1987) *A Basin Analysis Case Study: The Morrison Formation, Grants Uranium Region, New Mexico.* A.A.P.G. Studies in Geology No. 22, Tulsa, 391p.

UNRUG, R. (1989) Mineralization controls and source of metals in the Lufilian Fold Belt, Shaba (Zaire), Zambia, and Angola - a reply. *Econ. Geol.*, **84**, 963-973.

URBANEC, Z. (1966) Report UJV 1521

UZIEMBLO, N. H., L. E. THOMAS, L. H. SHOENLEIN, B. MASTEL, AND E. D. JENSEN (1987) Solids characterizaton from hydrothermal tests with spent fuel. In: *Scientific Basis for Nuclear Waste Management X*, (J. K. Bates and W. S. Seefelt, eds.), Mat. Res. Soc. Symp. Proc. Vol. 84. MRS, Pittsburgh, 161-171.

VANDERGRAAF, T. T. (1980) Leaching of irradiated UO_2 fuel. TR-100, Atomic Energy of Canada Limited Technical Record.

VAN LIERDE, W., J. PELSMAEKERS AND A. LECOCQ-ROBERT (1970) On the phase limits of U_4O_9. *Journ. Nucl. Mater.*, **37**, 276-285.

VAN LUIK, A. E. (1987) Uranium in selected endorheic basins as a partial analogue for spent fuel behavior in salt. In: *Natural Analogues in Radioactive Waste Disposal* (B. Côme and N. A. Chapman, eds.) Radioactive Waste Management Series, CEC, Graham and Trotman, London, 92-103.

VIER, D. T. (1944) USAEC, Report A-1277

VILKS, P., J. J. CRAMER, T. A. SHEWCHUK, J. P. A. LAROCQUE (1988) Colloid and particulate matter studies in the Cigar Lake natural analog program. *Radiochim. Acta*, **44/45**, 305-310.

VOCHTEN, R. (1990) Transformation of schoepite into different hydrated uranates. In: *ABSTRACTS, vol. 1, The 15th General Meeting of the IMA*, 28 June to 3 July, 1990, Beijing, China.

VOCHTEN, R., AND M. DELIENS (1980) Transformation of curite into meta-autunite: paragenesis data and electrokinetic properties. *Phys. Chem. Minerals*, **6**, 129-143

VOCHTEN, R., W. HUYBRECHTS, G. REMAUT AND M. DELIENS (1979) Formation of meta-torbernite starting from curite: crystallographic data and electrokinetic properties. *Phys. Chem. Minerals*, **4**, 281-290.

VOULTSIDIS, V., AND D. CLASEN (1978) Probleme und grenzbereiche der uranmineralogie. *Erzmetall.*, **31**, 3.

VOULTSIDIS, V., E. VON PECHMANN AND D. CLASEN (1982) Petrography, mineralogy and genesis of the U-Ni deposits, Key Lake, Saskatchewan, Canada. In: *Ore Genesis: The State of the Art* (G. C. Amstutz, *et al.*, eds.), Springer-Verlag, NY, 469-490.

WADSLEY, A. D. (1964) Inorganic non-stoichiometric compounds. In: *Non-stoichiometric Compounds* (L. Mandelcorn, ed.). Academic Press, New York, London, 98-209.

WALENTA, K. (1974) On studtite and its composition. *Am. Min.*, **59**, 167.

WALKER, G. W., AND J. W. ADAMS (1963) Mineralogy, international structure characteristics, and paragenesis of uranium-bearing veins in the conterminous United States. U. S. Geol. Surv. Professional Paper 455-D.

WANG, R., AND Y. B. KATAYAMA (1982) Dissolution mechanism for UO_2 and spent fuel. *Nucl. Chem. Waste Man.*, **3**, 83.

WANG, R., AND Y. B. KATAYAMA (1981) Electrochemical methods for leaching of spent fuel. *Nucl. Chem. Waste Man.*, **2**, p147.

WEBER, W. J., R. P. TURCOTTE AND F. P. ROBERTS (1982) Radiation damage from alpha decay in ceramic nuclear waste forms. *Radioactive Waste Management*, **2**, 295.

WERME, L., P. SELLIN, R. FORSYTH (1990) Radiolytically induced oxidative dissolution of spent nuclear fuel. SKB Report **90-08**.

WEST, J. M., I. G. MCKINLEY AND A. VIALTA (1989) The influence of microbial activity on the movement of uranium at Osamu Utsumi mine, Poços de Caldas, Brazil. In: *Scientific Basis for Nuclear Waste Management XII* (W. Lutze and R. C. Ewing, eds.), Mat. Res. Soc. Symp. Proc. Vol. 127. MRS, Pittsburgh, 771-777.

WHEELER, V. J., R. M. DELL, E. WAIT (1964) Uranium trioxide and the UO_3 hydrates. *J. Inorg. Nucl. Chem.*, **26**, 1829.

WHITE, G. D., AND E. R. GILBERT (1986) Comparison of the oxidation behavior of BNL, CRNL, and PNL UO_2 pellets. In: *Proceedings of the Third International Spent Fuel Storage Technology Symposium/Workshop, Vol. 2.* CONF-860417, U. S. Department of Energy, Seattle, WA.

WHITE, G. D., C. A. KNOX, E. R. GILBERT, A. B. JOHNSON, JR. (1983) Oxidation of UO_2 at 150-350°C. In: *Proceedings of the U. S. Nuclear Regulatory Commission Workshop on Spent Fuel/Cladding Reaction During Dry Storage,* NUREG/CP-0049, U.S.NRC, Gaithersburg, MD, 102-110.

WILDE, A. R. AND V. J. WALL (1987) Geology of the Nabarlek uranium deposit, Northern Territory, Australia. *Econ. Geol.*, **82**, 1152-1168.

WILLIS, B. T. M (1978) The defect structure of hyperstoichiometric uranium dioxide. *Acta Crystallogr.*, **A34**, 88.

WILLIS, B. T. M (1963) Positions of the oxygen atoms in $UO_{2.13}$. *Nature*, **197**, 755-756.

WILSON, C. N. (1988) Summary of results from the series 2 and series 3 NNWSI bare fuel dissolution tests. In: *Scientific Basis for Nuclear Waste Management XI* (M. J. Apted and R. E. Westerman, eds.), Mat. Res. Soc. Symp. Proc. Vol. 112. MRS, Pittsburgh, 473-483.

WILSON, C. N., AND C. J. BRUTON (in press) Studies on spent fuel dissolution behavior under Yucca Mountain repository conditions. In: *Proceedings American Ceramic Society Annual Meeting*, Indianapolis, IN, April 23-27, 1989.

WILSON, C. N., AND W. J. GRAY (1990) Measurement of soluble nuclide dissolution rates from spent fuel. In: *Scientific Basis for Nuclear Waste Management XIII* (V. M. Oversby and P. W. Brown, eds.), Mat. Res. Soc. Symp. Proc. Vol. 176. MRS, Pittsburgh, 489-498.

WILSON, C. N., AND H. F. SHAW (1987) Experimental study of the dissolution of spent fuel at 85°C in natural ground water. In: *Scientific Basis for Nuclear Waste Management X*, (J. K. Bates and W. S. Seefelt, eds.), Mat. Res. Soc. Symp. Proc. Vol. 84. MRS, Pittsburgh, 123-130.

WILSON, M. R., AND T. K. KYSER (1987) Stable isotope geochemistry of the alteration associated with the Key Lake uranium deposit, Canada. *Econ. Geol.*, **82(6)**, 1540-1557.

ZWAAN, P. C., C. E. S. ARPS AND E. DE GRAVE (1989) Vochtenite, $(Fe^{2+},Mg)Fe^{3+}[UO_2/PO_4]_4(OH)\cdot 12\text{-}13H_2O$, a new uranyl phosphate mineral from Wheal Basset, Redruth, Cornwall, England. *Mineral. Mag.*, **53**, 473-478.

APPENDIX A

MINERALS CONTAINING THE URANYL ION

Mineral names and formulae are based primarily on the current edition of and the supplement to *Glossary of Mineral Species* (Fleischer, 1987; 1989). A question mark (?) following a mineral name indicates a doubtful specie or uncertain formula.

U(IV) - U(VI) minerals	
α-U_3O_7 (?)	$UO_{2.33}$
ianthinite	$U^{4+}(UO_2)_5(OH)_{14}\cdot 3H_2O$
liandratite	$U(Nb,Ta)_2O_8$
moluranite	$H_4U^{4+}(UO_2)_3(MoO_4)_7\cdot 18H_2O$
orthobrannerite	$U^{4+}U^{6+}Ti_4O_{12}(OH)_2$
wyartite	$Ca_3U^{4+}(UO_2)_6(CO_3)_2(OH)_{18}\cdot 3\text{-}5H_2O$

Uranyl Oxide Hydrates	
ianthinite	$U^{4+}(UO_2)_5(OH)_{14}\cdot 3H_2O$
schoepite	$UO_3\cdot 2H_2O$
para·schoepite (?)	$UO_3\cdot 2H_2O$
meta·schoepite	$UO_3\cdot nH_2O$ (n<2)
studtite	$UO_4\cdot 4H_2O$
meta·studtite	$UO_4\cdot 2H_2O$

Alkali and Alkaline-earth Uranyl Oxide Hydrates

agrinierite	$(K_2,Ca,Sr)U_3O_{10}\cdot 4H_2O$
bauranoite	$BaU_2O_7\cdot 4\text{-}5H_2O$
becquerelite	$Ca[(UO_2)_6O_4(OH)_6]\cdot 8H_2O$
billietite	$Ba[(UO_2)_6O_4(OH)_6]\cdot 4\text{-}8H_2O$
calciouranoite	$(Ca,Ba,Pb)U_2O_7\cdot 5H_2O$
meta·calciouranoite	$(Ca,Ba,Pb)U_2O_7\cdot 2H_2O$
clarkeite (?)	$(Na_2,Ca,Pb)_2U_2(O,OH)_7$
compreignacite	$K_2[(UO_2)_6O_4(OH)_6]\cdot 8H_2O$
curite	$Pb_3[(UO_2)_8O_8(OH)_6]\cdot 3H_2O$
fourmarierite	$Pb[(UO_2)_4O_3(OH)_4]\cdot 4H_2O$
masuyite (?)	$Pb_3U_8O_{27}\cdot 10H_2O$
protasite	$Ba[(UO_2)_3O_3(OH)_2]\cdot 3H_2O$
rameauite	$K_2CaU_6O_{20}\cdot 9H_2O$
richetite (?)	$PbU_4O_{13}\cdot 4H_2O$
sayrite	$Pb_2[(UO_2)_5O_6(OH)_2]\cdot 4H_2O$
uranosphaerite (?)	$Bi_2U_2O_9\cdot 3H_2O$
vandenbrandeite	$Cu(UO_2)(OH)_4$
vandendriesscheite	$PbU_7O_{22}\cdot 12H_2O$
meta·vandendriesscheite	$PbU_7O_{22}\cdot nH_2O$ $(n<12)$
wölsendorfite	$(Pb,Ca)U_2O_7\cdot 2H_2O$

Uranyl Silicates	
beta-uranophane	$Ca(UO_2)SiO_3(OH)_2 \cdot 5H_2O$
boltwoodite	$HK(UO_2)(SiO_4) \cdot 1.5H_2O$
Na-boltwoodite	$(H_3O)(Na,K)(UO_2)(SiO_4) \cdot H_2O$
cuprosklodowskite	$(H_3O)_2Cu(UO_2)_2(SiO_4)_2 \cdot 2H_2O$
kasolite	$Pb(UO_2)(SiO_4) \cdot H_2O$
haiweeite	$Ca(UO_2)_2Si_6O_{15} \cdot 5H_2O$
meta·haiweeite	$Ca(UO_2)_2Si_6O_{15} \cdot nH_2O$ (n<5)
haiweeite-(Mg)	$Mg(UO_2)_2Si_6O_{15} \cdot 9H_2O$
lepersonite	$Ca(RE)_2U_{24}(CO_3)_8Si_4O_{76} \cdot 60H_2O$
oursinite	$(Co,Mg)(UO_2)_2Si_2O_7 \cdot 6H_2O$
sklodowskite	$(H_3O)_2Mg(UO_2)_2(SiO_4)_2 \cdot 2H_2O$
soddyite	$(UO_2)_2SiO_4 \cdot 2H_2O$
swamboite	$U^{6+}H_6(UO_2)_6(SiO_4)_6 \cdot 30H_2O$
uranophane	$Ca(UO_2)SiO_3(OH)_2 \cdot 5H_2O$
uranosilite (?)	$U^{6+}Si_7O_{17}$
weeksite	$K_2(UO_2)_2Si_6O_{15} \cdot 4H_2O$

Uranyl Carbonates

albrechtschraufite	$Ca_4Mg(UO_2)_2(CO_3)_6F_2 \cdot 17H_2O$
andersonite	$Na_2Ca((UO_2)(CO_3)_3 \cdot 6H_2O$
bayleyite	$Mg_2(UO_2)(CO_3)_3 \cdot 18H_2O$
bijvoetite-(Y)	$(Y,Dy)_2(UO_2)_4(CO_3)_4(OH)_6 \cdot 11H_2O$
grimselite	$K_3Na(UO_2)(CO_3)_3 \cdot H_2O$
joliotite	$(UO_2)(CO_3) \cdot nH_2O$
kamotoite-(Y)	$(Y,Nd,Gd)_2(UO_2)_4(CO_3)_3O_4 \cdot 14.5H_2O$
lepersonite	$Ca(Gd,Dy)_2(UO_2)_{24}(CO_3)_8(SiO_4)_4O_{12} \cdot 60H_2O$
liebigite	$Ca_2(UO_2)(CO_3)_3 \cdot 11H_2O$
mckelveyite	$Ca_3Na(Ca,U)Y(CO_3)_6 \cdot 3H_2O$
rabittite	$Ca_3Mg_3(UO_2)_2(CO_3)_6(OH)_4 \cdot 18H_2O$
roubaultite	$Cu_2(UO_2)_3(CO_3)_2O_2(OH)_2 \cdot 4H_2O$
rutherfordine	UO_2CO_3
schroeckingerite	$NaCa_3(UO_2)(CO_3)_3(SO_4)F \cdot 10H_2O$
shabaite-(Nd)	$Ca(RE)_2(UO_2)(CO_3)_4(OH)_2 \cdot 6H_2O$
sharpite	$Ca(UO_2)_6(CO_3)_5(OH)_4 \cdot 6H_2O$
swartzite	$CaMg(UO_2)(CO_3)_3 \cdot 12H_2O$
urancalcarite	$Ca(UO_2)_3(CO_3)(OH)_6 \cdot 3H_2O$
voglite	$Ca_2Cu(UO_2)(CO_3)_4 \cdot 6H_2O$
widenmannite	$Pb_2(UO_2)(CO_3)_3$
wyartite	$Ca_3U^{4+}(UO_2)_6(CO_3)_2(OH)_{18} \cdot 3\text{-}5H_2O$
zellerite	$Ca(UO_2)(CO_3)_2 \cdot 5H_2O$
meta·zellerite	$Ca(UO_2)(CO_3)_2 \cdot 3H_2O$
znucalite	$Zn_{12}(UO_2)Ca(CO_3)_3(OH)_{22} \cdot 4H_2O$

Uranyl Sulfates, Selenates, and Tellurates

coconinoite	$Fe^{3+}_2Al_2(UO_2)_2(PO_4)_4(SO_4)(OH)_2 \cdot 20H_2O$
johannite	$Cu(UO_2)_2(SO_4)_2(OH)_2 \cdot 8H_2O$
shroeckingerite	$NaCa_3(UO_2)_2(CO_3)_3(SO_4)F \cdot 10H_2O$
uranopilite	$(UO_2)_6(SO_4)(OH)_{10} \cdot 12H_2O$
meta·uranopilite	$(UO_2)_6(SO_4)(OH)_{10} \cdot 5H_2O$
xiangjiangite	$(Fe^{3+},Al)(UO_2)_4(PO_4)_2(SO_4)_2(OH) \cdot 22H_2O$
zippeite	$K_4(UO_2)_6(SO_4)_3(OH)_{10} \cdot 4H_2O$
Co-zippeite	$Co_2(UO_2)_6(SO_4)_3(OH)_{10} \cdot 16H_2O$
Mg-zippeite	$Mg_2(UO_2)_6(SO_4)_3(OH)_{10} \cdot 16H_2O$
Na-zippeite	$Na_4(UO_2)_6(SO_4)_3(OH)_{10} \cdot 4H_2O$
Ni-zippeite	$Ni_2(UO_2)_6(SO_4)_3(OH)_{10} \cdot 16H_2O$
Zn-zippeite	$Zn_2(UO_2)_4(SO_4)_3(OH)_{10} \cdot 16H_2O$
demesmaekerite	$Pb_2Cu_5(UO_2)_2(SeO_3)_6(OH)_6 \cdot 2H_2O$
derricksite	$Cu_4(UO_2)(SeO_3)_2(OH)_6$
guilleminite	$Ba(UO_2)_3(SeO_3)_2(OH)_4 \cdot 3H_2O$
marthozite	$Cu(UO_2)_3(SeO_3)_3(OH)_2 \cdot 7H_2O$
cliffordite	$U^{6+}Te_3O_9$
moctezummite	$PbU^{6+}Te_2O_8$
schmitterite	$U^{6+}TeO_5$

Uranyl Phosphates and Arsenates

althupite	$ThAl(UO_2)_7(PO_4)_4O_2(OH)_5 \cdot 15H_2O$
bergenite	$(Ba,Ca)_2(UO_2)_3(PO_4)_2(OH)_4 \cdot 5.5H_2O$
coconinoite	$Fe^{3+}{}_2Al_2(UO_2)_2(PO_4)_2(SO_4)(OH)_2 \cdot 20H_2O$
dewindtite (see renardite)	$Pb_{2-3}(UO_2)_{4-6}(PO_4)_{3-4} \cdot 7\text{-}10H_2O$
dumontite	$Pb_2(UO_2)_3O_2(PO_4)_2 \cdot 5H_2O$
francoisite-(Nd)	$(Nd,Y,Sm,Ce)(UO_2)_3(PO_4)_2O(OH) \cdot 6H_2O$
furongite	$Al_2(UO_2)(PO_4)_3(OH)_2 \cdot 13.5H_2O$
kamitugaite	$PbAl(UO_2)_5[(P,As)O_4]_2(OH)_4 \cdot 9.5H2O$
kivuite (?)	$(Th,Ca,Pb)H_2(UO_2)_4(PO_4)_2(OH)_8 \cdot 7H_2O$
moreauite	$Al_3(UO_2)(PO_4)_3(OH)_2 \cdot 13H2O$
mundite	$Al(UO_2)_3(PO4)_2(OH)_3 \cdot 5.5H2O$
parsonsite	$Pb_2(UO_2)(PO_4)_2 \cdot 2H_2O$
phosphuranylite	$(H_3O)_2Ca(UO_2)_3(PO_4)_2(OH)_4 \cdot 4H_2O$
phuralumite	$Al_2(UO_2)_3(PO_4)_2(OH)_6 \cdot 10H_2O$
phurcalite	$Ca_2(UO_2)_3(PO_4)_2(OH)_4 \cdot 4H_2O$
przhevalsite	$Pb(UO_2)_2(PO_4)_2 \cdot 4H2O$
pseudo-autunite (?)	$(H_3O)_4Ca_2(UO_2)_2(PO_4)_4 \cdot 5H_2O$
ranunculite	$(H_3O)Al(UO_2)(PO_4) \cdot 3H_2O$
renardite (?) (see dewindtite)	$Pb(UO_2)_4(PO_4)_2(OH)_4 \cdot 7H_2O$
threadgoldite	$Al(UO_2)_2(PO_4)_2(OH) \cdot 8H_2O$
triangulite	$Al_3(UO_2)_4(PO_4)_4(OH)_5 \cdot 5H_2O$
upalite	$Al(UO_2)_3(PO_4)_2O(OH) \cdot 7H_2O$
urancircite	$Ba(UO_2)_3(PO_4)_2 \cdot 12H_2O$
vanmeersscheite	$U^{6+}(UO_2)_3(PO_4)_2(OH)_6 \cdot 4H_2O$
meta·vanmeersscheite	$U^{6+}(UO_2)_3(PO_4)_2(OH)_4 \cdot 2H_2O$
vochtenite	$(Fe^{2+},Mg)Fe^{3+}(UO_2)_4(PO_4)_4(OH) \cdot 12\text{-}13H_2O$
walpurgite-(P)	$(BiO)_4(UO_2)_2(PO_4)_4 \cdot 2H_2O$
xiangjiangite	$(Fe^{3+},Al)(UO_2)_4(PO_4)_2(SO_4)_2(OH) \cdot 22H_2O$
yingjiangite	$(K_{1-x},Ca_x)(UO_2)_3(PO_4)_2(OH)_{1+x} \cdot 4H_2O$
arsenuranylite	$Ca(UO_2)_4(AsO_4)_2(OH)_4 \cdot 6H_2O$
asselbornite	$(Pb,Ba)(UO_2)_6(BiO_4)(AsO_4)_2(OH)_{12} \cdot 3H_2O$
hallimondite	$Pb(UO_2)(AsO_4)_2$
hügelite	$Pb_2(UO_2)_3(AsO_4)_2(OH)_4 \cdot 3H_2O$
kamitugaite	$PbAl(UO_2)_5[(P,As)O_4]_2(OH)_4 \cdot 9.5H2O$
walpurgite	$(BiO)_4(UO_2)_2(AsO_4)_4 \cdot 2H_2O$

Uranyl Phosphates and Arsenates (cont'd)

Autunite group	**$R_{1-2}(UO_2)_2(TO_4)_2 \cdot nH_2O$**
autunite	$Ca(UO_2)_2(PO_4)_2 \cdot 10\text{-}12H_2O$
Na-autunite	$Na_2(UO_2)_2(PO_4)_2 \cdot 8H_2O$
fritzcheite	$Mn(UO_2)_2[(P,V)O_4]_2 \cdot 10H_2O$
sabugalite	$HAl(UO_2)_4(PO_4)_4 \cdot 16H_2O$
salèeite	$Mg(UO_2)_2(PO_4)_2 \cdot 10H_2O$
torbernite	$Cu(UO_2)_2(PO_4)_2 \cdot 8\text{-}12H_2O$
trögerite-(P)	$UO_2(UO_2)_2(PO_4)_2 \cdot 8H_2O$
uranocircite	$Ba(UO_2)_2(PO_4)_2 \cdot 12H_2O$
uranospathite	$HAl(UO_2)_4(PO_4)_4 \cdot 40H_2O$
zeunerite	$Cu(UO_2)_2(PO_4)_2 \cdot 40H_2O$
arsenuranospathite	$HAl(UO_2)_4(AsO_4)_4 \cdot 40H_2O$
heinrichite	$Ba(UO_2)_2(AsO_4)_2 \cdot 10\text{-}12H_2O$
kahlerite	$Fe^{2+}(UO_2)_2(AsO_4)_2 \cdot 10\text{-}12H_2O$
novacekite	$Mg(UO_2)_2(AsO_4)_2 \cdot 12H_2O$
trögerite	$UO_2(UO_2)_2(AsO_4)_2 \cdot 8H_2O$
uranospinite	$Ca(UO_2)_2(AsO_4)_2 \cdot 10H_2O$
Meta·autunite group	**$R_{1-2}(UO_2)_2(TO_4)_2 \cdot nH_2O$**
chernikovite (hydrogen autunite)	$(H_3O)_2(UO_2)_2(PO_4)_6 \cdot 2H_2O$
bassetite	$Fe^{2+}(UO_2)_2(PO_4)_2 \cdot 8H_2O$
meta·ankoleite	$K_2(UO_2)_2(PO_4)_2 \cdot 6H_2O$
meta·autunite	$Ca(UO_2)_2(PO_4)_2 \cdot 6H_2O$
meta·torbernite	$Cu(UO_2)_2(PO_4)_2 \cdot 8H_2O$
meta·uranocircite	$Ba(UO_2)_2(PO_4)_2 \cdot 8H_2O$
meta·uranocirciteII (?)	$Ba(UO_2)_2(PO_4)_2 \cdot 6H_2O$
Na-meta·autunite	$(Na_2,Ca)(UO_2)_2(PO_4)_2 \cdot 8H_2O$
uramphite	$(NH_4)_2(UO_2)_2(PO_4)_2 \cdot 4\text{-}6H_2O$
abernathyite	$K(UO_2)(AsO_4) \cdot 4H_2O$
meta·autuniteII (?)	$Ca(UO_2)_2(AsO_4)_2 \cdot 4\text{-}6H_2O$
meta·heinrichite	$Ba(UO_2)_2(AsO_4)_2 \cdot 8H_2O$
meta·kahlerite	$Fe(UO_2)_2(AsO_4)_2 \cdot 8H_2O$
meta·kirchheimerite	$Co(UO_2)_2(AsO_4)_2 \cdot 8H_2O$
meta·lodevite	$Zn(UO_2)(AsO_4)_2 \cdot 10H_2O$
meta·novacekite	$Mg(UO_2)_2(AsO_4)_2 \cdot 4\text{-}8H_2O$
meta·uranospinite	$Ca(UO_2)_2(AsO_4)_2 \cdot 8H_2O$
meta·zeunerite	$Cu(UO_2)_2(AsO_4)_2 \cdot 8H_2O$
Na-uranospinite	$(Na_2,Ca)(UO_2)_2(AsO_4)_2 \cdot 5H_2O$

Uranyl Vanadates

ferghanite	$(UO_2)_3V_2O_8 \cdot 6H_2O$
rauvite	$Ca(UO_2)_2V_{10}O_{28} \cdot 16H_2O$
unnamed (?)	$Ca\text{-}U\text{-}V\text{-}O\text{-}H_2O$
unnamed (?)	$Pb\text{-}U\text{-}V\text{-}O\text{-}H_2O$
uvanite (?)	$(UO_2)_2V_6O_{17} \cdot 15H_2O$
carnotite group	
carnotite	$K_2(UO_2)_2V_2O_8 \cdot 3H_2O$
curienite	$Pb(UO_2)_2V_2O_8 \cdot 5H_2O$
francevillite	$(Pb,Ba)(UO_2)_2V_2O_8 \cdot 5H_2O$
fritzcheite	$Mn(UO_2)_2[(P,V)O_4]_2 \cdot 10H_2O$
margaritasite	$(Cs,K,H_3O)(UO_2)_2V_2O_8 \cdot H_2O$
rauvite	$Ca(UO_2)_2V^{5+}{}_{10}O_{28} \cdot 16H_2O$
sengierite	$Cu_2(UO_2)_2V_2O_8 \cdot 6H_2O$
strelkinite	$Na_2(UO_2)_2V_2O_8 \cdot 6H_2O$
tyuyamunite	$Ca(UO_2)_2V_2O_8 \cdot 8H_2O$
meta·tyuyamunite	$Ca(UO_2)_2V_2O_8 \cdot 3H_2O$
vanuralite	$(H_3O,Ba,Ca,K)_2(UO_2)_2V_2O_8 \cdot 4H_2O$
vanuranylite (?)	$(H_3O,Ba,Ca,K)_{1.6}(UO_2)_2V_2O_8 \cdot 4H_2O$

Uranyl Molybdates and Tungstates

calcurmolite	$Ca(UO_2)_3(MoO_4)_3(OH)_2 \cdot 11H_2O$
cousinite	$Mg(UO_2)_2(MoO_4)_2(OH)_2 \cdot 5H_2O$
iriginite (?)	$U^{6+}(MoO_4)_2(OH)_2 \cdot 3H_2O$
moluranite	$H_4U^{4+}(UO_2)_3(MoO_4)_7$
tengchongite (?)	$U^{6+}{}_6Mo^{6+}{}_2O_{25} \cdot 12H_2O$
umohoite	$(UO_2)(MoO_2)(OH)_4 \cdot 2H_2O$
uranotungstite	$(Ba,Pb,Fe^{2+})(UO_2)_2(WO_4)(OH)_4 \cdot 12H_2O$

APPENDIX B

REPORTED U(VI) MINERALOGY OF SELECTED URANIUM DEPOSITS.

All deposits contain uraninite unless specified (coffinite exists where noted)

Koongarra deposit (Alligator Rivers), Australia

schoepite	vandendriesscheite
fourmarierite	curite
kasolite	sklodowskite
uranophane	renardite/dewindtite
sabugalite	torbernite
autunite	meta·salèeite
meta·torbernite	phosphuranylite

Mary Kathleen Deposit, Australia

beta·uranophane	uranophane
"gummite" (mixed uranyl oxide hydrates)	

Osamu Utsumi mine, Minas Gerais, Brazil

none reported (except uraninite)

Cigar Lake, Saskatchewan, Canada

α-U_3O_7

Rabbit Lake, Saskatchewan, Canada

(all occur as precipitates at the surface)	
boltwoodite	sklodowskite
tyuyamunite	uranophane

Beaverlodge, Canada

cuprosklodowskite	fourmarierite
kasolite	masuyite
sklodowskite	uranopilite
vandendriesscheite	zippeite

Cornwall District, England

autunite	bassetite
johannite (?)	torbernite
uraconite	zeunerite
zippeite	

Polmottu, Finland

coffinite

Limousin Region, France

autunite	bassetite
billietite	ianthinite
parsonite	sharpite
torbernite	uranospathite
uranophane	

Oklo, Gabon

francevillite	wölsendorfite
uranocircite	uranospathite

Krunkelbach mine, Menzenschwand, Germany

uranyl oxide hydrates	uranyl silicates
uranyl phosphates	uranyl arsenates
amorphous uranyl-Al-Si-hydroxide	uranyl tungstates

Needle's Eye, Scotland

none reported (except uraninite)

Orphan mine, Arizona, USA

bayleyite	meta·torbernite
meta·zeunerite	torbernite
uranophane	zeunerite

Midnite mine, Spokane, Washington, USA

autunite	phosphuranylite
sklodowskite	torbernite
uranophane	zippeite

Marysvale District, Utah, USA

beta-uranophane	dickite
phosphuranylite	shroeckengerite
torbernite	tyuyamunite
umohoite	uranophane
uranopilite	zippeite

Katanga District, Shaba, Zaire

becquerelite
bijvoetite-(Y)
cuprosklodowskite
curite
dervicksite
diderichite
fourmarierite
ianthinite
joliotite
lepersonite
masuyite
meta·schoepite
meta·torbernite
phosphuranylite
protasite
richetite
rutherfordine
sayrite
schmitterite
shabaite-(Nd)
siengenite (?)
soddyite
swamboite
uranophane
uranocircite
umohoite
vandendriesscheite
wyartite
zippeite
beta-uranophane
billietite
curiènite
demesmaekite
dewindtite
dumontite
guilleminite
iriginite
kasolite
liebigite
marthozite
meta·studtite
parsonsite
phurcalite
renardite
roubaltite
salèeite
schoepite
sengierite
sharpite
sklodowskite
studtite
torbernite
urancalcarite
uranopilite
vandenbrandeite
wölsendorfite
zeunerite-(As)

APPENDIX C

UNIVERSITY OF NEW MEXICO URANIUM-MINERAL COLLECTION

AQUISITION

DMNH:	**Denver Museum of Natural History**
LANL:	**Los Alamos NationaL Laboratory**
CSM:	**Colorado School of Mines**
HM:	**Harvard Mineralogical Museum**
MM:	**Moravskè Museum (Brno, Czechoslovakia)**
USNM:	**United States National Museum**
AMNH:	**American Museum of Natural History**

(* indicates number assigned by UNM)

Africa

Musonoi mine, Shaba (Katanga), Zaire

cuprosklodowskite	CSM(*MC1)
guilleminite	CSM(67-57)
marthozite	HM(124720)
torbernite	CSM(*MT1)
uraninite	UNM(339)

Kasolo mine, Shaba (Katanga), Zaire

curite	CSM(TM20643)
sklodowskite	DMNH(14502)
torbernite/kasolite	CSM(69-55)

Shinkolobwe mine, Shaba (Katanga), Zaire

mixed U-oxide hydrates	CSM(*SG1)
autunite (or torbernite, w/ alt.)	CSM(*SA1)
bequerelite	HM(*UNM·464)
bequerelite	HM(10902)
bequerelite	HM(86785)
bequerelite	HM(87442)
billietite	CSM(*SB1)
billietite	HM(*UNM·469)
billietite	HM(104455)
billietite (w/ uraninite)	HM(104456)
curite	CSM(*SC1)
curite	DNMH(58-97)
curite	DNMH(58-98)
curite	HM(86777)
curite (w/ fourmarierite & torbernite)	HM(GU-2)
curite w/ kasolite	HM(105749)
dewindtite (w/ kasolite)	HM(105718)
fourmarierite (w/curite, dewindtite)	HM(87085)
fourmarierite (w/curite, kasolite)	HM(108209)
fourmarierite (w/uranophane)	HM(105752)
ianthinite	HM(*UNM·465)
ianthinite	HM(2222)
ianthinite (w/ alt.)	HM(*UNM·451)
kasolite	CSM(*SK1)
kasolite	HM(105729)
masuyite	HM(106524)
meta·torbernite	CSM(*ST1)
meta·torbernite	CSM(76-23)
parsonsite (w/ U-silicates)	HM(86778)
rutherfordine	CSM(*SR1)
schoepite (w/β-uranophane)	CSM(*SS2)
schoepite (w/becquerelite & ianthinite)	CSM(87090)

Shinkolobwe mine, Shaba (Katanga), Zaire [cont'd]

sklodowskite	HM(86773)
soddyite	HM(86775)
soddyite/sklodowskite	CSM(*SS1)
studtite	HM(*UNM·454)
studtite	HM(109081)
torbernite	CSM(87-045)
uraninite	HM(*UNM·437)
uraninite (w/alt.)	CSM(*SU1)
uraninite (w/ gold)	CSM(10749)
uraninite (w/alt.)	CSM(108)
uranophane	CSM(*SU2)
uranophane	HM(105727)
vandenbrandeite	CSM(*SV1)

Namibia

boltwoodite	(Swakopmund)	HM(114695)
rutherfordine	(Morogorro)	CSM(68-55)

Asia

India

clarkeite	(Ajmer district, Rajputana)	HM(UN-14)

Japan

thorogummite	(Fukusima Prefecture)	CSM(TM20711)

Australia

Northern Territories

phosphuranylite	(Katherine mine)	CSM(68-118)
saleèite	(Ranger deposit)	CSM(81-138)
uraninite, phosphuranylite	(Pallite mine)	CSM(TM20541)
uraninite (w/alt.)	(El Sharan mine)	CSM(TM12232)
uraninite	(Nabarlek)	DMNH(13298)
uraninite	(Rum Jungle)	DMNH(6756)

Northwest Territories, Canada

cuprosklodowskite	(Eldorado mine; Great Bear Lake)	DMNH(13287)
uraninite, vandendriesscheite	(Great Bear Lake)	CSM(68-59)
uraninite	(Eldorado mine; Great Bear Lake)	CSM(TM4705)
uraninite	(Eldorado mine; Great Bear Lake)	HM(*UNM·436)
uraninite	(Eldorado mine; Great Bear Lake)	HM(*UNM·438)
uraninite (w/alt.)	(Labine Pt., Great Bear Lake)	CSM(10627)
uraninite	(Great Bear Lake)	UNM(254)
uraninite	(Great Bear Lake)	UNM(352)
uraninite	(Great Bear Lake)	UNM(374)
uraninite	(Great Bear Lake)	UNM(378)
uraninite	(Great Bear Lake)	HM(96613-b)
uraninite	(Great Bear Lake)	HM(96611)
uraninite	(Great Slave Lake)	UNM(345)
vandendriesscheite	(Great Bear Lake)	HM(92568)

Ontario, Canada

unknown	(Faraday mine; Bancroft)	CSM(68-109)
uraninite	(Perry Sound; Spider's Bay)	CSM(TM10978)
uraninite	(Faraday mine, Bancroft)	UNM(340)
uraninite	(Wilberforce)	UNM(343)
uraninite	(Camray property, Theano Pt., S. Ste. Marie Reg.)	UNM(354)
uraninite	(Theano Pt., Sault. Ste. Marie Reg.)	UNM(377)
uraninite	(Cardiff Township)	UNM(375)

Saskatchewan, Canada

beta-uranophane	(Nisto mines)	DMNH(13291)
uraninite	(Rabbit Lake)	DMNH(13289)
boltwoodite	(Rabbit Lake)	DMNH(13290)
unknown	(Beaverlodge)	DMNH(15895)
"uranium ore"	(Beaverlodge)	CSM(V-5)
"uranium ore"	(Beaverlodge)	CSM(EL-1)
uraninite	(Beaverlodge)	UNM(350)
uraninite (w/alt.)	(Goldfield area, Beaverlodge)	UNM(351)
"impact breccia"	(Claude Trench)	CSM(C-3)
"hydrothermally altered quartzite"	(Cluff Lake)	CSM(C-1)
"cluff breccia"	(Cluff Lake)	CSM(C-6)
uraninite	(near Nunn Lake, east of Lac La Ronge)	UNM(346)
carnotite	(Lac La Ronge)	UNM(376)
uraninite	(Foster Lake)	UNM(348)
uranium ore	(Key Lake)	LANL(KL762-521)
uranium ore	(Key Lake)	LANL(KL762-522)
uranium ore	(Key Lake)	LANL(KL768-580)
uranium ore	(Key Lake)	LANL(KL768-581)
uranium ore	(Key Lake)	LANL(KL785-457)
uranium ore	(Key Lake)	LANL(KL756-329)
uranium ore	(Key Lake)	LANL(KL755-288)
uranium ore	(Key Lake)	LANL(KL5085-306)
uranium ore	(Key Lake)	LANL(KL5085-330)
uranium ore	(Key Lake)	LANL(KL5085-281)
uranium ore	(Key Lake)	LANL(KL779-413)

Arizona, USA

uraninite w/ Cu-mins.	(Alpha mbr., Kaibab LS, Flagstaff)	CSM(TM11498)
"pitchblende"	(Huskon #7 mine, Cameron)	CSM(TM10899)
uraninite/autunite	(Chee #8 "C"mbr., Chinle Fm, Cameron)	CSM(TM11478)
kasolite	(Red Hills mine, Mojave Co.)	DMNH(13272)
uraninite (w/pyrite)	(Monument Valley, 20mi. N of Kayenta)	DMNH(15852)
carnotite	(Monument #2 mine, Monument Valley)	CSM(TM11582)
tyuyamunite	(Monument #2 mine, Monument Valley)	UNM(381)
bequerelite	(Monument #2 mine, Monument Valley)	UNM(382)
uraninite (w/alt.)	(Monument #2 mine, Monument Valley)	UNM(383)
carnotite	(Monument #2 mine, Monument Valley)	UNM(384)

California, USA

mixed U-oxide hydrates		(Masonville) DMNH(6603)

Colorado, USA

fourmarierite	(Mica Lakes region, Hahn's Peak)	HM(*UNM·458)
carnotite ore	(Jo Dandy mine, Montrose Co.)	CSM(TM7387)
torbernite/autunite	(Larimer)	CSM(TM7323)
torbernite/autunite	(Larimer)	CSM(TM7313)
torbernite/autunite	(Larimer)	CSM(83.168)
uraninite	(Schwartzwalder mine, Jefferson Co.)	CSM(TM20395)
"pitchblende"	(Moffat Co.)	CSM(TM10968)
"pitchblende"	(Moffat Co.)	CSM(TM10970)
"pitchblende"	(Caribou mine)	CSM(66.66.3)
"pitchblende"	(near Sargents))	CSM(TM20174)
uraninite	(Paradox Valley)	CSM(TM12329)
uraninite (w/alt.)	(Marshall Pass, Saguache Co.)	CSM(TM12229)
boltwoodite (w/ uraninite)	(Marshall Pass, Saguache Co.)	HM(*UNM·439)
liebegite	(Schwartzwalder mine, Jefferson Co.)	CSM(72.46.5-6)
liebegite	(Schwartzwalder mine, Jefferson Co.)	DMNH(9773)
liebegite	(Schwartzwalder mine, Jefferson Co.)	DMNH(9105)
autunite	(Denver-Goden U mine, Jefferson Co.)	CSM(TM20601)
"pitchblende"/carnotite	(Marshall Pass, Saguache Co.)	CSM(*CP1)
uraninite	(Schwartzwalder mine, Jefferson Co.)	DMNH(6979C)
uraninite	(Wood mine, near Central City, Gilpin Co.)	DMNH(12616)
uraninite	(Cherokee mine, Central City, Gilpin Co.)	DMNH(14700-C)
uraninite	(Cherokee mine, Central City, Gilpin Co.)	DMNH(14689)
uraninite (organic-rich)	(Lumsden mine, Mesa Co.)	DMNH(14715)
uraninite	(Billiken Load, Critchel, Jefferson Co.)	DMNH(15499)

Connecticut, USA

uraninite	(Hale's feldspar Quarry, Portland)	CSM(TM6745)
uraninite (w/alt.)	(Rock Landing Quarry, Haddam Neck)	UNM(373)
uraninite	(Branchville)	UNM(402)

Idaho, USA

uraninite	CSM(69.121)

New Hampshire, USA

autunite/uranophane	(Ruggles mine, Grafton Center)	CSM(7999)
autunite	(Ruggles mine)	CSM(TM8000)
clarkeite/uraninite	(Ruggles mine)	UNM(401)
curite/uraninite	(Ruggles mine)	UNM(398)
fourmarierite(?)	(Ruggles mine)	UNM(400)
mixed U-oxide hydrates	(Ruggles mine)	CSM(712.1)
uraninite (w/alt.)	(Ruggles mine)	CSM(TM6740)
uraninite (w/alt.)	(Ruggles mine)	DMNH(13279)
uraninite (w/alt.)	(Ruggles mine)	CSM(TM6758)
uraninite (w/alt.)	(Ruggles mine)	CSM(711:3:1)
uraninite (w/uranophane)	(Ruggles mine)	CSM(TM3524)
uraninite (w/alt.)	(Ruggles mine)	UNM(341)
uraninite (w/alt.)	(Ruggles mine)	UNM(342)
uraninite (w/alt.)	(Ruggles mine)	UNM(344)
uraninite (w/alt.)	(Ruggles mine)	UNM(396)
uraninite, uranophane, autunite	(Ruggles mine)	UNM(370)
uranophane	(Ruggles mine)	UNM(399)
uranophane/uraninite	(Ruggles mine)	UNM(397)
mixed U-oxide hydrates	(probably Ruggles mine)	UNM(408)
rutherfordine	(Grafton Cntr.)	DMNH(13280)
torbernite	(Grafton Cntr.)	CSM(TM3549)
uraninite (w/alt.)	(Grafton Cntr.)	DMNH(6154)
uraninite (w/alt.)	(Grafton Cntr.)	DMNH(6573)

New Mexico, USA

coffinite	(Valencia Co.)	CSM(11258)
uraninite	(Valencia Co.)	DMNH(13269)
coffinite (w/zippeite)	(Ambrosia Lake, Grants)	CSM(80.216)
uranophane (?)	(Guy #5 claim, San Miguel Co.)	CSM(TM6230)
uranophane	(Poison Canyon, Prewitt)	HM(1798)
rutherfordine	(Grants)	CSM(1229.2)
tyuyamunite	(Haystack mine, Grants)	DMNH(15866)
uraninite (in Todilto LS)	(Valencia Co.)	DMNH(13270)
uraninite	(Section 33 mine, near Grants)	UNM(369)

North Carolina, USA

uraninite (w/alt.)	(Flat Rock mine, Mitchell Co.)	DMNH(3284)
uraninite (w/alt.)	(Flat Rock mine, Mitchell Co.)	UNM(332)
mixed U-oxide hydrates	(Flat Rock mine, Mitchell Co.)	HM(127527)
uraninite (w/alt.)	(Chesnut Flats mine, Mitchell Co.)	UNM(338)
uraninite (w/alt.)	(Chestnut Flats mine, Mitchell Co.)	UNM(136)
uraninite (w/alt.)	(Emily Knob mine, Mitchell Co.)	UNM(135)
uraninite (w/alt.)	(No. 20 mine, Mitchell Co.)	UNM(333)
uraninite (w/alt.)	(No. 20 mine, Mitchell Co.)	UNM(334)
uraninite (w/alt.)	(No. 20 mine, Mitchell Co.)	UNM(335)
uranospathite	(Mitchell Co.)	CSM(503.1H)
phosphuranylite	(Mitchell Co.)	CSM(5960)
uraninite	(Mitchell Co.)	DMNH(7206)
clarkeite	(Spruce Pine)	CSM(2026.1)
clarkeite	(Spruce Pine)	DMNH(13283)
clarkeite	(Spruce Pine)	HM(*UNM·453))
clarkeite	(Spruce Pine)	HM(*UNM·460))
clarkeite	(Spruce Pine)	HM(*UNM·461))
uraninite	(Spruce Pine)	HM(*UNM·434)
uraninite (w/mixed U-oxide hydr.)	(Spruce Pine)	HM(91208)
uraninite (w/alt.)	(Fanny Gauge mine, Burnsville, Yancey Co.)	DMNH(1228)
clarkeite	(Fanny Gauge mine, "Newdak," Yancey Co.)	HM(*UNM·459)
uraninite	(Webb mine, Yancey Co.)	UNM(336)
uraninite	(Webb mine, Yancey Co.)	UNM(337)

Pennsylvania, USA

uranothorianite	(Easton)	UNM(403)

South Dakota, USA

meta-autunite	(Bob Ingersoll mine, Keystone, Pennington Co.)	DMNH(14496)

Utah, USA

schoepite	(Delta (Pick) mine, Emery Co.)	CSM(TM3828)
schoepite	(Hidden Splendor mine, Emery Co.)	HM(*UNM·463)
boltwoodite	(Delta mine, San Rafael Swell, Emery Co.)	HM(111-A)
thucolite	(Temple Mt., San Rafael Swell, Emery Co.)	CSM(87.132)
uvanite	(Temple Rock., San Rafael Swell, Emery Co.)	CSM(1443 H)
uraninite	(White Canyon, San Juan, Co.)	UNM(394)
uraninite	(Happy Jack mine, San Juan, Co.)	UNM(353)
uraninite	(Happy Jack mine)	UNM(386)
uraninite	(Happy Jack mine)	UNM(387)
uraninite	(Happy Jack mine)	UNM(388)
uraninite	(Happy Jack mine)	UNM(389)
uraninite	(Happy Jack mine)	UNM(393)
uraninite	(Happy Jack mine)	UNM(395)
uraninite/schoepite	(Happy Jack mine)	CSM(*HJU1)
uraninite, w/ mixed U-sulfates	(Happy Jack mine)	UNM(372)
zippeite	(Happy Jack mine)	DMNH(14565)
zippeite	(Happy Jack mine)	DMNH(14565)
uraninite/schoepite	(Happy Jack mine)	CSM(*HJU1)
uraninite	(Mi Vida mine, San Juan Co.)	DMNH(15879.4)
uraninite	(Mi Vida mine)	DMNH(13262)
uraninite	(Mi Vida mine)	UNM(247)
uraninite/tyuyamunite	(Mi Vida mine)	UNM(407)
zippeite	(Oyler mine, Capital Reef, Wayne Co.)	UNM(385)
uraninite	(Seven Mile Canyon, Moab)	UNM(390)
uraninite	(Seven Mile Canyon)	UNM(392)
schroeckingerite	(Seven Mile Canyon)	UNM(391)
pitchblende & becquerellite	(Moenkopi/Chinle contact)	CSM(TM11680)
uranophane	(near Callao)	UNM(380)

Washington, USA

meta-autunite	(Daybreak mine, Spokane)	DMNH(8367)
autunite	(Spokane)	UNM(371)

Wyoming, USA

schroekingerite	(Wamsutter)	CSM(203)
uranophane	(Silver Cliff mine, Lusk)	UNM(249)
urananium ore	(Shirley Basin)	UNM(379)

South America

Argentina

boltwoodite	(Mina Chiquita, Quebrada del Tigre, Cordoba)	DMNH(13293)
uraninite (w/alt.)	(Sonia mine, La Rioja Province)	DMNH(14501)

Brazil

uraninite	(Boquieran Pegmatite, Rio Grande do Norte)	DMNH(13294)

Czechoslovakia

uraninite-"pitchblende"	(Annaberg)	CSM(TM7675)
liebigite	(Jachymov)	DMNH(3288)
uraninite	(Jachymov)	UNM(255)
uraninite	(Jachymov)	UNM(347)
uraninite	(Jachymov)	UNM(406)
uraninite	(Jachymov)	HM(21171)
uraninite	(Jachymov)	HM(105917)
uraninite	(Jachymov)	HM(J36a)
uraninite	(Jachymov)	HM(96537)
uraninite	(Jachymov)	HM(71110)
uraninite	(Jachymov)	USNM(91983)
"uranopilite"	(Jachymov)	CSM(5933)
"uranopilite"	(Jachymov)	CSM(5936 SHS)
uranophane	(Jachymov)	DMNH(3304)
torbernite	(Jachymov)	CSM(5947)
voglite	(Jachymov)	DMNH(3289)
zippeite	(Jachymov)	DMNH(3303)
autunite	(Johanngeorgenstadt)	CSM(8603)
johannite	(Johanngeorgenstadt)	DMNH(13296)
mixed U-oxide hydrates	(Horní Hoštice)	MM(a837)
fourmarierite	(Horní Hoštice)	MM(A4602)
masuyite	(Horní Hoštice)	MM(A4605)
studtite	(Horní Hoštice)	MM(A4600)
uraninite (w/alt.)	(Nová Ves)	MM(11937)
fourmarierite	(Zálesí)	MM(A4606)
uraninite w/alt.	(Zálesí)	MM(22168)
uraninite w/alt.	(Zálesí)	MM(a1439)
uraninite w/alt.	(Zálesí)	MM(12529)
mixed U-oxide hydrates	(Zálesí)	MM(11235)
unknown U-oxide hydrate	(Zálesí)	MM(11230)
unknown U-oxide hydrate	(Zálesí)	MM(15400)
uraninite	("Hohenthal-Schacht" in Mansfield)	HM(*UNM·428)

Europe (cont'd)

England

uranospathite	(Redruth, Cornwall)	CSM(TM10042)
torbernite/"scorudite"	(Phoenix, Cornwall)	CSM(5952SHS)
torbernite	(Gunnislake mine, Cornwall)	CSM(TM9937)

France

sabugalite	(Marnac)	CSM(68-58)

Germany (united)

trögerite	(Schneeberg, Saxony)	CSM(5942)
uranosphaerite	(Schneeberg, Saxony)	AMNH(16209)
uranosphaerite	(Schneeberg, Saxony)	USNM(5892)
uraninite	(Schneeberg, Saxony)	CSM(711-4H)
uranospinite	(Weisser Hirsch mine, Neustädtel, Schneeberg)	DMNH(3298)
uranophane	(Weisser Hirsch mine)	DMNH(3297)
uranocircite	(Bergen, Saxony)	UNM(405)
zeunerite	(Daniels mine, Saxony)	DMNH(3293)
uraninite (w/ ianthinite?)	(Wölsendorf)	DMNH(13297)
uraninite	(Wölsendorf)	HM(*UNM·426)
mixed U-oxide hydrates	(Wölsendorf)	HM(WBG-1)

Norway

curite / kasolite / uranophane	(Fone, Gjerstad)	HM(*UNM·452)
curite w/ uranophane, uraninite	(Fone, Gjerstad)	HM(*UNM·466)
uraninite and curite	(Fone, Gjerstad)	HM("4")
uraninite	(Fone, Gjerstad)	HM(104723)
uraninite	(Bjertnes, Krödern)	HM(*UNM·425)

Europe (cont'd)

Portugal

saleèite	(Cunha Baixa mine)	CSM(80-214)

Spain

uranospathite	(Pedro Alvaro, Salamanca)	CSM(C-19-2)

Undetermined Localities

boltwoodite w/calcite	HM(120787)
vandendriesscheite	HM(*UNM·470)
uraninite (w/alt.) (w/ feldspar & muscovite)	HM(107488)
uraninite w/ becquerelite & carnotite	HM(*UNM·485)
schoepite w/ masuyite & ianthinite (?)	HM(86786)

Appendix D

SCANNING ELECTRON MICROGRAPHS OF SELECTED URANYL MINERALS

Uranyl Oxide Hydrates

Schoepite	$UO_2(OH)_2 \cdot H_2O$
Meta·schoepite	UO2(OH)2
Billietite	$Ba[(UO_2)_6O_4(OH)_6] \cdot 4\text{-}8H_2O$
Becquerelite	$Ba[(UO_2)_6O_4(OH)_6] \cdot 4\text{-}8H_2O$
Fourmarierite	$Pb[(UO_2)_4O_3(OH)_4] \cdot 4H_2O$
Curite	$Pb_3[(UO_2)_8O_8(OH)_6] \cdot 3H_2O$
Vandenbrandeite	$Cu(UO_2)(OH)_4$

SCHOEPITE $UO_2(OH)_2 \cdot H_2O$

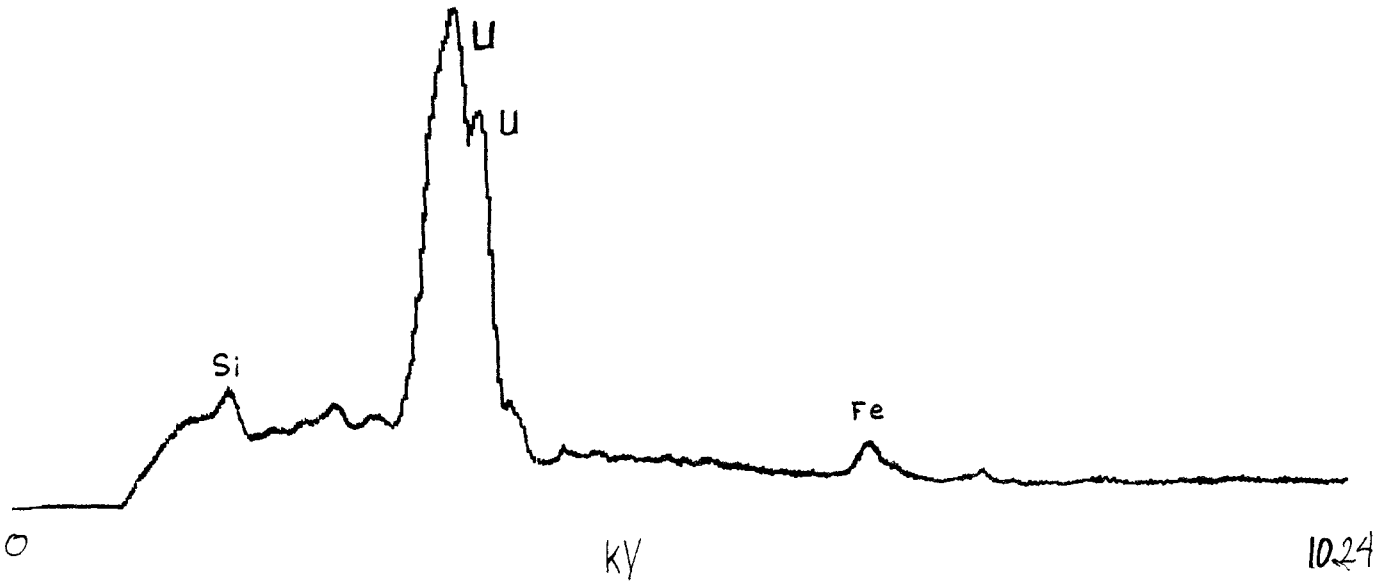

META·SCHOEPITE **UO2(OH)2**

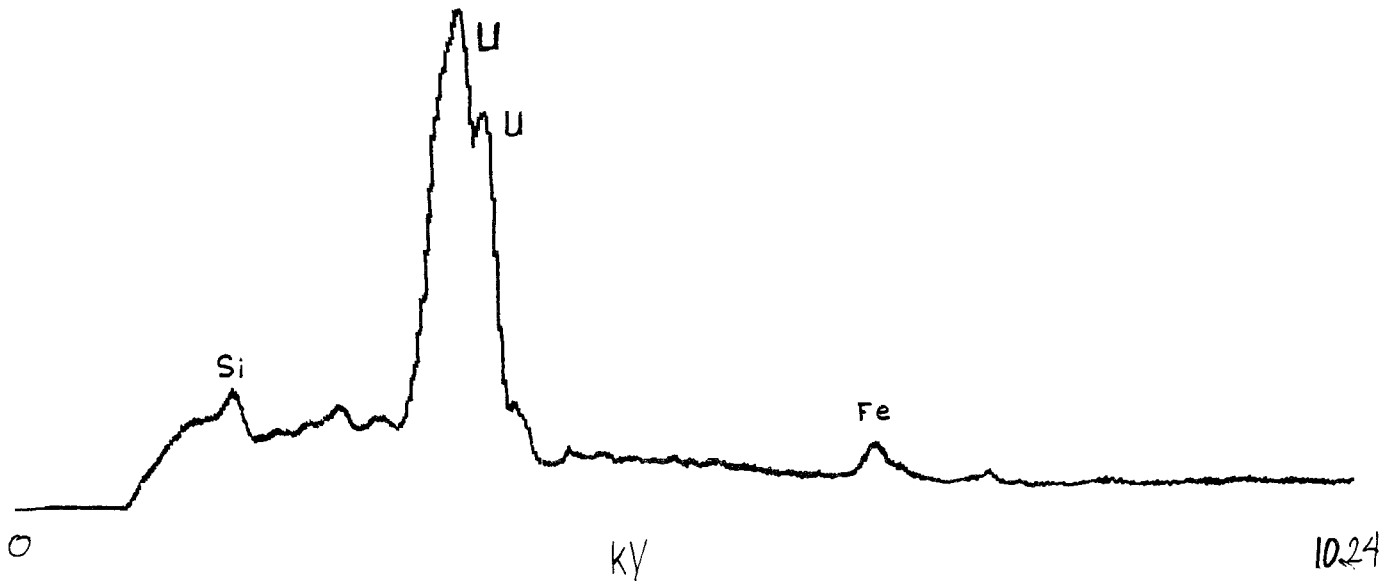

BILLIETITE $BA[(UO_2)_6O_4(OH)_6]\cdot 4\text{-}8H_2O$

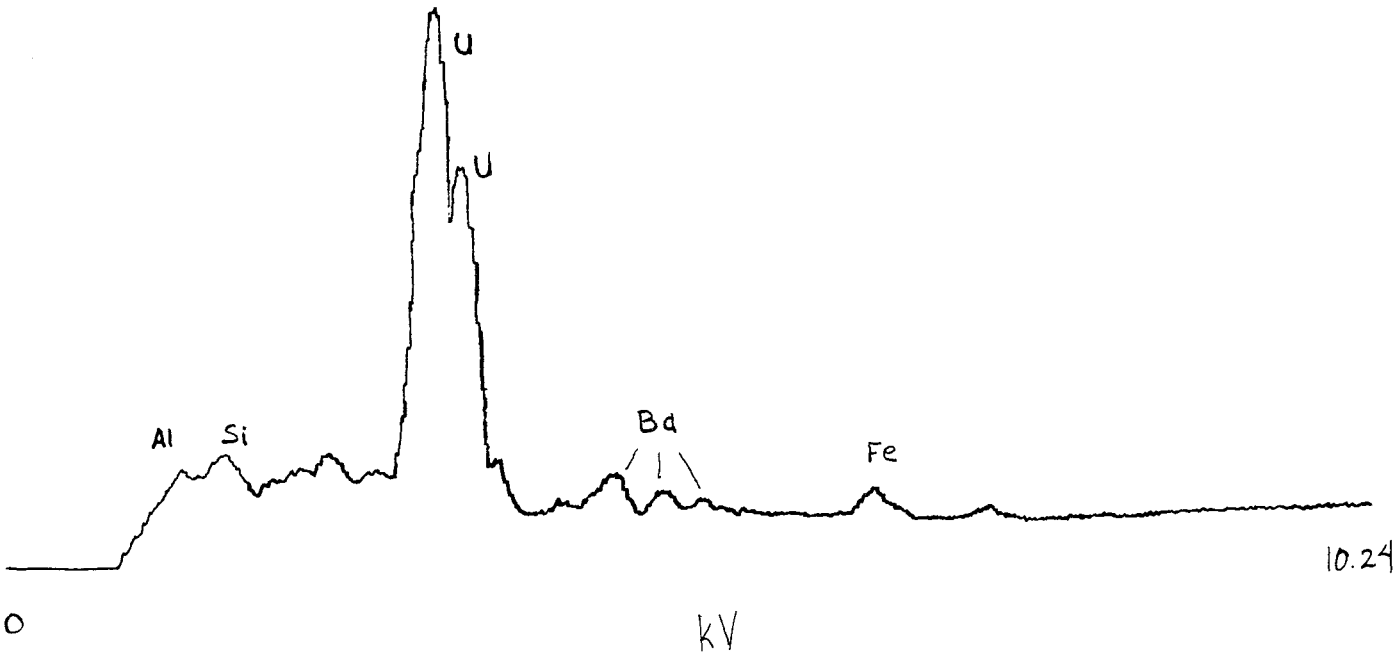

BECQUERELITE $BA[(UO_2)_6O_4(OH)_6]\cdot 4\text{-}8H_2O$

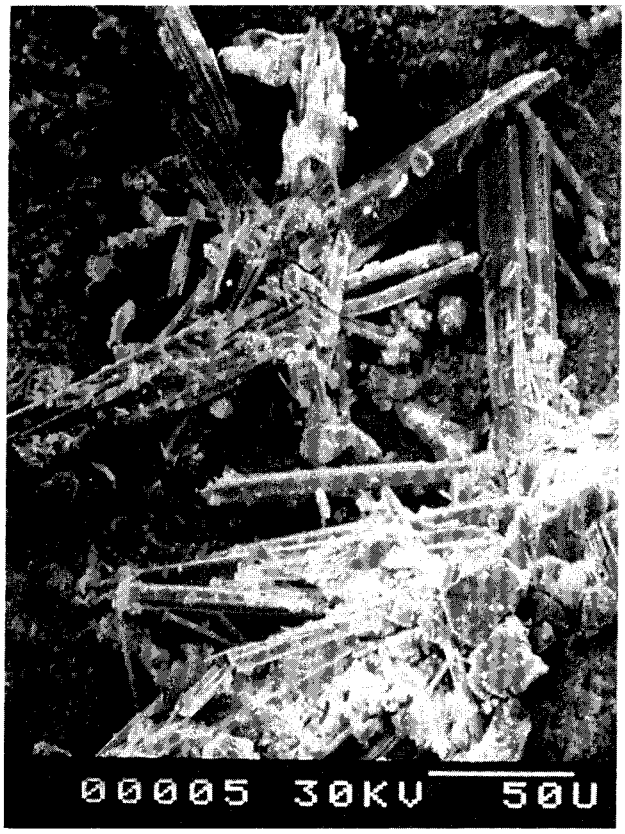

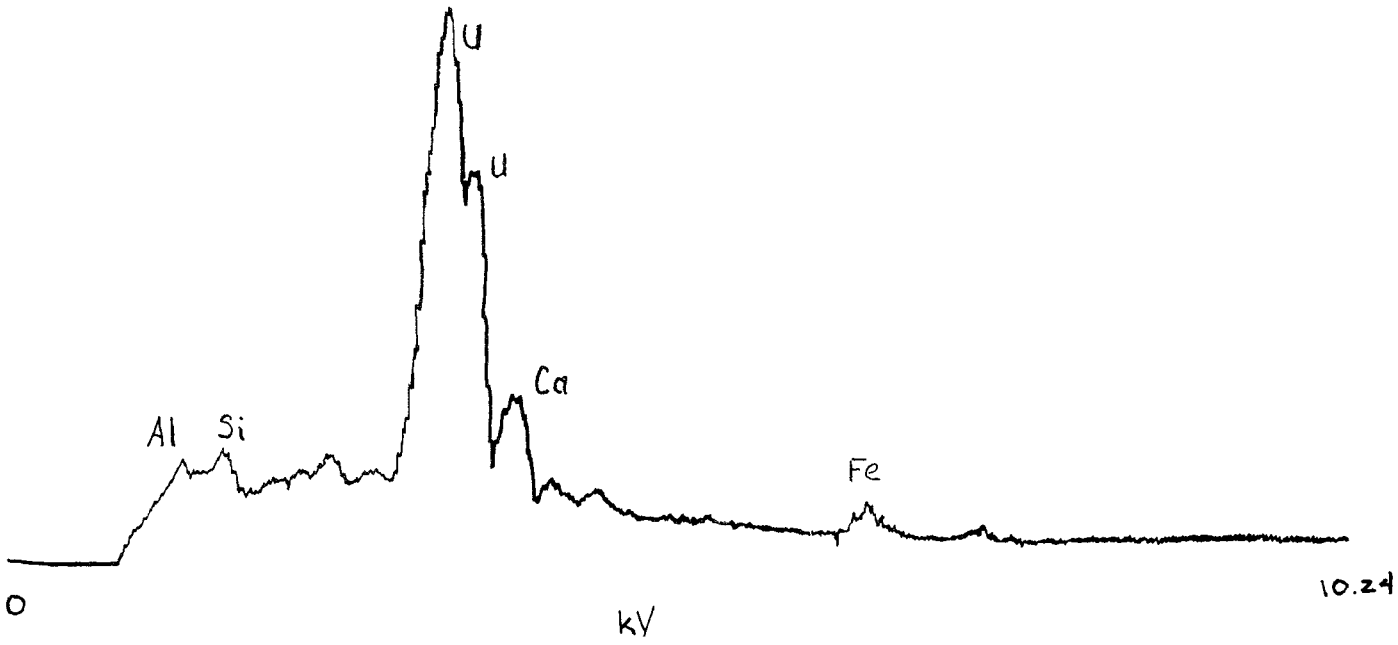

CURITE $PB_3[(UO_2)_8O_8(OH)_6]\cdot 3H_2O$

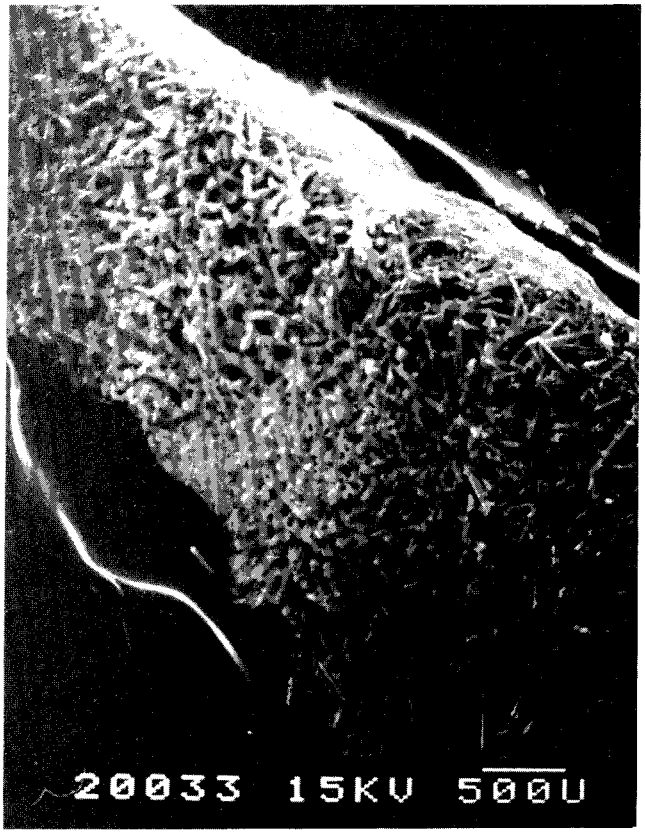

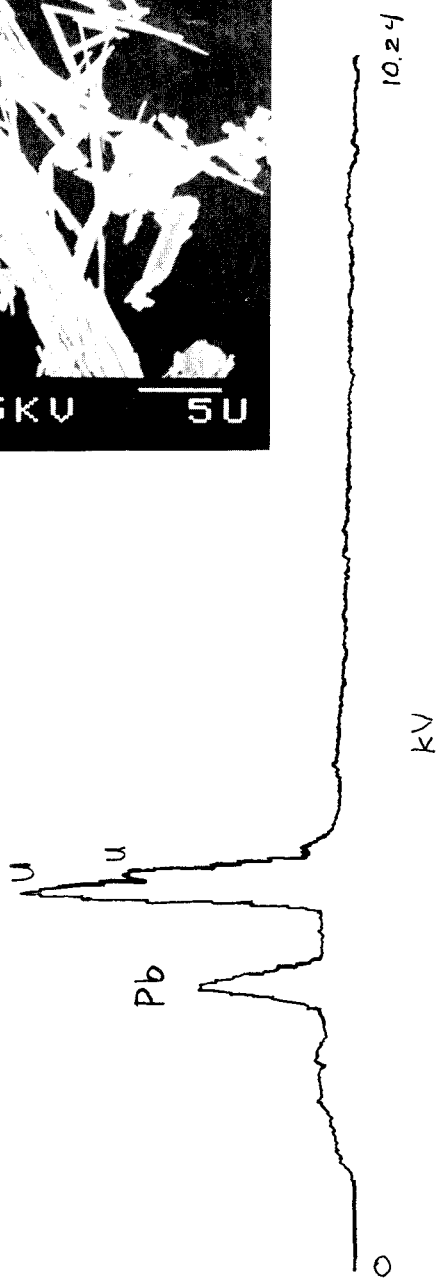

FOURMARIERITE $PB[(UO_2)_4O_3(OH)_4]\cdot 4H_2O$

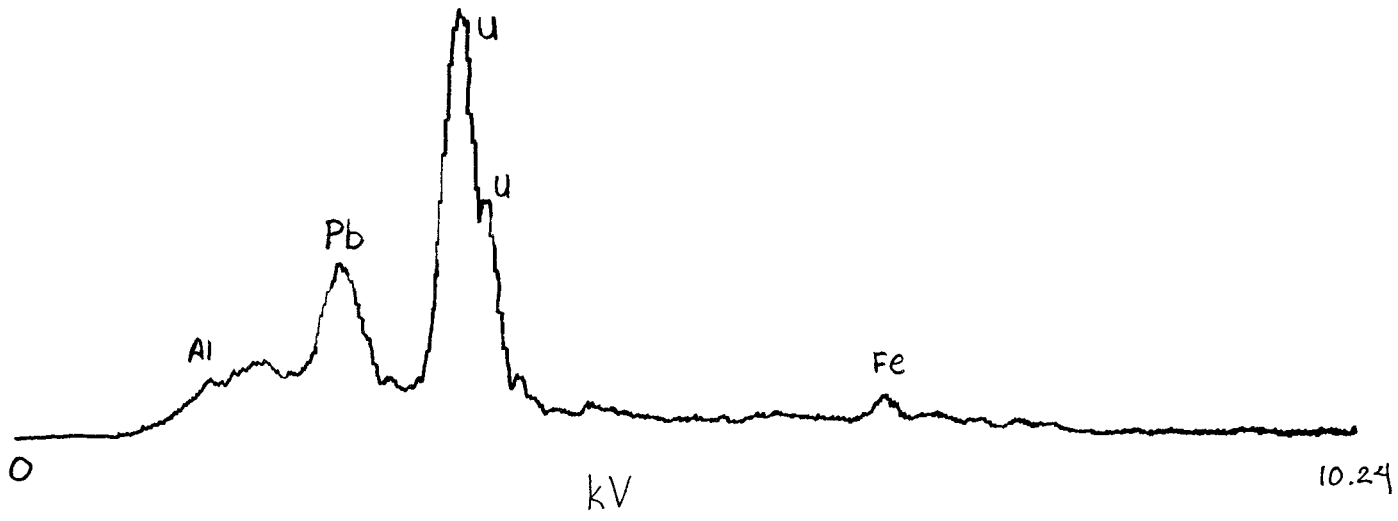

VANDENBRANDEITE $CU(UO_2)(OH)_4$

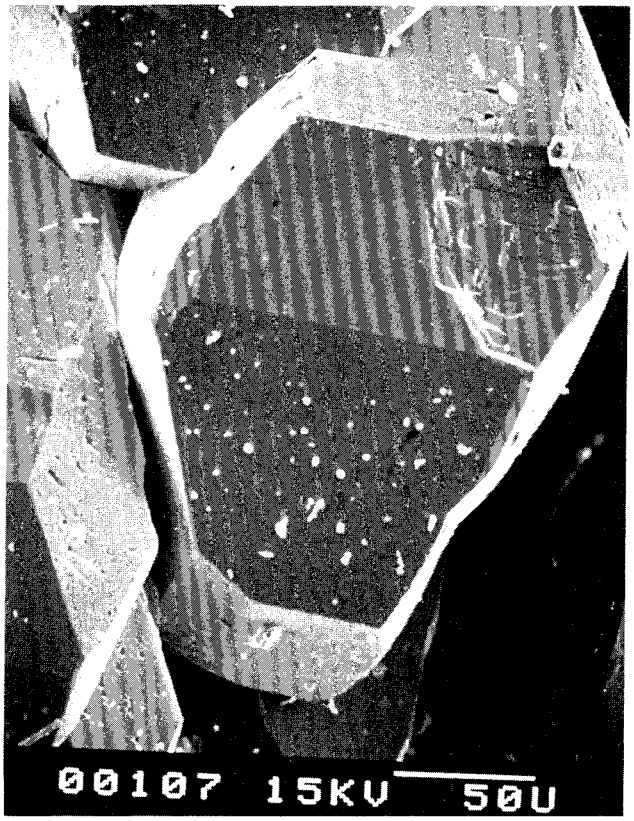

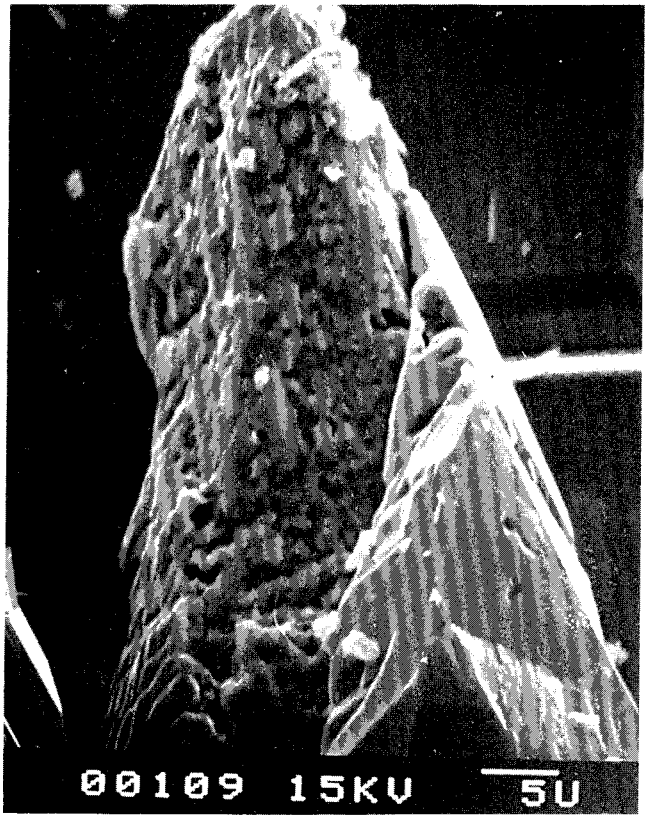

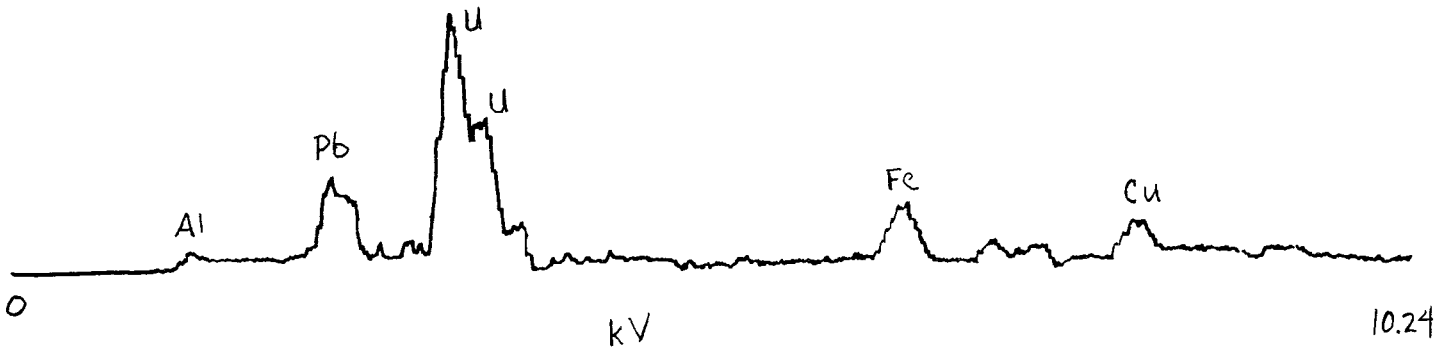

Uranyl Silicates

Soddyite	$UO_2(SiO_4)\cdot 2H_2O$
Uranophane	$Ca(UO_2)(SiO_3)(OH)_2\cdot 2H_2O$
Kasolite	$Pb(UO_2)(SiO_4)\cdot H_2O$

SODDYITE $UO_2(SIO_4)\cdot 2H_2O$

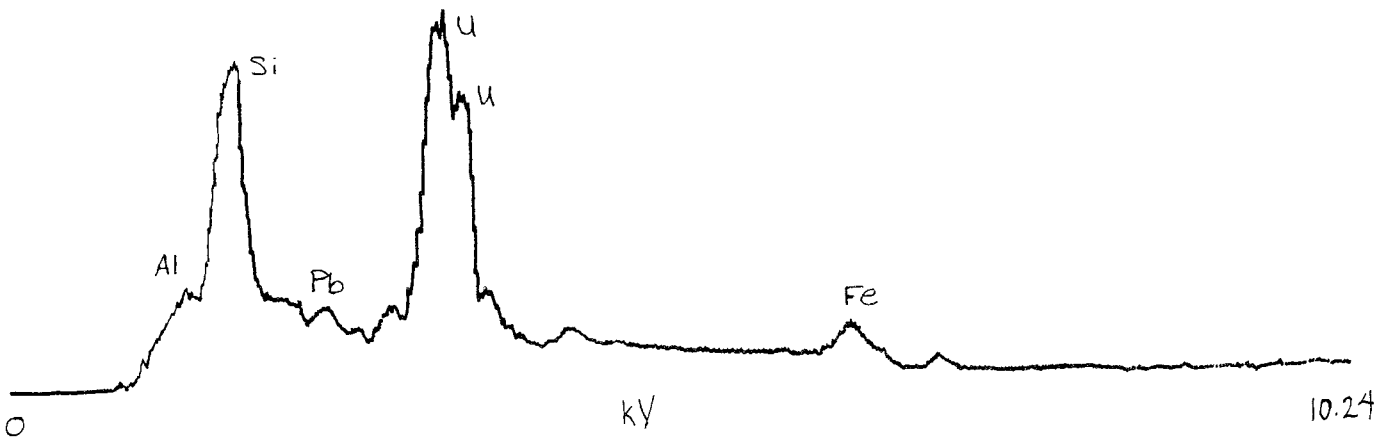

URANOPHANE $CA(UO_2)(SIO_3)(OH)_2 \cdot 2H_2O$

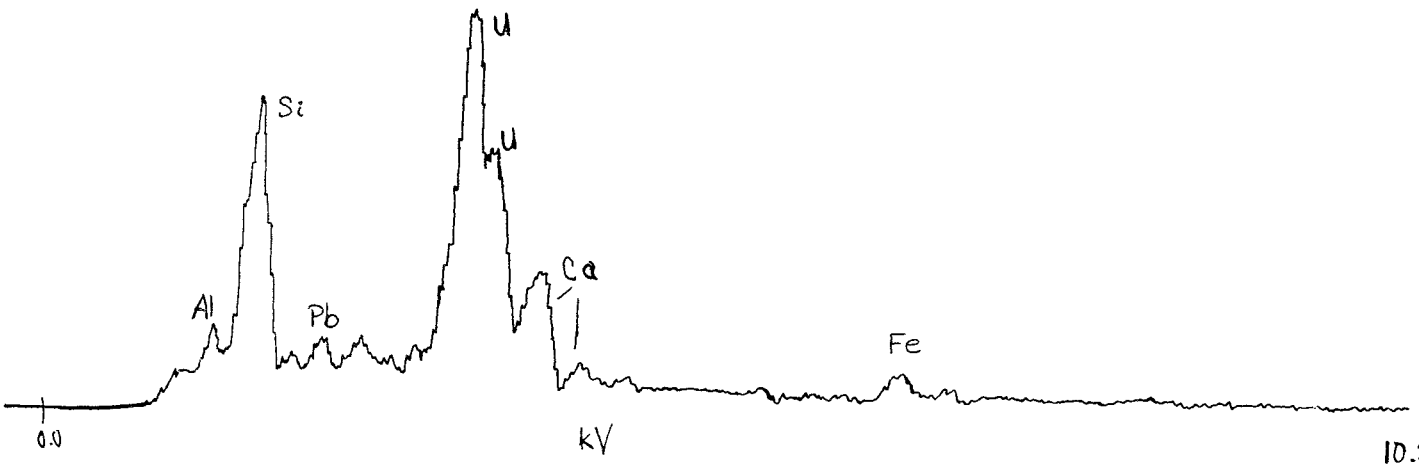

KASOLITE $PB(UO_2)(SIO_4)\cdot H_2O$

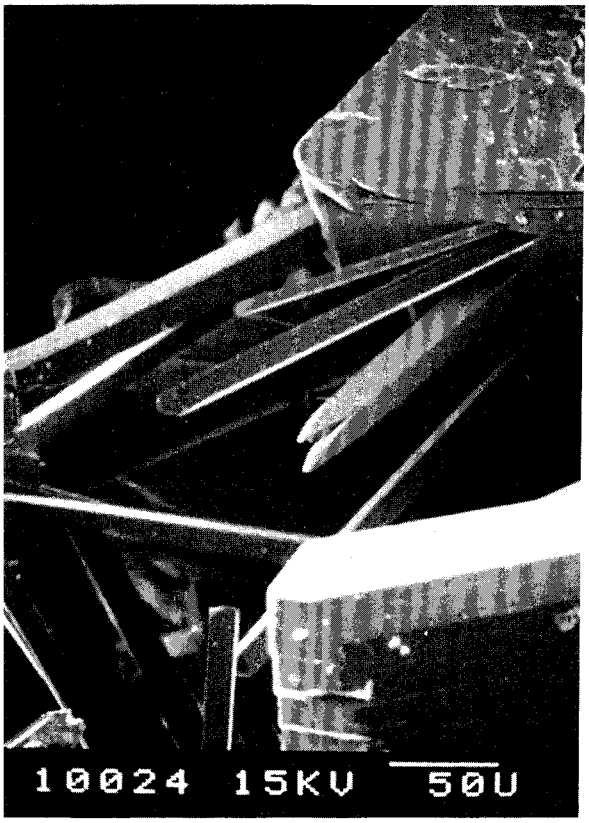

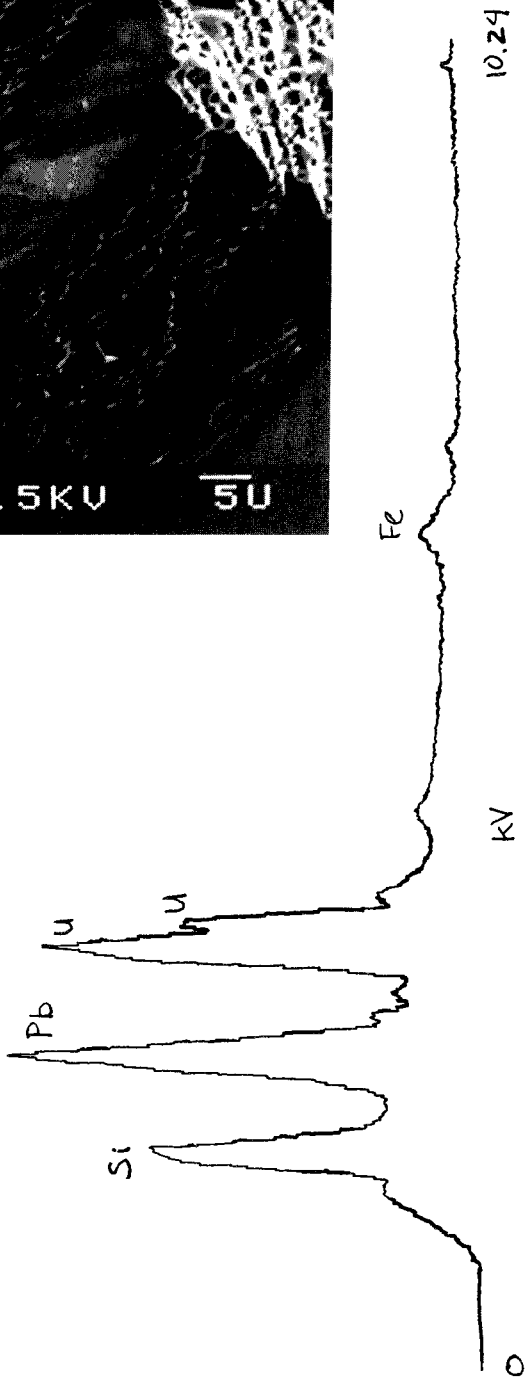

Uranyl Phosphates

Torbernite	$Cu(UO_2)_2(PO_4)_2 \cdot 8\text{-}12H_2O$

TORBERNITE $CU(UO_2)_2(PO_4)_2 \cdot 8\text{-}12H_2O$

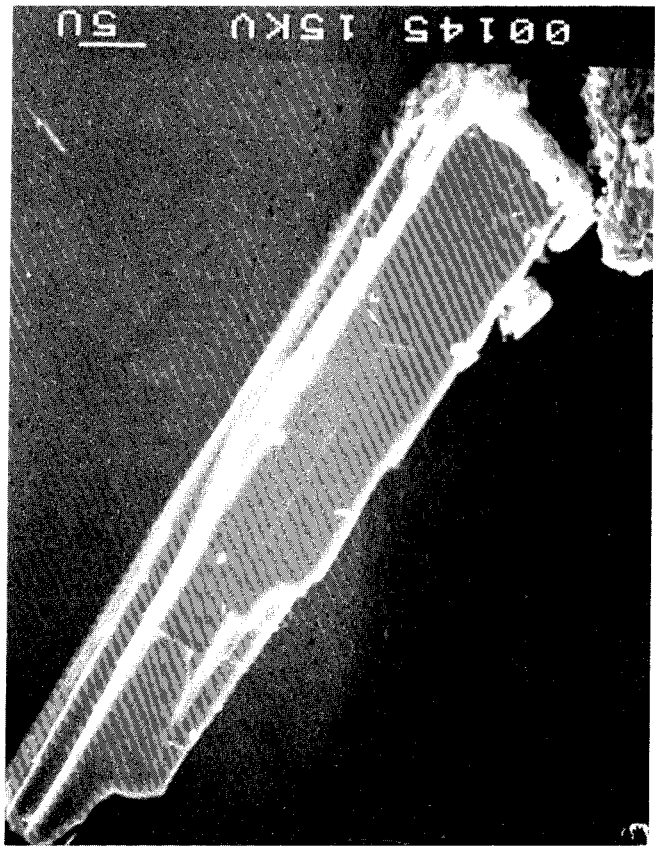

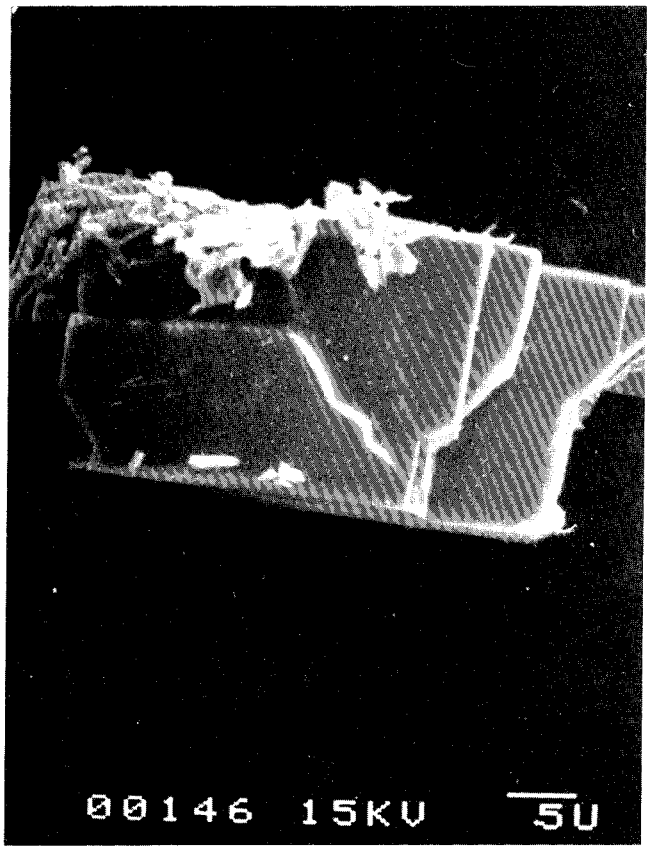

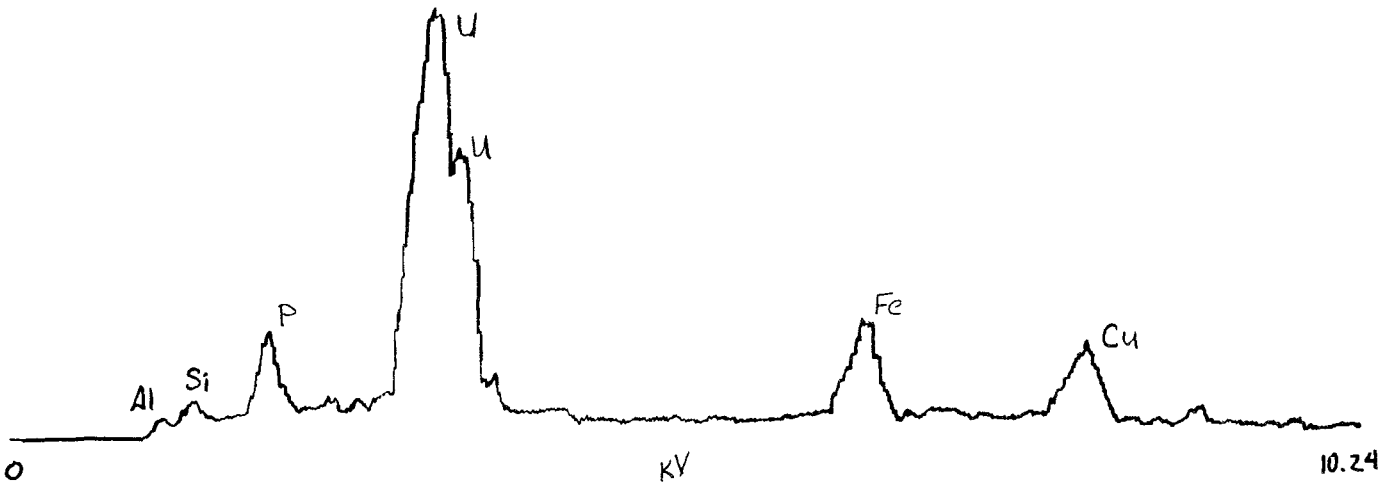

Uranyl Carbonates

Rutherfordine	$UO_2(CO_3)$

RUTHERFORDINE $UO_2(CO_3)$

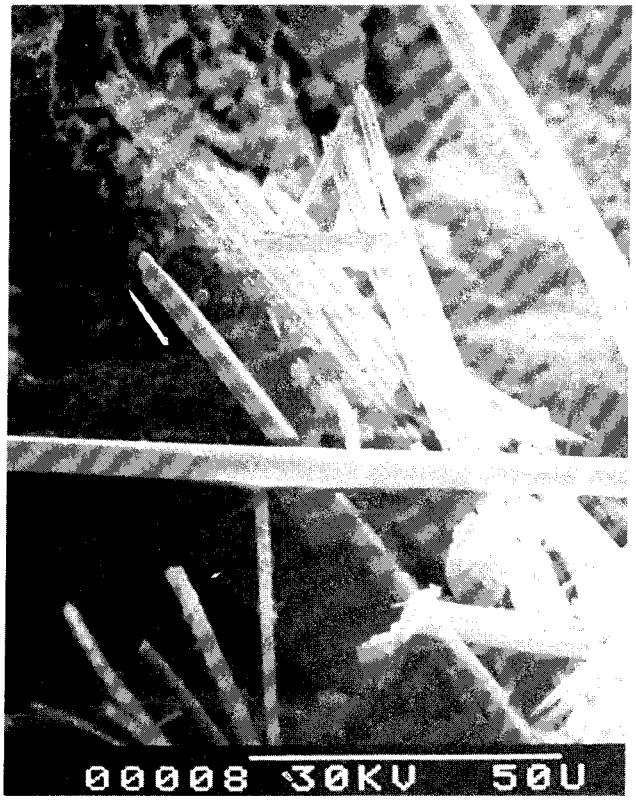

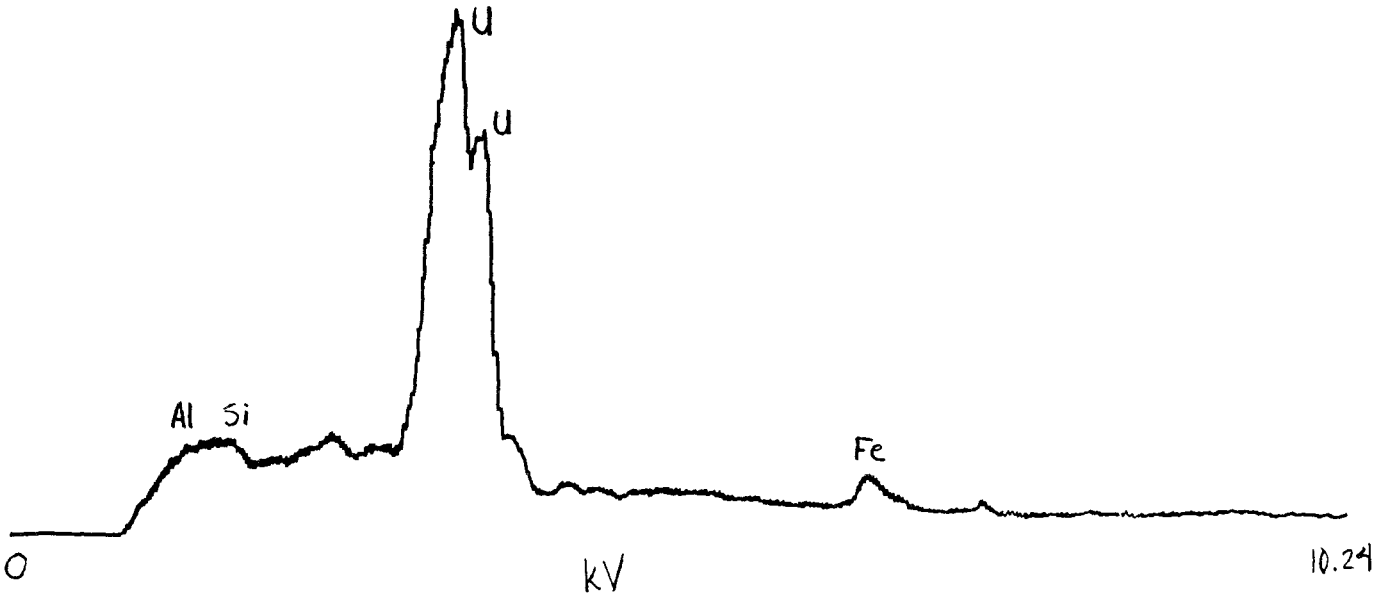

List of SKB reports

Annual Reports

1977-78
TR 121
KBS Technical Reports 1 – 120
Summaries
Stockholm, May 1979

1979
TR 79-28
The KBS Annual Report 1979
KBS Technical Reports 79-01 – 79-27
Summaries
Stockholm, March 1980

1980
TR 80-26
The KBS Annual Report 1980
KBS Technical Reports 80-01 – 80-25
Summaries
Stockholm, March 1981

1981
TR 81-17
The KBS Annual Report 1981
KBS Technical Reports 81-01 – 81-16
Summaries
Stockholm, April 1982

1982
TR 82-28
The KBS Annual Report 1982
KBS Technical Reports 82-01 – 82-27
Summaries
Stockholm, July 1983

1983
TR 83-77
The KBS Annual Report 1983
KBS Technical Reports 83-01 – 83-76
Summaries
Stockholm, June 1984

1984
TR 85-01
Annual Research and Development Report 1984
Including Summaries of Technical Reports Issued during 1984. (Technical Reports 84-01 – 84-19)
Stockholm, June 1985

1985
TR 85-20
Annual Research and Development Report 1985
Including Summaries of Technical Reports Issued during 1985. (Technical Reports 85-01 – 85-19)
Stockholm, May 1986

1986
TR 86-31
SKB Annual Report 1986
Including Summaries of Technical Reports Issued during 1986
Stockholm, May 1987

1987
TR 87-33
SKB Annual Report 1987
Including Summaries of Technical Reports Issued during 1987
Stockholm, May 1988

1988
TR 88-32
SKB Annual Report 1988
Including Summaries of Technical Reports Issued during 1988
Stockholm, May 1989

1989
TR 89-40
SKB Annual Report 1989
Including Summaries of Technical Reports Issued during 1989
Stockholm, May 1990

Technical Reports

List of SKB Technical Reports 1991

TR 91-01
Description of geological data in SKB's database GEOTAB
Version 2
Stefan Sehlstedt, Tomas Stark
SGAB, Luleå
January 1991

TR 91-02
Description of geophysical data in SKB database GEOTAB
Version 2
Stefan Sehlstedt
SGAB, Luleå
January 1991

TR 91-03
1. The application of PIE techniques to the study of the corrosion of spent oxide fuel in deep-rock ground waters
2. Spent fuel degradation
R S Forsyth
Studsvik Nuclear
January 1991

TR 91-04
Plutonium solubilities
I Puigdomènech[1], J Bruno[2]
[1]Enviromental Services, Studsvik Nuclear, Nyköping, Sweden
[2]MBT Tecnologia Ambiental, CENT, Cerdanyola, Spain
February 1991

TR 91-05
Description of tracer data in the SKB database GEOTAB
SGAB, Luleå
April, 1991

TR 91-06
Description of background data in the SKB database GEOTAB
Version 2
Ebbe Eriksson, Stefan Sehlstedt
SGAB, Luleå
March 1991

TR 91-07
Description of hydrogeological data in the SKB's database GEOTAB
Version 2
Margareta Gerlach[1], Bengt Gentzschein[2]
[1]SGAB, Luleå
[2]SGAB, Uppsala
April 1991

TR 91-08
Overview of geologic and geohydrologic conditions at the Finnsjön site and its surroundings
Kaj Ahlbom[1], Sven Tirén[2]
[1]Conterra AB
[2]Sveriges Geologiska AB
January 1991

TR 91-09
Long term sampling and measuring program. Joint report for 1987, 1988 and 1989. Within the project: Fallout studies in the Gideå and Finnsjö areas after the Chernobyl accident in 1986
Thomas Ittner
SGAB, Uppsala
December 1990

TR 91-10
Sealing of rock joints by induced calcite precipitation. A case study from Bergeforsen hydro power plant
Eva Hakami[1], Anders Ekstav[2], Ulf Qvarfort[2]
[1]Vattenfall HydroPower AB
[2]Golder Geosystem AB
January 1991

TR 91-11
Impact from the disturbed zone on nuclide migration – a radioactive waste repository study
Akke Bengtsson[1], Bertil Grundfelt[1],
Anders Markström[1], Anders Rasmuson[2]
[1]KEMAKTA Konsult AB
[2]Chalmers Institute of Technology
January 1991

TR 91-12
Numerical groundwater flow calculations at the Finnsjön site
Björn Lindbom, Anders Boghammar,
Hans Lindberg, Jan Bjelkås
KEMAKTA Consultants Co, Stockholm
February 1991

TR 91-13
Discrete fracture modelling of the Finnsjön rock mass
Phase 1 feasibility study
J E Geier, C-L Axelsson
Golder Geosystem AB, Uppsala
March 1991

TR 91-14
Channel widths
Kai Palmqvist, Marianne Lindström
BERGAB-Berggeologiska Undersökningar AB
February 1991